SELF-SENSING COMPOSITES: CURE MONITORING

by

ANDREW DERMOT TOMLIN

A thesis submitted to the
University of Birmingham
for the degree of
MASTER OF RESEARCH

School of Metallurgy and Materials
University of Birmingham
December 2010

Abstract

The ability to monitor the cure kinetics at the fibre-matrix interface and the effects induced by the presence of silane coupling agents was the main focus of this study. E-glass reinforcing fibres were used as chemical sensors to eliminate the potential problems associated with implanting a foreign body into a composite structure in the form of an optical fibre. This study demonstrated conclusively that E-glass reinforcing fibres can be used to monitor the cure of an epoxy/amine resin system *in-situ*; the data generated via evanescent wave spectroscopy (EWS) using the reinforcing E-glass fibres showed excellent correlation with conventional transmission Fourier transform infrared spectroscopy over a range of temperatures. EWS via E-glass fibres was used to study the effects of the following coupling agents on the cure behaviour: (i) 3-glycidyloxypropyltrimethoxysilane (GPS); and (ii) 3-aminopropyltriethoxysilane (APS). The epoxy and amine functional groups in the resin system were affected by the presence of the silane coupling agents during cure. Increased GPS concentration induced faster rates of epoxy conversion, but reduced the final degree of epoxy conversion. The amine functional groups of the curing resin were converted at faster rates with APS treatment, but the final degree of amine conversion was reduced.

Acknowledgements

I am indebted to my supervisors, Professor Gerard Franklyn Fernando and Doctor Liwei Wang. I am extremely grateful to have worked with two extraordinary people.

I thank Professor Alison Davenport for her support during the latter stages of my study.

I also wish to thank the sensors and composites group.

Contents

List of Figures

List of Tables

Glossary

ATR-	attenuated total reflectance
DGEBA-	diglycidyl ether of bisphenol-A
DSC-	differential scanning calorimetry
EWS -	evanescent wave spectroscopy
FBG-	fibre Bragg grating
FTIR -	fourier transform infrared
IR-	infrared
NA-	numerical aperture
NIR -	near infrared
PCA-	principal component analysis
RTM-	resin transfer moulding
SMA-	standard sub-minature adaptor
UV-	ultraviolet

Chapter 1

1. Introduction

There are three major elements that characterise a composite; the matrix, the reinforcement and the interface. The matrix can be a metal, ceramic or polymer, the reinforcement can be particulates, short-fibres or continuous fibres, and the interface is the region between the matrix and reinforcement. The selection and combination of materials for the three phases produces a composite with specific properties that the selected materials on their own could not achieve. This flexibility allows their final properties to be tailored to the requirements of the intended end-use application. Each phase plays a significant role in determining how the composite structure will perform during service.

In the present study the chief area of interest concerns the matrix phase, where thermosetting polymer systems are monitored throughout the cure process. The term “cure” is generally used when referring to cross-linking reactions. A wealth of techniques are available to monitor cure and the use of optical fibres as sensors have received much interest since their commercial introduction in the early seventies (Udd, 1995). The aim of this project is to further develop the technology where the conventional reinforcing fibres act as pseudo optical fibre sensors. This will enable evanescent wave infrared spectroscopy to be carried out through the glass fibres with the resin acting as the cladding. The primary aims of this study are to: (i) demonstrate that E-glass fibres can be used as sensors to for cure monitoring; and (ii) investigate the effect of surface-treatments on the cure behaviour.

The subsequent sections of the thesis are structured as follows: Chapter 2 provides: (i) an explanation for the motivation for undertaking this research; (ii) relevant background information concerning epoxy resins and cure monitoring techniques; (iii) a review of the literature concerning evanescent wave spectroscopy and silane coupling agents. Chapter 3 describes the cure monitoring experimental procedures used in this study. Chapter 4 presents the results obtained accompanied with in-depth discussion, concentrating on how silane treated E-glass fibres affect the cure kinetics of an epoxy resin. Chapter 5 assembles appropriate conclusions from the findings and briefly details any recommended further research.

Chapter 2

2. Literature review

2.1 Cure monitoring

Cure monitoring is the tracking of the cross-linking process of a thermosetting resin. It is achieved by the measurement of physical, optical, spectral, thermal etc. quantities and the changes that occur in relationship to the cure condition, either directly or indirectly (Skordos, 2003). In addition to achieving improved matrix-dominated properties, economical and environmental advantages may also be obtained (Bang *et al.* 2001) as will be discussed subsequently.

2.1.1 Cure kinetics

The cure kinetics of the resin system is affected by many factors (Crosby *et al.* 1996) (Figure 2.1).

Figure 2.1: Determinants of the cure kinetic of a resin system.

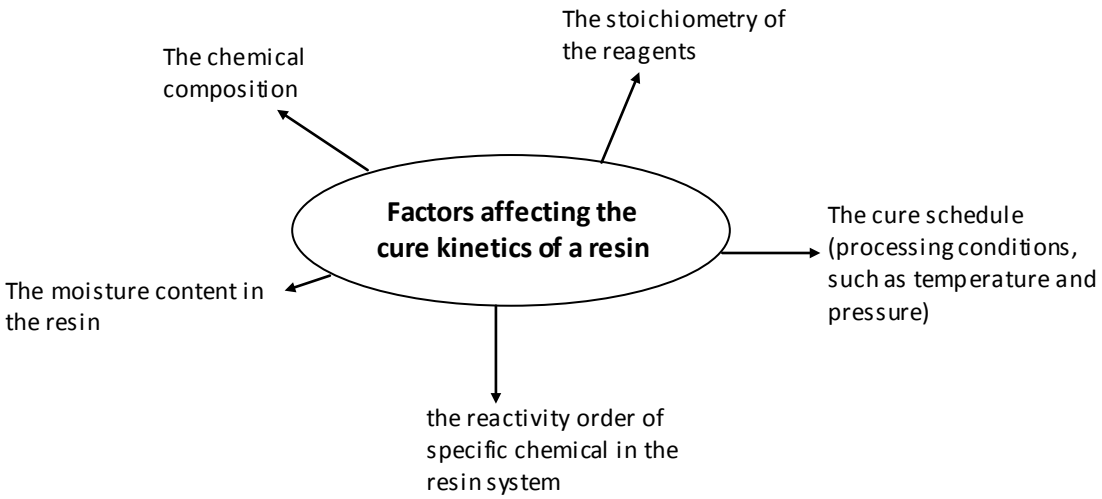

The matrix-dominated properties are therefore influenced by the cure kinetics, determining properties such as interlaminar shear strength, resin failure strain, void content and crosslink density (Doyle *et al.* 1998). In general, composite manufacturers use a pre-defined cure schedule for a particular resin system. However, these processing conditions may not actually consider the chemical state of the resin. Depending on storage conditions (storage time, temperature, freeze/thaw cycles, collective time spent out of the required temperature) the chemical state of the resin will vary between each use (Lodeiro and Mulligan, 2005). Yu *et al.* (2009) studied the ageing of epoxy prepegs at different humidity conditions using near-infrared (NIR) spectroscopy; the authors noticed that humid conditions increased epoxy cure conversion. If a more 'flexible approach' can be

introduced by understanding the cure kinetics, composite properties can be more specific to their applications requirements by enhancing the cure schedule (Crosby *et al.* 1996).

2.1.2 Residual stresses

Cross-linking reactions are exothermic; this creates an issue with respect to thermal management of the composite perform. The manufacture of a polymer composite involves the presence of two dissimilar materials (e.g. the matrix and reinforcing fibres) and so at the particular processing temperature the materials will expand differently. The heat within the composite preform needs to be monitored; traditionally, thermocouples are used. Thermocouples only provide temperatures local to their location, i.e. the edges of the preform (Tuncol *et al.* 2007). This is especially a problem for large, bulky and complicated performs. Differential thermal expansion of the key components (i.e. the fibres and matrix) can result in the development of residual stresses when the composite is cooled down from the processing temperature. The resin contraction of the matrix cross-linking can also contribute to the development of residual stresses (Hahn, 1984). Warping of composites, commonly known as 'spring-back', is caused by residual stresses (Leng and Asundi, 2002).

2.1.3 Legislation, product-value and costs

There is a need to increase the efficiency of the manufacturing process of a composite, as it is the most critical and costly stage (Liu, 1993). In addition to providing the most optimum product, the composites industry must now seriously consider the issues concerning environmental preservation and sustainable development. These added pressures are applied by government directives, for example, the waste incineration directive (2000/76/EC) was set-up to protect the environment from air, water and oil pollution. The consideration for the raw materials being used, the process of manufacture and the end-of-life policies are all aspects that will be assessed against environmental standards. In composite manufacturing, much can be done to become environmentally cleaner and more energy efficient.

Sensors systems can be used to recognise significant changes in the characteristic of the curing process to facilitate the decision making concerning the processing conditions. For instance, power can be economised and CO_2 emissions can be reduced, by identifying the point of vitrification, which signifies completion of cure (Karkanas, 1997); the curing of the material can consequently be stopped, thus reducing the cure duration. This assurance of quality eliminates the otherwise possibility of producing an inadequate and vitrified thermoset material, which will be in a permanent state and so contribute to waste; as well as exhausting all the resources used during its production process (Mulligan, 2003). This is also relevant to safety critical applications; lengthy quality control

procedures can be facilitated and assist quicker launch dates into the market place, especially when introducing new resin systems and batch to batch variations (Mulligan, 2003).

Concerning a more 'flexible approach', it is of significance to mention there are many fabrication techniques available (Figure 2.2).

Figure 2.2: Polymer composite fabrication techniques.

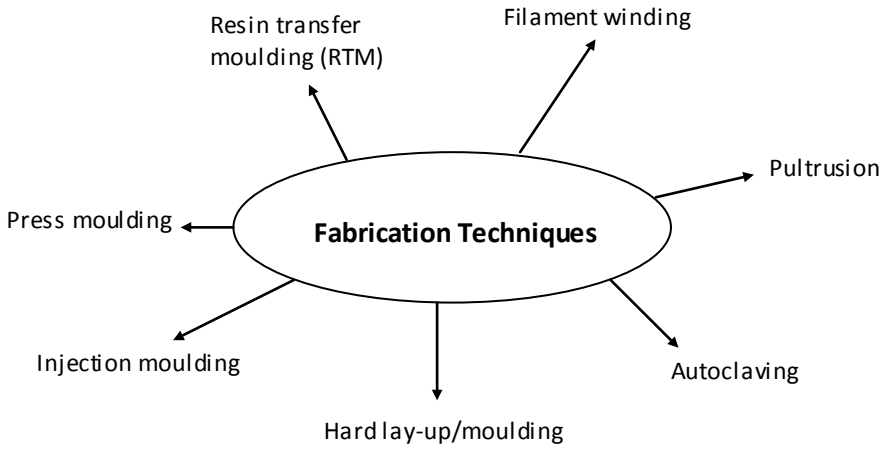

With each technique, the curing environment will be different, such as temperature and thickness disparities regarding the composites geometry; factors the cure schedule may not account for. This accentuates the need to implement a monitoring system that compensates for these differences to permit adjustments to the processing conditions in real-time (Roberts and Davidson, 1993). If the fabricator has information identifying particular stages during cure, decisions regarding the processing conditions can be made with assurance of a more efficient fabrication process. For example, if stages of low-viscosity and the moments before reaching gelation can be identified; in the case of filling a mould, the quality of fibre impregnation can be improved by applying pressure at the optimum times, which will help reduce porosity.

So, there is a demand for monitoring the rate and state of cure of a composite; the parameters of interest are monitored by particular process monitoring techniques (see Section 1.3). By satisfying each of the just mentioned issues economical gains are also available.

2.2 Curing of epoxy resins

The cure of a liquid thermosetting pre-polymer is characteristically achieved by the application of heat, curing the initial viscous liquid state into a highly cross-linked solid. Other activation methods of cross-linking include light (Koran & Kürschner, 2001), microwaves (Azzarri *et al.* 2003) and electron beam (Zhang *et al.* 2002). During this transition (liquid to solid), chemical, physical and mechanical properties of the resin are modified. The curing is accomplished by a series of complex chemical reactions, creating linked monomer units from the protraction and cross-linking of the initial pre-polymer molecules producing networks of high molecular weight. When the curing of the material proceeds (from its initial state), there will become a point at which the flow of the material ceases. Here, the material has reached gelation caused by the increasing molecular weight (accompanied by an increase in viscosity), also referred to as the rubber phase (Troughton, 2008). As the curing continues, further reactions take place enhancing the number and density of 3-D structural cross-links leading the material to vitrify, (Chen *et al.* 1999). If curing extends beyond vitrification, the risk of degradation to the material becomes more probable. The end of cure can be defined when no further reactions can occur and the product is a hard, solid material usually possessing a T_g higher than that of the cure temperature. The degree of cure is of much interest and can be defined as the 'percentage of un-reacted species conversion as compared to a fully cured material', (Lodeiro and Mulligan, 2005). Once the material accomplishes a fully cured state, no further reactions can take place, even if the curing time and temperature is increased. On occasions the material is subjected to a second stage of curing, termed as 'post-cure'; an elevated temperature is used to enable further cross-linking and increase the materials T_g. This process helps prevent degradation of the material, reducing the effect of strong exothermic reactions that are characteristic during cross-linking when commencing first time cure at high temperatures, as opposed to a second stage of curing.

2.2.1 Epoxy resin and amine hardner

An extensive body of literature is available concerning the process of cross-linking kinetics for thermoset resins, especially for epoxy resins. Reactive epoxy rings (also termed oxirane rings) partly comprise their pre-polymer state (Fig. 2.3), once the resin has cured to a high molecular weight cross-linked network, no more reactive epoxy rings may be present as they have been consumed in the cross-linking reactions. So, whether in a pre-polymer or cured state, the "epoxy resin" name is relevant for the two situations (Karkanas, 1997). The three-membered-strained ring-containing oxygen is the functional group of epoxy resin that acts as the reactive site for cross-linking (Varma *et al.* 2001).

Figure 2.3: The epoxy (oxirane) ring structure.

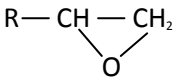

The widespread attention that epoxy-based resin systems receive is partly because of their extensive use in aerospace applications. In the 1940s, the reaction between bisphenol A and epichlorohydrin was the first marketed epoxy resin (Karkanas, 1997). Their nature permits a flexible approach to tailor desired properties, by adapting different backbone structures and molecular weights (Varma *et al.* 2001).

To produce the cured material, curing agents are used (referred to as hardeners) which react with the epoxies active functional groups and are what provide the 'linkages' in the rigid crosslinked structure; consequently providing their desirable qualities. These include: chemical resistance, flexibility, adhesiveness, castability and dimensional stability. A number of hardeners are obtainable, usually comprised of sulphur, oxygen or nitrogen. In the case of this study the latter is of interest; amines containing nitrogen are a commonly used curing agent.

2.2.2 Epoxy-amine cure reactions

It is the opening of the oxirane rings with active hydrogen atoms that produce cross-linking and polymerization. This is achieved by using a hardener, which acts as a reagent to crosslink with the greatly reactive strained epoxide ring; a common type of hardener is an amine. During the epoxy-amine cure reaction, it is well documented and generally accepted that two main reactions occur (Barton, 1985; Smith, 1961):

Primary epoxy-amine addition

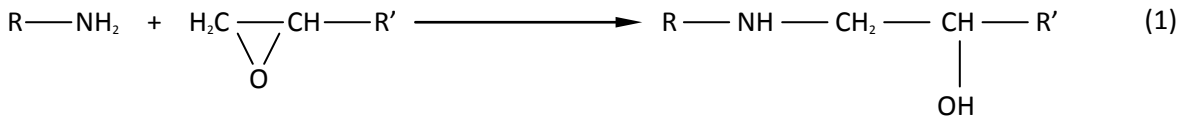

(1)

From the first reaction (Eqn. 1) the Nitrogen atom (N) on the primary amine couples with a carbon atom on the epoxy group. As a result a carbon-oxygen bond is broken, thus producing two more functional groups:

(i) secondary amine group; and

(ii) hydroxyl (OH) group

A further reaction is now seen with the secondary amine group (i) also reacting with the epoxy ring (Eqn.2) producing tertiary amine groups and an obvious increase in molecular weight.

Secondary epoxy amine addition

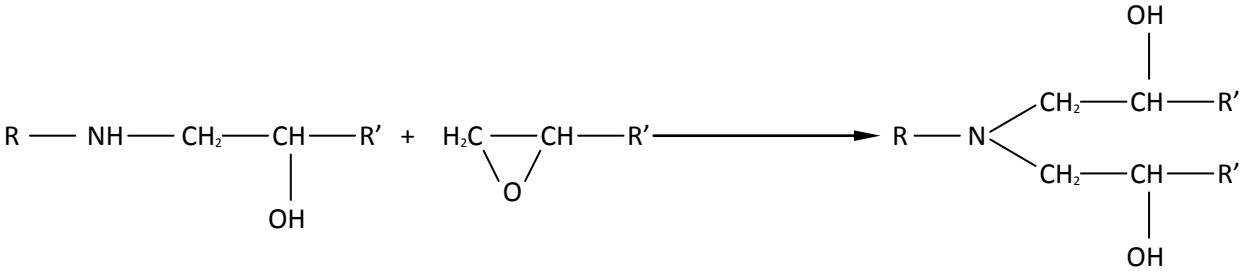

(2)

The hydroxyl formed (ii) also takes part in the reaction acting as a catalyst (Smith, 1961) (Eqn. 3)

Hydroxyl-epoxy (also referred to as etherification)

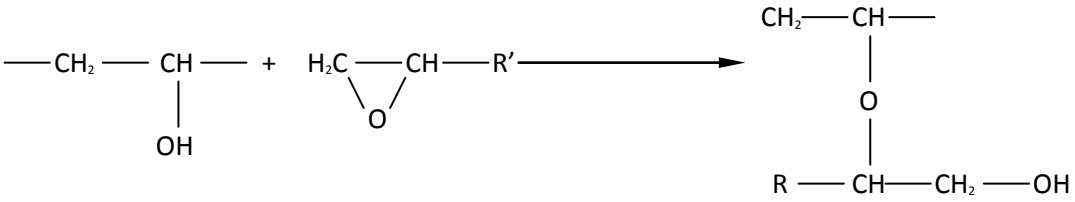

(3)

This additional reaction of the epoxy molecules with the hydroxyl groups can arise when the amine is existent in less than stoichiometric concentrations (Karkanas, 1997). By identifying the key functional groups involved in the cross-linking reactions, their consumption in the reactions can be tracked by using sensors to provide an absorption spectrum at different intervals during cure.

2.3 Cure monitoring techniques

A wide range of thermoset cure monitoring techniques are available and they function by detecting property changes in the material; these measurements are then used to indicate the cure state. Kazilas (2002) divided the techniques into three areas (Table 1).

Table 1: Cure monitoring techniques and examples (Kazilas, 2002).

Cure Monitoring Technique	**Example**
Thermal monitoring	Differential scanning calorimetry (DSC) is an established technique used for thermal monitoring, measuring properties such as the enthalpy of the reaction and the glass transition temperature (Tg), (Zvetkov *et al.* 2008).
Optical methods	Fourier transform infrared (FTIR) spectroscopy and Raman spectroscopy are both examples of optical methods used to monitor cure, that can provide data alternative to the DSC for analysis of cross-linking kinetics, (Merad *et al.* 2009).
The response of the resin system to a small external excitation (i.e. acoustic, electric, magnetic or mechanical).	Acoustic cure monitoring (Ultrasound); subjecting ultrasound to the curing material, its propagating velocity can be measured as a function of cure duration to indicate the state of cure (Harrold and Sanjana, 1986).

Though there is an abundant resource of techniques that can monitor the cure of thermosetting resins, a wealth of considerations must be addressed to determine their effectiveness as potential industrial processes. Fernando and Degamber (2006) underline some of these concerns by comparing thermal (DSC) and spectral (FTIR) data (Table 2).

Table 2: Comparison between DSC and FTIR data (Fernando & Degamber, 2006).

Thermal (DSC) data	**Spectral (FTIR) data**
The housings of the curing sample are of different materials, substrate-catalysed reactions are therefore possible.	
Measurements are taken from heat activated processes in the case of the DSC.	Vibrational characteristics are considered in FTIR spectroscopy.
The DSC uses conductive heating.	The activation of cure with FTIR experiments is difficult to design without experiencing thermal gradients in the sample during cure, relying on conductive and radiative heating.
The sample mass is less for DSC experiments and heat transfer is consequently affected.	
Atmospheric conditions can also be different between the two	

This has led to motivation of combining the two techniques (Johnson *et al.* 1992) in order to find a solution. The following sections will concentrate on the techniques relevant to this study.

2.3.1 Optical fibres and the self-sensing concept

Depending upon the measurand of interest (strain, temperature, chemical concentration, etc.), an optical fibre based technique is available for that purpose. In regards to this study, the techniques for cure monitoring with the aid of an optical fibre sensor are of interest and can be divided into qualitative or quantitative methods. A qualitative approach relies on the correlation between a specific property of the resin as a result of the cure conditions, e.g. time and temperature; whereas, a quantitative method produces information of specific chemical activity that are involved in the reaction taking place. There are numerous different types of practice that are available to monitor cure via optical fibre sensors (Table 3).

Table 3: Established techniques used to monitor the curing process.

Spectroscopy techniques	Non-spectroscopy tecniques
Ultraviolet (UV) (Merschman & Tilotta, 1998)	Strain monitoring (O'Dwyer *et al.* 1998)
Infrared (IR) (Mijovic & Andjeli, 1995)	Temperature monitoring (Liu *et al.* 1997)
Raman (Hong *et al.* 1993)	Ultrasonics (Mitra & Booth, 1998)
Chemiluminescence (Schweinsberg & George, 1986)	Dielectric (Bidstrup *et al.* 1989)
Fluorescence decay (Muhs *et al.*1990)	Nuclear magnetic resonance (NMR) (Challis *et al.* 2003)

As established previously, there is a demand for sensors that can obtain quantitative data *in-situ* and in real time. A great body of literature exists regarding the practicality of using optical fibres as light guides via total internal reflection for process monitoring. In the late fifties, a technique known as dielectric cure monitoring was introduced and has become firmly established as a prospective sensory system; however a significant concern with this technique is its susceptibility to electromagnetic interference (Kang *et al.* 2002). Optical fibre sensors are immune to electromagnetic interference and hence eliminate costs concerning the shielding of electrical-based techniques (Chen *et al.* 2004) broadening their eligibility to be used in composite processing equipment (Powell *et al.* 1998). They are also extremely sensitive to changes of the light propagating through the fibre, such as intensity, frequency, polarization and phase modulations. These attributes have facilitated their use in monitoring a wide range of material states during and after cure, such as temperature and strain (Montanini and D'acquisto, 2007), acoustic emission (Read *et al.* 2002) and vibration (Johnson *et al.* 1999) monitoring. Among other merits of optical fibre sensors, is their small size and light weight allowing feasible integration into the composite matrix (Lee, 2003). However, the incorporation of a foreign body into the host structure introduces a number of practical matters that must be approached with caution.

Firstly, in the composite structure a diameter and thermo-mechanical mismatch (Melin *et al.* 1999) is present between the optical fibre sensor and the surrounding reinforcing fibres. This affects inter-fibre spacing (Benchekchou and Ferguson, 1998) creating resin rich areas which encourage stress concentrations, that act as crack initiation sites causing delamination under mechanical loads (Her *et al.* 2010). Secondly, fibre reinforced polymer composites are used in safety critical applications (Okoli, 2001) and the deployment of a 'foreign body' may require recertification of the structure before it can be used, increasing cost. If successful deployment of the optical fibre sensor into the composite structure is achieved, further questions will be raised regarding its long term effect on the

composites structure, as well as its dependability and resilience with time. For example the sensor will need to withstand the operating temperature and/or pressures during composite processing. Silica optical fibres are regularly used as sensors and their brittle nature (Chang *et al.* 2009) require the need for an external protective system (Kin-Tak *et al.* 2001). This causes further implications regarding the sensing regions exposure to the measurand and the possible effects the surface chemistry can have on the cross-linking kinetics of the matrix. Lastly, there are concerns surrounding interconnection between the embedded sensor and interrogation apparatus.

Embedding fibres creates a list of considerations: protecting the sensor with coatings, survivability in service conditions, effect on properties and the durability of the interface between the sensor, matrix and fibres. A part solution to these problems is to use the reinforcing fibres as the sensors. Hayes *et al.* (1997) used the commercially available quartz fibres as a 'self-sensing fibre' to act as a light guide, concluding that the quartz fibres 'proved more sensitive to impact damage than the conventional optical fibres used in the study'. By comparing the mechanical properties of the quartz fibres to the E-glass fibres; they are similar in nature. It has been found that in the case of E-glass fibre reinforced epoxy composites, cure monitoring can take place by utilising E-glass optical properties converting them into light guides; hence the name self-sensing composites (Kister *et al.* 2001). This is possible when using an epoxy resin with a refractive index lower than that of the E-glass fibre. The radiating energy can then attain total internal reflection converting the reinforcing fibre into a waveguide. However, the disadvantage with this method is that Kister *et al.* (2003) only measured light absorption in the conventional intensity-based approach. This poses a problem of obtaining invalid conclusions of the collected quantitative chemical information during the cure, as there is chance of drift from the light source and/or detector.

2.3.2 Total internal reflection and evanescent waves

The word "evanescent" originates from Latin, "*evanescere"* which translates to disappear; this is apposite as the intensity of the evanescent wave decays exponentially with distance from the interface at which it was created. Evanescent wave spectroscopy can monitor the cross-linking process involved in the processing conditions of an epoxy resin system and relies on total internal reflection to take place through the sensor.

The speed of light is a physical constant that is usually considered when travelling through a vacuum. However, when light travels through another medium, such as glass or plastic, its speed will change. The index of refraction, , is related to the speed of light for a given material; the ratio of the speed of light in vacuum ( ) to the speed of light in the medium ( ) is defined as the index of refraction (Serway *et al.* 2008).

(4)

As the speed of light changes from one media to another, so does its wavelength. The index of refraction can also be expressed in terms of wavelength, where is the wavelength in vacuum and is the wavelength in the medium (Serway *et al.* 2008):

(5)

It has been established that the speed of light changes and the wavelength changes, as light passes through different media, however the frequency of light stays constant. Wavelength and frequency are related by the following equation (Bailey & Wright, 2003):

(6)

where is the speed of the wave, is the frequency and is the wavelength.

As a light ray strikes the boundary between two media of differing refractive indices the light ray's velocity is altered. At this point it causes a bend in the lights direction; this is known as refraction, and so it creates an angle-of-refraction, (Anderson *et al.* 2004). By measuring the angles from the normal to the interface of light passing through into , the angle of incidence it related to the angle of the transmitted light into by Snell's Law (Lekakou *et al.* 2006):

(7)

Figure 2.4: Refraction of light bewteen media of differing refractive indices.

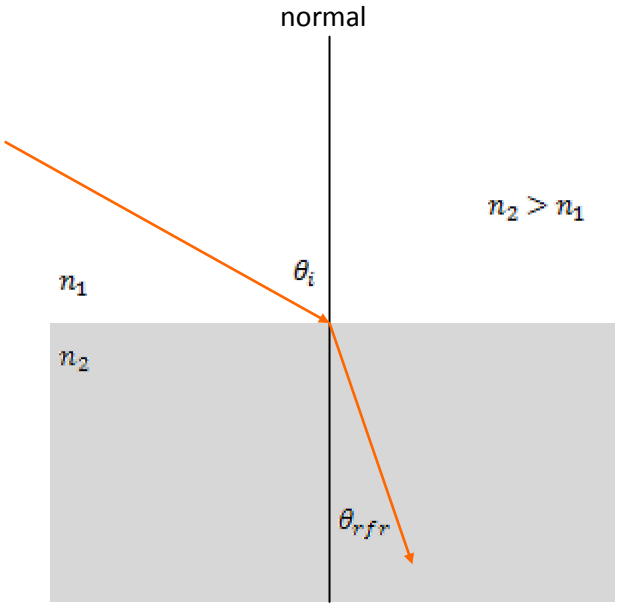

As light crosses the boundary into a medium with a higher refractive index, the light will be refracted and transmitted towards the normal. Light can be refracted away from the normal if this is reversed, i.e. by passing light through a medium with a lower refractive index. This is significant, because at a particular angle, the light travelling from to , when will bend (refract) at 90°, i.e. along the interface. This angle is known as the critical angle, ; it is a specific value of , achieved when (Pedrotti and Pedrotti, 2006). So, when and , the critical angle is governed by (Pedrotti and Pedrotti, 2006):

( ) (8)

When is greater than the critical angle total internal reflection is attained.

Figure 2.5: Total internal reflection is achieved when the angle of incidence is greater than the critical angle.

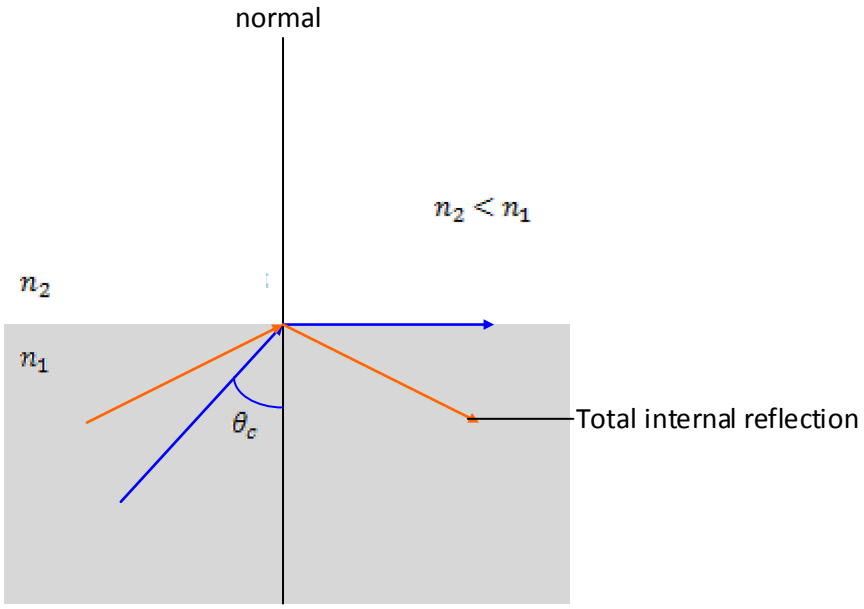

The potential light ray paths can now be discussed (Fig. 2.6) for a core with a refractive index that is higher than the refractive index of the cladding, . Air possessing a refractive index is a third medium that can also be considered , its refractive index being lower than both and . The light ray is directed at the fibre/air interface at angle , consequently at the interface the ray is reflected, as well as being refracted towards the fibre surface, which continues to penetrate through the material . The penetrating light ray then reaches and strikes the cladding/fibre boundary at an angle of , displayed at point 3. At the point at which is greater than the critical angle total internal reflection is attained shown at point 4. In a scenario where angle is smaller than the

critical angle refraction takes place penetrating into the cladding before eventually escaping with some internal reflection occurring also.

Figure 2.6: A diagram illustrating the potential light ray paths through an E-glass fibre and the surrounding resin that occur during total internal reflection (Anderson *et al.* 2004).

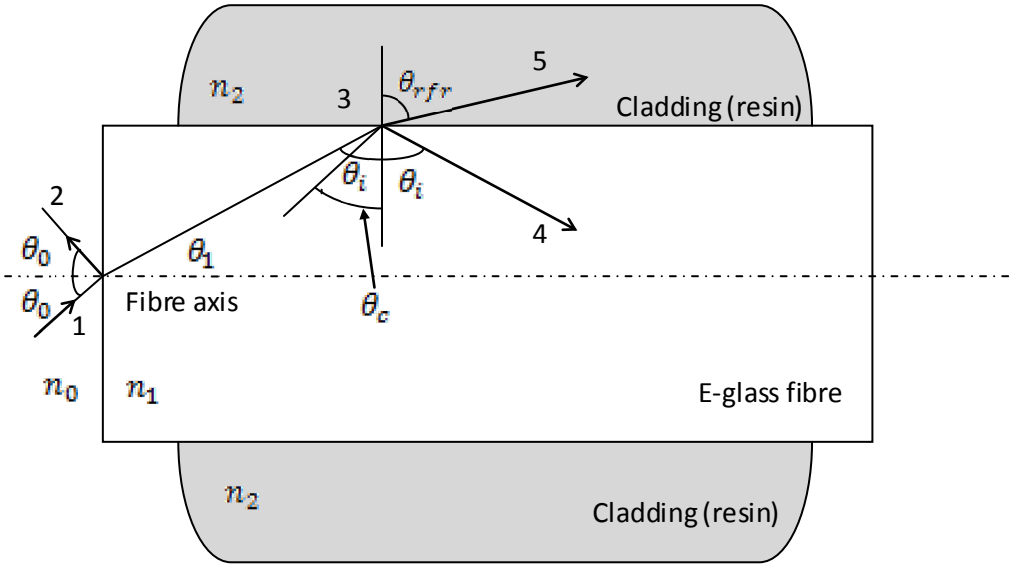

As a result of interaction between the incident light and the reflected light a standing wave disturbance is present close to the interface. A non-transmitting field is created as a result through minor infiltration of the incident light into the cladding (the evanescent wave), as described by Xu *et al*. (1996). The amplitude of the evanescent wave decays exponentially and the distance from the surface to where the intensity falls to 1/e of that at the interface is known as the penetration depth. The penetration depth of the evanescent wave can be estimated by (Fernando & Degamber, 2006):

(9)

where is the refractive index of the E-glass fibre and is the refractive index of the epoxy-amine resin system, represents the lights wavelength and represents the angle of incidence at the fibre/resin interface. With reference to infrared spectroscopy, the infrared radiation of the evanescent field is absorbed by the analyte at specific frequencies according to the vibrating molecules of the analyte and their absorption frequencies (Garton, 1989). Depending on the absorption band of the analyte, the incident light will be reflected at an attenuated frequency. By analysing the difference between the input wavenumber and output wavenumber an absorption

spectrum can be generated. If the principles associated with this technique are applied to the E-glass fibre and the epoxy resin system it is possible to obtain spectra in the NIR region.

2.3.3 Review of infrared evanescent wave spectroscopy

IR spectroscopy relies on the ability of certain molecules to absorb infrared radiation. Atoms within the molecules vibrate; the frequency of these vibrations is dictated by the strength and length of their bonds and by the atom's mass. The molecules bonds have a natural vibrating frequency; radiation in the infra-red region that is equivalent to this vibrating frequency is absorbed by these bonds, which results in the molecules vibrations. The information obtained from the infra-red spectrum helps identify the composition of the chemical bond or functional group and its concentration, with reference to the position of the absorption peak and the intensity of the peak (Fernando, 2005). Additionally, the shift in baseline of the spectra is associated with the change in refractive index (Degamber *et al*., 2003, Doyle *et al*., 1998). Due to the bond's distinctive vibrational frequency, it can be assigned to a specific wavelength range and therefore be identified easily (Table 4). Weyer (1985) and Stark, *et al.* (1986) provide helpful studies in NIR spectroscopy and its use for qualitative and quantitative analysis that can be used to identify certain peaks from obtained spectra. Druy and Elandjian (1988) employed the chalcogenide glass fibre as an evanescent sensor used to gather cure data of a graphite/epoxy prepeg. A stripped portion of the fibre exposed the region to the epoxy prepeg during the cure reaction to track the absorption band of the –NH bending mode at 3367cm^{-1}. Xu *et al.* (1996) shows that for an epoxy/amine resin system, the absorption peaks associated with the primary amine and epoxy functional groups can be clearly assigned in the near-infrared region. The motivation to use NIR spectroscopy over MIR and FIR spectroscopy is the clearer separation between absorption bands with little overlap (Poisson *et al.* 1996).

Table 4: Characteristic Near-IR absorption peaks for an epoxy resin system (Mijovic *et al.* 1995).

Wavenumber (cm^{-1})	Peak assignment
7000	-OH stretching vibrations
6682 6670 6570 6080	$-NH_2$ stretching vibrations
5969	aromatic ring C-H stretch combination
4536	epoxide combination

An *in-situ* method of monitoring the formation of a polymer network in the mid-infrared range has been demonstrated successfully by Anne, *et al.* (2009). Chalcogenide glass of a Se-Sb-Ge-Ga system was the choice of optical fibre because of its acceptance of radiation in the mid-infrared range and higher temperature tolerance, when compared to the commonly used TAS glass ($Te_2As_3Se_5$). Spectra received in the mid-infra red region are infamously difficult to identify specific vibrational bonds due to convoluted overlapping. The authors utilise a technique known as principal component analysis (PCA). The light guide was approximately 400 µm in diameter, but the sensing region was reduced to 100 µm in diameter to increase sensitivity (Le Coq *et al.* 2002). This was achieved by drawing the fibre at an increased speed during forming and by a chemical treatment which 'congruently' dissolved the glass. The tapered region was set up in a mould, the resin was injected into the mould (which was pre-heated at 180 °C) and came into contact with the sensor, a quasi isothermal cure was then carried out for 3 hours. The results were interpreted in two ways, firstly in the range 970 – 1130 cm^{-1} the evolution of integrated transmission spectra was plotted against cure duration. This data illustrated three stages during the cure process:

(i) 0 – 40 min: transmission was constant and so it can be inferred no reactions were taking place;

(ii) 40 – 120 min: a decrease in transmission inferring that curing was in process and

(iii) 120 – 180 min: transmission was constant indicating the end of cure.

Secondly, principal component analysis (PCA) was used producing a 'map' in the region between 970 and 1130 cm^{-1}. PCA is a technique used when the absorption bands cannot be clearly assigned to the vibrational bonds due to dense overlapping. PCA functions by considering the coefficients of linear combinations derived from 'spectra factors' of the raw spectra and arranging the factors in accordance to their weight. Data points in spaces signified the initial spectra and illustrated similar results compared to the integrated transmittance, in that three distinct regions exist. A large concentration of data points at the bottom right hand corner of the map indicates the period before curing begins, from 60 to 100 min a separation occurs with data points distributed along a parabola indicating that cure is in progress. End of cure was inferred by the collection of data points in one area on the left hand side of the map at the end of the parabola. The 2S2G fibre successfully monitored polymerisation process of an industrial resin, achieved at temperatures of 200 ^{o}C; the PCA analysis could be a future prospect for analysis on an industrial scale.

Powell *et al*. (1998) employed the evanescent wave method and used a high refractive index (n=1.65) optical fibre with a 20 cm portion of the cladding removed at the mid-point of the 1.5 m length fibre. After the sensor was prepared, it was placed within a glass tube before being placed in a thermostatically controlled water bath ensuring the de-clad region was immersed in the water bath. Connected to the ends of the optical fibre were a Bentham Instruments scanning monochromator and an InGaAs photodiode detector. From the spectra collected a rising baseline was identified as a main feature seen in the spectra; caused by the changing refractive index as a function of cure, identifying the increase in molecular weight. The evanescent wave spectroscopy (EWS) technique proved to show good correlation in comparison to the transmission sensor and refractive index sensor, with faster cure rates at higher temperatures. Powell *et al.* (1998) successfully demonstrated that from the spectra obtained characteristic absorption peaks could be identified and their involvement in the cure reactions could be monitored. Papers by Doyle (1998) and Crosby (1996) also show similar results.

A study by Chailleux *et al*. (2001) used F2 glass optical fibre with a high refractive index (n=1.62) to sense the cure of diglycidyl ether of bisphenol-A (DGEBA) resin using isophorone diamine (IPD) as the hardener. A portion of the optical fibre cladding was removed to allow contact of the resin to the sensor. To ensure good light guiding properties for evanescent wave transmission, the following refractive index relation had to be obeyed: $n_{core} > n_{medium} > n_{cladding}$. In comparison with the degree of cure from a differential scanning calorimeter (DSC), the evanescent sensor showed good ability to monitor the degree of cure. The possible damage to the optical fibre sensing region caused by the mechanical removal of the cladding and also the angle of incidence could have been affected from

the movement of the optical fibre at the light source, thus affecting the degree of evanescence and output signal (Fernando & Degamber, 2006); attributing a possible disadvantage with using optical fibre sensors. Dunkers *et al*. (1997), collected spectra using evanescent wave Fourier transform near infrared spectroscopy. Here they used an optical fibre 'mini-bundle', consisting of three, 150 µm high index (n=1.612) fibres. By using this 'mini-bundle' it increased signal-to-noise (S/N) ratio by providing increased optical throughput. A fibre used with a very small core radius increased its fragility and sensitivity to flow variation and hence reduced the signal-to-noise (S/N) ratio (Lew *et al.* 1984). This also introduced microbends in the fibre that might cause loss of light beams striking the core/cladding interface at an angle less than the critical angle.

Evident from the literature, EWS allows the identification of specific absorption peaks, which can then be assigned to specific functional groups. The concentration of the functional group of interest can be tracked during cure of the resin by reviewing the intensity of its assigned peak with time. Any change in the refractive index of the resin can also be obtained from the shift in baseline of the spectra.

2.4 Glass fibres and silane coupling agents

The production of glasses has existed for thousands of years. Conventionally, glasses are inorganic and non-metallic. The following definition is made possible due to two common traits that glasses possess; "an amorphous solid completely lacking in long range, periodic atomic structure, and exhibiting a region of glass transformation behaviour" (Shelby, 2005). In the case of using two dissimilar materials, such as an epoxy resin (organic polymer) and glass fibre (mineral based fibre), an attachment between the two to create a water resistant bond is not possible; a third intermediate material is required (Plueddemann, 1991).

At the beginning of the 1940s improvement in the performance of composite materials was made possible with the introduction of high strength and high modulus glass fibres. Albeit, these new composites provided good strength properties, they were not however being utilised to their full potential; prolonged exposure to atmospheric moisture deteriorated their properties drastically. This predicament created the need for a new mechanism to be used to combat this apparent loss of adhesion between the glass and resin and in the mid-1950s silane coupling agents were successfully employed to enhance composite properties (Owen, 2002). Glass fibre polymer matrix composites are still to do this day a popular material to use, moderately attributable to the advancement in coupling agents.

The glass fibre surfaces nature is critical to how it interacts and adheres with the resin matrix. It is of importance to understand that during fibre production the surface properties of the glass fibre can be modified (such as processing conditions and post-treatments), which in turn affect adhesion properties and so affecting the composite performance (Miller & Ishida, 1990). During the fabrication of glass fibres, they are coated with a "size" at the time of drawing; among the ingredients are three important elements:

(i) lubricant preventing damage;
(ii) binder for strand integrity and
(iii) a coupling agent for bonding to the matrix.

The silane coupling agent comprises a small percentage of approximately 0.1 – 0.5% in the sizes composition (Britcher *et al.* 1999)

The mechanism that provides the enhancement in the properties of composites as a result of the silane treatment, has attracted much interest. The postulated processes and mechanisms that provide these effects have been debated for many years, with scientific research supporting for and against arguments on the numerous theories that exist. The adhesion mechanism is extremely

complex, how the bonding occurs is reliant on the fibre's and matrix's atomic arrangement, molecular conformation and chemical constitution; as well as the morphological properties of the fibre and the diffusion coefficient of the elements in each component (Kim & Mai, 1998).

2.4.1 Adhesion mechanisms of the silane coupling agent

Organo-silane coupling agents are generally used to treat the surfaces of E-glass fibre in order to improve the bonding between the fibres and the matrix. A silane coupling agent has the general molecular formula (Sever *et al.* 2008):

$$R' - Si - (OR)_3 \qquad (10)$$

The R' group is a reactive functional group, such as epoxy that is selected to bond with the organic resin matrix. The OR group is also a reactive functional group, hydrolysis of the alkoxy groups on the silane takes place in aqueous solution to form a solution of silane-triols $RSi(OH)_3$ (Plueddemann, 1991); as illustrated in equation 11. By modifying the pH of the solution, hydrolysis of the alkoxy groups is encouraged. Depending on the weight percentage (wt %) of the silane used and the type of functional alkyl group, the cure kinetics can be affected (Jones, 2007).

Hydrolysis equation

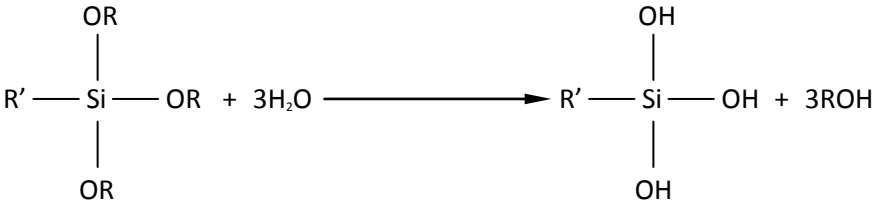

(11)

Plueddemanm (1991) suggests the OR group can also react directly with the hydroxide groups (Si-OH) on the glass fibre surface to form oxane bonds (Si-O-Si) (equation 12). It is the silanol groups (the triols) formed in aqueous solution (-OH) that can then react with the hydroxyl groups present on the glass fibre surface, via hydrogen bonding (Hull, 1981). This occurs after the silane solution is applied to the glass fibre surface and then dried under certain conditions. It is at this point that the silanol and Si-OH on the glass fibre surface undergoes a reversible condensation process, yielding a polysiloxane structure (Plueddemann, 1988) with the formation of oxane bonds between the silane and glass surface (Si-O-Si), (Plueddemann,1991). The efficiency of the coupling agent is dictated by the nature of treatment and drying conditions (Wang *et al.* 2009).

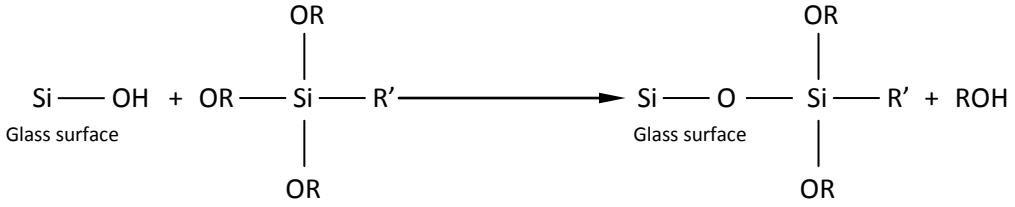

(12)

In addition to the direct condensation reaction in Equation 12; another condensation reaction can also be considered between the silanol groups of the organo-silane and the silanol groups present on the glass. During this reaction, the silanol groups can condense with the adjacent silane forming a polymer film on the surface (Equation 13).

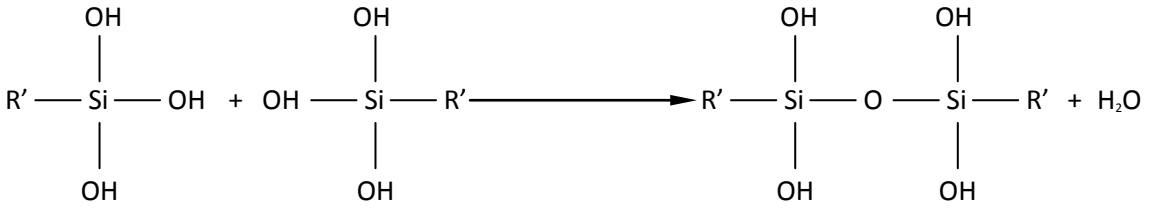

(13)

After these reactions, the R groups are free to crosslink with reactive functional groups of the uncured resin matrix (i.e. the amine and epoxy) and generate the characteristic covalent bond, 'coupling' the glass to the cross-linked resin. This provides a wealth of benefits, which include, enhanced adhesion, improved composite strength, improved strength retention and protection of the interfacial bond from water attack (Sever *et al.* 2008).

The choice of silane coupling agent for this study is in accordance with the theory of this mechanism; 3-aminoproyltrimethoxysilane (APS) and 3-glycidyloxypropyltrimethoxysilane (GPS) both have primary functional groups of amine and epoxy, respectively.

3-aminoproyltrimethoxysilane (APS)

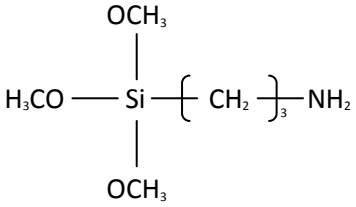

(14)

3-glycidyloxypropyltrimethoxysilane (GPS)

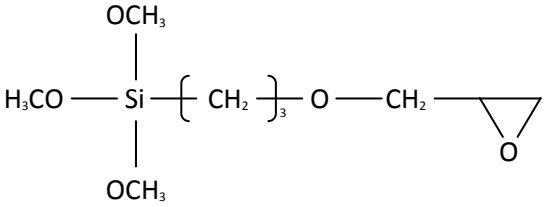

(15)

It would be naive to accredit the chemical bonding theory as the sole contributor to the unique bonding mechanism that appears with silane coupling agents. Ishida and co-workers (1982), demonstrate that adhesion at the interface is far from simple, indicating that mechanical

interlocking is also present. The authors reasoned that a vinyl silane (VTS) had limited use as a coupling agent in comparison to the amino silane, APS; because the VTS exhibits a highly cross-linked layer, which causes the vinyl functional groups to be inaccessible. APS on the other hand, exhibits the ability to accept the migration of resin into molecular pores creating a semi-interpenetrating network. This was deduced by a carrying out warm (50°C) and hot water (100°C) washing testing the extractability of the hydrolysed silane deposit. Loosely adsorbed material (soluble oligomeric component) was removed during warm water washing and linear hydrolysable components were removed from the silane deposit with hot water washing, (Jones, 2007). It is the loosely adsorbed component that is perceived to vacate the silane deposit and migrate to the resin matrix, permitting the matrix resin to take residence into the now empty molecular pores.

The other theories proposed have not had as much acceptance as the chemical bonding theory, however one should not dismiss them. They can also play a vital role in understanding why the coupling agent has such a profound effect on properties of composites. The surface wettability theory, explains that an adhesive bond can impart sufficient strength by the means of physical adsorption alone, providing the adhesive fully wets the substrate. The ability to achieve these conditions is extremely difficult and after considerations of external factors, such as water, the strength of the bond cannot be maintained just via physical adsorption. It could be suggested that the chemical bonding theory has the chief role and once this mechanism has been satisfied, properties can further be improved by increasing the wetting of a resin onto the treated fibre surface.

Another explanation considers the interdiffusion of atoms or molecules across the boundary formed between the resin matrix and coupling agent. Plueddemann (1991), states that a thermodynamic equilibrium must exist between the two constituents for interdiffusion to take place. Interdiffusion and the interpenetrating network (IPN) offers an explanation (excluding the chemical bonding theory) for the bonding of glass fibres and polymer resins via silane coupling agents, (Ishida & Koenig, 1978; Plueddemann, 1988; Plueddemann & Stark 1980)). This notion is clearly represented in an illustration from Plueddemann (1988). The formed interphase develops dissimilar physical, chemical and mechanical properties compared to the bulk properties of the fibre and matrix, (Al-Moussawi *et al.* 1993). Ishida & Koenig (1979) and Sung *et al.* (1981) provided interesting findings for γ-methylamino-propyltrimethoxysilane (γ-MPS) and γ-amino-propyl-triethoxysilane, respectively, supporting the case for interdiffusion.

An additional theory is that of electrostatic attraction; if the fibre and matrix display a difference in electrostatic charge, this can assist the attractive forces of bonding, with the charge density dictating

the bond strength, (Kalantar & Drzal, 1990). Though this contribution is minimal, but would take greater responsibility in the presence of a silane, (Plueddemann, 1991)). As reported by Plueddemann (1988), acidic or natural reinforcements bond favourably in the presence of silanes, the degree of success however, is not so common for alkaline surfaces. Mechanical and reaction bonding are among other explanations for how the silane coupling agent interacts with its substrate.

2.4.2 Silane coupling agents and their effect on mechanical properties

Bjorksten and Yaeger (1952) compiled data and found that specific silane treatments of polyester laminates improved wet-strength. Ahagon and Gent (1975) examined failure strength for an elastomer adhered to a glass substrate, via interfacial chemical bonding. The density of the chemical bonds was altered via the treatment of the glass substrate with combinations of vinyl- and ethylsilanes at differing percentages. A synthetic rubber was applied to the silane treated glass substrate and cured *in-situ* by a free radical process. By increasing the portion of the vinylsilane relative to the ethysilane, a proportional increase in adhesion was observed and thus credited to the formation of interfacial bonds to the vinyl groups present on the glass substrate. The examinations were conducted at low rates of detachment and at high temperatures (considered to be near equilibrium conditions). Comparatively the vinylsilane treatment was 35 times stronger than the ethylsilane; covalent and dispersion bond strengths are similar to this difference indicating the presence and functionality of interfacial chemical bonds, (Ahagon & Gent, 1975; Miller & Ishida, 1990).

Wang *et al*. (1999) report findings on the mechanical performance of the fibre/matrix interface of a polymer composite using surface treated reinforcing E-glass fibres. In the case of determining flexural strength and modulus, a three-point bend test was used, conducted under wet and dry conditions. For fracture toughness the mode of fracture used was Mode-I using a compact tension (CT) specimen. The composites with γ-Aminopropyltriethoxysilane (APS) and δ-Aminobutyltriethoxysilane (ABS) treatment showed enhanced flexural strength and modulus. Additionally, the ABS and APS-treated composites demonstrated improved fracture toughness, with critical strain energy release rate (G_c) increasing from 10.5 kJ/m^2, to 14.3 kJ/m^2 and 17.1 kJ/m^2 for the untreated composite, ABS treated and APS treated, respectively. The critical stress intensity factor (K_c) followed a similar trend, increasing from 17.1MN/m$^{3/2}$, to 19.9 MN/m$^{3/2}$ and to 22.3 MN/m$^{3/2}$ for the untreated composite, ABS treated and APS treated, respectively. Keusch *et al.* (1997) compiled data on mechanical performance for E-glass reinforced epoxy uni-directional composites; the reinforcing E-glass fibres were sized with different treatments, and showed similar results to Wang *et al*. (1999). Of interest to the current project, only treatments 1 and 2 will be discussed. Treatment 1 was an amino-silane coupling agent and treatment 2 was unsized/as-

received E-glass. In all the cases of testing UD laminates with coupling agent treatment surpassed the properties of unsized UD laminates for properties: interfacial shear strength, interlaminar shear strength, transverse tensile strength and static longitudinal tensile strength.

For silane treatment, an optimum concentration can be applied to the glass fibre to achieve optimum mechanical properties (Park and Jin, 2001). The issues with pre-treating the fibres in an acidic solution to regenerate silanol groups (Gonzalez-Benito *et al.*, 1999) were not considered; Sever *et al.* (2008) provided research that evaluated the effects of acid activation and silane treatment on the mechanical properties of a glass fibre/epoxy composite. They evaluated mechanical property disparities between differently treated E-glass fabric, formed in a hand lay-up technique with an epoxy resin and hardener: (i) as-received; (ii) heat cleaned E-glass fabric then subjected to γ-GPS (γ-glycidoxypropyltrimethoxysilane) treatment; and lastly (iii) heat cleaned E-glass fabric treated with an acid activation procedure using hydrochloric acid aqueous solution, finally being subjected to γ-GPS treatment. The composites interlaminar shear strength (ILSS) and tensile and flexural properties were determined by ASTM D2344 short-beam analysis, ASTM standard D-3039 tensile test and ASTM D 790 three-point bending test, respectively. The fracture surfaces were examined using a scanning electron microscope (SEM). The composites that were acid activated prior to silane treatment drastically reduced its tensile strength in comparison with the other two conditions. The tensile properties were further reduced with increasing hydrochloric acid concentration. It has been identified acid activation increases the population of silanol groups with an aminosilane, and so provides a better quality 'veneer' of the fibre augmenting the degree of silanization (Gonzalez-Benito *et al.* 1999). The result reported by Sever *et al.* (2008) illustrates the existence of a trade off between the corrosion of the reinforcing fibres receive from being in contact with the acid reducing their mechanical properties, and hence the properties of the overall composite, and the degree of silanization. Small differences were observed between as-received and silane-treated fibres for tensile strength. The notion that composites demonstrate similar behaviour under tensile load is exemplified with all three conditions showing similar properties in tensile modulus. The heat-cleaned E-glass fabric with silane treatment provided the greatest fibre/matrix adhesion increasing its flexural strength, via chemical bonding. As discussed previously, the fibres that received acid treatment produced a significantly weaker composite compared to the other conditions, but this time with regards to flexural strength. ILSS provided similar results that were observed for flexural strength. Heat-cleaned fibres with silane treatment provided enhanced properties compared to the as-received fibres. Acid activated fibres diminished ILSS in comparison to the as-received condition; the cause of this being attributed to loss of fibre strength as a result of being deteriorated chemically. SEM analysis illustrated a higher degree of adhesion for silane-

treated heat-cleaned fibres compared to the as-received fibres, further supporting the results from the mechanical testing. This is determined by large amounts of resin adhering to the fibres surface from fracture. It was observed for the acid activated heat cleaned fibres, interfacial adhesion was also very good with larger and uniform amounts of resin bonding to the fibres surface after fracture. This good interfacial bonding is not relayed to the results obtained from the mechanical testing. The conclusion was that the corrosion to the fibre as a result of acid treatment had a far greater effect on the properties of the composite, therefore consideration must be taken to find a correct balance of acid activation to increase silanization, but not to a concentration that damage to the fibre will outweigh the advantages obtained from the corrosive treatment.

Wu *et al.* (1997) recognised the importance of understanding the interphase region and the adhesion mechanisms occurring, in order to tailor these processes to provide the desired composite properties. The authors pointed out that the basis of interactions that occur is relevant to the glass surface composition, which can be modified significantly with respect to how the fibre is formed and the application method of the sizing. E-glass fibres possess a high concentration of silanol groups on their surface (Thomason and Adzima, 2001) attributed to fibre forming in the presence of water (Feuston & Garofalini, 1990) and so E-glass fibres' isoelectric point (IEP) is relatively low in the range between 3 and 4 (Mader *et al.* 1996). The IEP is the pH of a surface that carries no electrical charge (Wu *et al.* 1997). The IEP indicates the most favourable pH, if this is satisfied for the glass fibre and its silanol groups and of the silanol groups of the coupling agent, they will possess a minimum charge; this facilitates the advancement between one another for hydrogen bonding and siloxane formation (Plueddemann, 1991). Mechanical properties of glass fibre reinforced polyester composites were examined with different silane-treatments. Methacryloxy and amino were the silanes used, with one, two or three Si-0H groups present for each silane. Two different glass compositions were used and produced into unidirectional composite rods, that were subsequently sized and in some cases immersed in boiling water for three days. It was determined that the organic 'tail' of the coupling agent helps to dictate composite properties, characterised by angular-dependent X-ray photoelectron spectroscopy (ADXPS). Appropriate selection of the coupling agents tail group with the resin, was found to improve strength properties of the composite over chemisorption when dry-tested. Though, when the composite was exposed to heat and water it was found that chemisorption played a primary role in maintaining the strength properties of the composite rather than tail group compatibility.

2.4.3 Silane coupling agents and their effect on cure kinetics

Palmese *et al.* (1999) published results concerning glass fibre sizings and their effect on the cure kinetics for a commercial vinyl-ester resin system. Commercial S-2 glass fibres were used, and in

order to identify the composition of their sizings, the fibres were stripped using acetone and then analysed using Fourier transform infra-red (FTIR) spectroscopy. The method of stripping the fibres from the sizing was not efficient. The different sizings were referred to as, 463, 449, 365, and 933 and from the spectra obtained, all showed the presence of "silane-derived silicon", with 463 seeming to have a higher absorption of these functional groups compared to the others. Unbound epoxy also seemed to be present in 463, 449 and 365 when compared to spectra of EPON-828, with no signs of epoxy for 933. Differential scanning calorimetry (DSC) was used for cure monitoring. Using an empirical rate expression, the reaction rate constants found for the filled systems were higher than the "neat" resin. Secondly, thermogram data illustrated quicker cure rates for filled systems during an isothermal cure at 110 °C.

The effectiveness of the coupling agent is in part contributed by specific aspects that can influence their adsorption onto the (glass) surface in question. Provatas, *et al.* (1998) highlight these key aspects as: the solvent used, molecular weight and polydispersity of the polymer, the polymer concentration, time allowed for adsorption, number of reactive or surface interactive groups per polymer molecule, the reaction temperature, the pH in aqueous systems, the type of post-treatment, and the substrate.

Olmos *et al.* (2005) conducted a study comparing two techniques that analysed the curing of an epoxy matrix reinforced with silica microparticles, FT-NIR spectroscopy and fluorescence spectroscopy. The authors used a tagging method that is made possible by tracking the fluorescence response of molecules that can be chemically bonded to the interface. The molecules are known as fluorophores allowing their response to be tracked and thus provide information concerning the cross-linking process. Fluorescence groups were added by tagging only the epoxy matrix and secondly tagging only the interface. Surface treatments in the form of silane coupling agents were applied to the silica particles, these were; 3-aminopropylmethyldiethoxysilane (APDES) and 3-aminopropyltriethoxysilane (APTES). An UV excitable reactive fluorophore was used to tag either the polymer matrix or the interphases of the matrix and filler. The tagging of both areas of interest is necessary, because independent analysis of the cure reactions is required for both regions (the bulk matrix and the interphases of the composite). A 100% conversion process takes place between the reaction of the fluorophore (1-pyrenesulfonyl chloride) and primary amines (Olmos *et al.* 2005). As a result of this reaction it can be inferred, depending on the specific interest, that the part of the molecule accountable for its colour (chromophore) are all chemically bonded either to the bulk matrix or the surface of the particles.

The authors carried out FTIR spectroscopic analysis for a non-tagged sample (APTES-IR), this served to act as a control and so, by comparison, it was determined that the fluorophore in the bulk tagged sample (APTES-B-Py) did not affect the cross-linking reactions. In the interface tagged sample (APTES-I-Py) however the fluorophore was perceived to affect activation energy in comparison with APTES-B-Py; by altering the hydrophilic character of the siloxane coating (APTES), the activation energy was increased.

The spectra obtained from the fluorescence response allowed clear band assignments of the fluorophores. The assigned band at 450-650nm, is regarded as the 'emission from an excited charge transfer complex formed between the amino groups of the coating and the pyrene moieties in the ground estate'. It is this band that experiences a more intense peak when at the interface in comparison to the bulk matrix. This is because; at the interface the silane coating provides an increased concentration of amino groups that can consequently surround the fluorophore molecules. The number of amino groups present in the APTES treatment was more so than for the APDES treatment. And so, the previous claim is further supported, with the 450-650nm band making a greater involvement to the spectrum from APTES results compared to APDES results. It is inferred that the opened structure of APDES compared to APTES, is responsible for the increased effect on the extent of the cure reactions at the interface. Mechanical testing by Hamada *et al.* (1994), determined that APDES treatment was more effective in increasing interfacial strength than APTES surface treatment in glass fibre reinforced epoxy composites. These findings indicate that because APTES treatment deposits a more concentrated area of amino groups at the interface it can permit augmented siloxane cross-linking reducing the composites interfacial strength. Hamada *et al.* (1994), postulate that this cross-linked structure acts as a barrier restricting further reactions between the epoxy matrix and silane organofunctional groups, which are also in agreement with Iglesias *et al.* (2002). It can therefore be assumed, the APDES treatment can participate in interpenetration with the matrix resin more readily.

Results reported by Lenhart *et al.* (2000), Palmese and McCullough (1994) and others, motivated Gonzalez Benito (2003) to investigate further, the differences in cure kinetics from the glass-fibre surface to the bulk epoxy/amine matrix. The angular distance of the points of the microscopic areas of interest was measured using a novel FTIR imaging technique; this being a single glass fibre impregnated with the polymer system between two salt plates (CaF_2). The epoxy peak at 915 cm^{-1}, is traditionally a popular band to use for conversion in cure analysis, however due to signal-to-noise issues making analysis of the band inconclusive, the changes in the OH band was used as an alternative. The cure of the polymer system (at room temperature) derived from the technique was

perceived to be similar to those obtained via more conventional techniques (Gonzalez-Benito *et al.* 2001), and thus supporting the choice of the OH groups as the band of interest. The IR absorption illustrated the existence of a structural gradient between the glass-fibre surface and bulk epoxy. As expected for all locations, the OH absorbance increased, though this increase was more pronounced at the bulk (than at the fibre surface) of the resin system during cure. The increased OH absorbance indicates faster cross-linking kinetics at the bulk matrix, hence contributing to the structural gradient that exists (Mikes *et al.* 2001). Also noticeable, was that at the beginning of cure there was a higher concentration of hydroxyl groups present at the interface compared to the bulk; this was due to water molecules being absorbed by the silanol groups present at the glass fibre surface (Gonzalez-Benito *et al.* 1999;1996). The concentration of active amine is perceived to be more predominant at the glass-fibre interface, increasing the cross-linking rate with distance from the glass fibre. Two probable causes for the increased fraction of amine groups were proposed: (i) favourable interactions between the amine groups and OH groups (of the fibre surface); and (ii) the smaller molecules of the amine hardener, can diffuse with more efficiency through the silane layer than the larger molecules of the epoxy.

It has been established that the cross-linking of a resin system can be affected by the presence of a silane coupling agent. Generally, the silane will be present at the interface between the reinforcement and the resin matrix (as a surface treatment to the reinforcement) and so cross-linking is more likely to be affected at the reinforcement interface than towards the bulk resin matrix. For example, if an APS treatment is used on glass fibre in an epoxy matrix, it would be expected that the increased concentration of amino groups would increase cross-linking.

2.5 Surface characterisation

To understand the mechanisms that occur at the interface, characterisation techniques are required. The enormous scope of the type of bonding that can transpire, obviously points out that the 'interface' is specific to the 'fibre-matrix system', (Kim & Mai, 1993); this statement demonstrates the complexity of characterisation and the need for it. Surface characterisation is important for this research, as it is essential to determine the interactions according to the surface chemistry of as-received and treated E-glass fibres, and the epoxy/amine resin. Defining the sizing layer composition and distribution, the fibre sizing molecular interactions, gradients and microphases in the fibre surface composition, can help to assist with predicting and controlling the influence of coatings/sizes on processability and composite performance (Thomason and Dwight, 1999).

2.5.1 Atomic force microscopy

Atomic force microscopy (AFM) was first patented in 1986 after the invention by Binnig *et al.* (1986), revolutionising analysis at the nanoscale. The principle behind this type of microscopy relies on a 'tip' in a cantilever system to experience attractive and repulsive atomic forces via interaction with the surface of interest, thus replicating a 3-dimensional topographical image. The cantilever traverses the samples surface detecting short-range chemical forces, van der Waals forces and electrostatic forces, consequently the motion of the cantilever is detected by reflecting a laser off the back of the cantilever to a photo detector (Yongho & Wonho, 2008).

There are frequently used variations on the AFM with respect to the modes that can be used and the different ways of accurately detecting the cantilevers motion. As previously mentioned Binnig *et al*. (1986) developed the first AFM that functioned in 'contact' mode (tip/sample interaction). Martin *et al*. (1987) extended this approach introducing the 'non-contact' mode, where the distance between the tip and sample is of a very small magnitude (tens to hundreds of angstroms) and the cantilever oscillates close to its resonant frequency. Typically, the tip is opposed by the van de Waals forces causing a change in its vibrating amplitude, this change is identified and measured as a force gradient which signifies variations in the tip to sample distance, that can finally be depicted as a topographical image. Such that the forces between the tip and sample are low, it makes this technique extremely desirable for softer samples. Zhong *et al.* (1993) provided the next major development in AFM, presenting the 'tapping' mode (also known as intermittent contact AFM), a very similar method to Martin *et al.* (1987) with one fundamental difference. The difference is explained in the name 'tapping', as the oscillating tip is situated nearer to the sample allowing the tip to periodically touch (tap) the sample. Tapping mode AFM has become an important and

established technique, by eliminating the restrictions associated with non-contact and contact mode AFM (Eaton, 2010).

Griswold *et al.* (2005) adsorbed γ-aminopropyltrimethoxysilane (APS) at different weight percentages onto the surface of optical glass fibres before embedment into a polymer matrix. The possible effects the silane had on the formed interface were interpreted using AFM and nano-indentation. Care was taken to clean the fibres thoroughly, as a clean substrate is of paramount importance to classify that the surface treatment is known. APS was adsorbed onto glass fibres from 0, 0.1, 1.0, 3.0 and 5.0 wt% aqueous solutions. After treatment the fibres were immediately embedded into an epoxy adhesive (trade name Hysol 608) which was subsequently cured for 24 hours. To characterise the interphase region using AFM, the sample was firstly prepared by microtoming. Microtoming is a common technique used to obtain thin slices of polymer for microscopic examination and was chosen because it was understood physical and chemical alterations of the surface were less likely for this technique when compared to conventional polishing techniques. Microtoming allows for the production of a very flat surface, keeping height differences between the phases (matrix, interphase and fibres) to a minimum. The AFM used to carry out imaging was a Nano Scope IIIa; tapping mode was selected, with light tapping being applied to locate an appropriate region for hard tapping to then be employed to obtain the true topographic nature of the interphase. To acquire accurate images, a scan speed of less than 1 Hz was used, to prevent the tip from jolting as it scanned perpendicular to the fibre at the fibre-matrix interphase. Once the interphase region of interest was located, its width can be established ready for nano-indentation with the chosen area possessing no debonding, pits, debris and voids. Indentations were applied at a force of 16 μN, with several indents performed on a sample with identical parameters. Tapping mode was implemented again to capture the topographic image of the indents, enabling the authors to confirm their location. The captured images allowed interphase thickness to be calculated, taking numerous measurements on separate fibres to establish “the statistical distribution of the interphase thickness”. Increasing APS concentration provided very clear results of augmented interphase thickness. To an extent, modulus of the imaged region can be inferred with the interphase regions in the authors’ captured images appearing darker in contrast to the matrix; when the tip experiences a softer surface (in this case the interphase) a shift in drive frequency transpires, as a consequence of the tip requiring increased energy to keep it a constant amplitude. All interphase regions were determined softer than the bulk matrix; this was further supported via the nanoindentation results.

Gao and Mader (2002), studied unidirectional E-glass fibre reinforced epoxy composites imaging the topography of the samples via AFM in tapping mode, as well as an indentation technique to measure mechanical responses. The authors provided contradictory results to those found by Griswold *et al.* (2005). Phase imaging was also conducted in conjunction with the scanning in tapping mode, which distinguishes variances in material properties over a selected area. The authors found that the modulus of the bulk matrix was of no significant difference to the interphase's modulus, in the case of the unsized fibre/epoxy sample. This suggests that the epoxy matrix cannot form a significant interphase with unsized glass fibres. The E-glass fibres sized with APS/PU however, did show a property gradient between the bulk matrix and reinforcing fibre. The authors define the interphase as a region with a modulus being 10% greater than the matrix modulus; on that condition they determined the interphase thickness to be 300 nm. The amine curing agent was suggested to migrate and preferentially diffuse into the silane sizing; as a consequence an amine-rich region is formed next to the glass fibre. The increased amine concentration influenced the chemical interactions holding it responsible for the property gradient. The modulus of the interphase decreased with increasing distance from the fibre surface. Correlation can be assigned to the fact that an increased concentration of amine at the fibre surface, will completely satisfy the number of epoxy groups and increase cross-link density; in addition the sizing layer will directly react with the epoxy providing strong interfacial adhesion.

Liu *et al.* (2008) provide research with AFM in tapping mode, investigating the interaction of γ-Aminopropylltriethoxysilane (APS) with E-glass fibre surfaces. Surface topography was examined for differently treated E-glass fibres: (i) APS coated; (ii) warm water extracted and (iii) hot water extracted. The extent of removal of the silane layer was increased incrementally; warm water was used to extract the physisorbed silane deposit, with hot water extracting the chemisorbed silane deposit. Images were obtained in air using an etched silicon probe cantilever, oscillating at a nominal resonant frequency of 300 kHz. A 1 µm by 1 µm image was captured at a particular location on the surface of the differently treated fibres; the images were not illustrated in 3-D format, but colour shading indicated the depth of troughs and peaks, the brightest points indicating depth of 5 nm. The application of a silane coating created a multifarious surface topography. There is a disordered array of peaks and troughs, with a height variation of less than 6.4 nm, caused by remaining hydrolysed APS molecules (Liu *et al.* 2008). The warm water extracted treatment reduced the height variation to less than 4.5 nm, providing a more consistent topographical structure. Before water extraction the surface topography consisted of both physisorbed and chemisorbed silane deposit, this is observed in the more complex surface nature in the AFM image. A more ordered structure (but still heterogeneous in nature) was visible after warm water extraction, with the

removal of the physisorbed residue revealing the chemisorbed layer. After hot water extraction, it has been suggested that of the chemisorbed silane deposit, at the ends of the crosslinked network, the randomly coiled chains are extracted hydrolytically; hence the induced development of “pits” or “pores” observed in the AFM images.

AFM has proven a useful tool to study surface topography at the nanoscale. Different surface treatments to glass fibres can be characterised depending on the surface texture generated by that particular treatment (Gupta *et al.* 2000). It is of agreement that increasing silane concentration to the glass fibre surface increases the interphase thickness, however the effect the silane has at the interface has been disputed. For example, APS inhibits the curing of the epoxy contributing to a softer interphase (Griswold *et al.* 2005), whereas Gao and Mader (2002) believe the increase in concentration of APS, increases the number of available amines to cross-link with the epoxy molecules enhancing the modulus. The next chapter describes the experimental procedures taken to help establish and reinforce existing findings, as well as potentially providing new ideas.

Chapter 3

3. Experimental

3.1 E-glass fibre bundles

Continuous un-sized electrical grade glass fibre bundles were used as the light guiding material, supplied by PPG Industries (UK). Approximately 2500 individual fibre filaments constituted the fibre bundle (Fig. 3.1), with each filament consisting of an approximate diameter of 15 ± 3 µm. The refractive index of the E-glass preform was 1.56 and was measured at 589.6 nm and 20 °C. To facilitate inter-connection between equipment, the ends of the bundle were potted into sub-miniature A-type (SMA) connectors using a lower refractive index resin (EPO-TEK® 314 (Promatech Ltd)), which was subsequently cured at 120 °C for 3 hours. The potential for light transmittance and absorption of the fabricated sensor was optimised by polishing the potted ends using an APC 8000 polisher (SENKO Advanced Composites Ltd).

Figure 3.1: Photograph of an E-glass fibre bundle potted into a pair of sub miniature A-type (SMA) connectors.

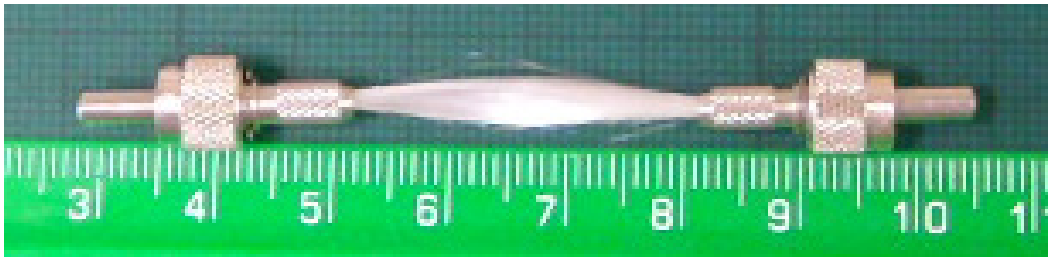

3.2 Epoxy/amine resins system

3.2.1 LY 3505/XB 3403

Araldite LY 3505 supplied by Huntsman Advanced Materials was one of two resin systems used for cure monitoring in this study, which is a Bisphenol A/F epoxy resin. The hardener used for the experiments was the XB 3403 (polyoxypropylene diamine), also provided by Huntsman Advanced Materials. The two substances, LY 3505 and XB 3403 were weighed at the stoichiometric ratio of 1:0.35, respectively. The two components were then mixed thoroughly and consequently degassed in a vacuum chamber at -20 in Hg for approximately 15 minutes. During the transmission experiments the mixed resin and was cured at 40 °C, 50°C, 60°C and 70°C for 1200, 900, 400 and 500

minutes, respectively. During the EWS experiments the mixed resin was cured at 40 °C, 50°C, 60°C and 70°C for 64, 52, 60 and 50 minutes, respectively.

3.2.2 EPO-TEK 310M®

With reference to the EWS experiments, it was necessary to use a resin system whose refractive index was lower than that of E-glass. The resin system used in the current study with E-glass was a two-component resin system, EPO-TEK 310M® (Promatech Ltd, UK); the resin and hardener were weighed out to give a stoichiometric ratio of 1:0.55 (epoxy:amine). The components were mixed and degassed in the same way as described previously. The refractive index of the resin system was 1.50. During the transmission experiments, the mixed resin was cured at 35°C, 45°C, 55°C and 65°C for 900, 500, 300 and 200 minutes, respectively. During the EWS experiments, the mixed resin was cured at 35°C, 45°C, 55°C and 65°C for 900 minutes.

3.3 Silane treatment

The coupling agent used in this study was 3-glycidoxypropyltrimethoxysilane (GPS) (Sigma-Aldrich, UK) and was used as-received. A 0.1 wt% GPS solution was prepared using a mixture of ethanol and distilled water (4:1) and the pH was adjusted to 4 using acetic acid. The exposed portion of fibre bundle (Fig. 3.1) was immersed in this solution for one hour at room temperature. After this period, the solution was drained and the fibre bundle was dried at room temperature for two hours. Subsequently, the silane-treated fibre bundle was dried in the oven at 100 °C for three hours. 0.5, 1 and 3 wt% silane solutions were also prepared in a similar manner and applied to the E-glass fibre bundles.

3.4 Cure monitoring: conventional transmission spectroscopy

Spectra were collected during cross-linking from 1100 to 4000 cm^{-1} via a Bruker MATRIX™ -F duplex FT-NIR spectrometer (Bruker Optics Ltd, UK) at a resolution of 4 cm^{-1} and with 64 scans. A CUV-TLC-50F temperature-controlled cuvette holder (± 0.02 °C) (Ocean Optics Inc., Netherlands), accommodated a demountable optical glass cuvette with a path length of 1 mm (Starna, UK). A syringe was used to dispense the mixed resin system into the glass cuvette. With reference to Figure 3.2a, two low-OH optical fibre probes were used to deliver and collect light from the spectrometer's housed light source and InGaAs detector.

Figure 3.2: The experimental set-up for: (a) conventional transmission spectroscopy and (b) evanescent wave spectroscopy.

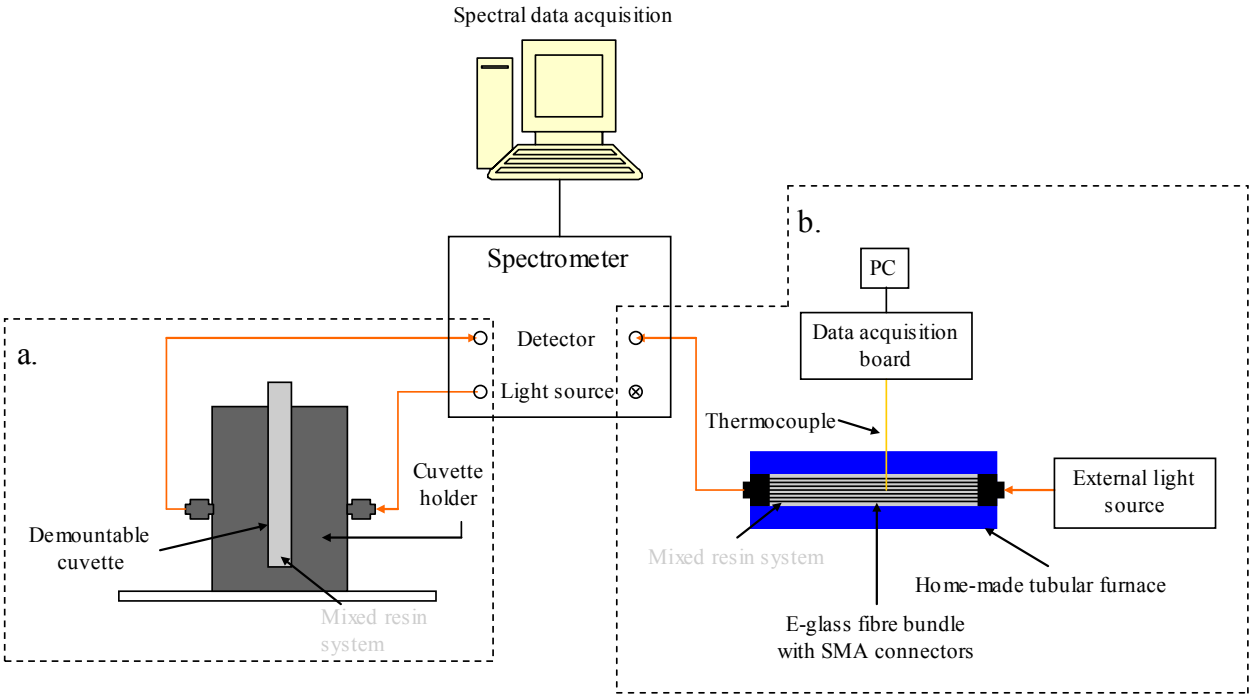

3.5 Cure monitoring: evanescent wave spectroscopy

The Bruker Optics Ltd spectrometer (used with the conventional transmission FTIR spectroscopy) was used to acquire spectra during the cross-linking. Spectra were obtained over 128 scans instead of 64 scans. This was necessary because of the poorer transmission characteristics of the E-glass. An external white light source, WLS100 (Bentham Instruments Ltd., UK) was used to illuminate the glass fibre bundle. The fibre bundle with the SMA connectors (Figure 3.1), were impregnated thoroughly with the degassed resin system. The fibre bundle was secured in a custom-made oven and maintained at the required isothermal temperature (± 0.2 °C). Prior to any experiments being undertaken, the oven was calibrated by using a thermocouple; the thermocouple was then used to monitor temperature and provide temperature control during the curing of the resin system. Fig. 3.2b illustrates the experimental set-up.

3.6 Cure monitoring: Fourier transform infrared – Attenuated total reflection spectroscopy

A Nicolet Magna-IR 850 Fourier transform infra-red attenuated total reflectance (FTIR-ATR) spectrometer equipped with a DTGS KBr detector was used to collect cure kinetic data of the resin system. Spectra was collected in the mid infra-red range (700-4000 cm^{-1}) at a resolution of 4 cm^{-1} and with 100 scans. Before commencing a cure reaction a background spectrum was taken and this was subtracted from the subsequent spectra collected over 350 minutes. A thermocouple was used for temperature control.

3.7 Surface characterisation

3.7.1 Atomic force microscopy

A Digital Instrument D 3100 scanning Probe Microscope was used to perform AFM of GPS treated E-glass fibres operating in the tapping mode. Tapping mode reduces the chances of scraping and thus practically eradicates any lateral force, secondly low forces are used which reduces damage to softer samples imaged in air and lastly, higher lateral resolution was expected (compared to contact mode). Images were acquired at room temperature in air using a tapping mode silicon probe (MPP-1110) cantilever with a tip radius of 8 nm. The spring constant of the cantilever (k) was 40N/m and the nominal resonant frequency was 300 kHz.

Chapter 4

4. Results and discussion

4.1 Cure monitoring: LY3505/XB3403 resin system

4.1.1 Comparison: transmission and evanescent wave spectroscopy

Figure 4.1 compares the transmission and evanescent wave absorbance spectra at the start of the cure reaction. The spectra were obtained using the LY3505 and XB3403 epoxy resin system that was cured at 70°C. The relevant peaks are highlighted in Figure 4.1. Both techniques are in agreement with the peak assignments; the primary amine, CH and epoxy peaks are assigned to the absorbance peaks at 4900 cm^{-1}, 4600 cm^{-1} and 4500 cm^{-1}, respectively. These findings were apparent for all temperatures. A summary of the peaks of interest in Figure 4.1 are summarised in Table 4.

Figure 4.1: Absorption spectra of LY3505 and XB3403 via transmission and evanescent wave spectroscopy.

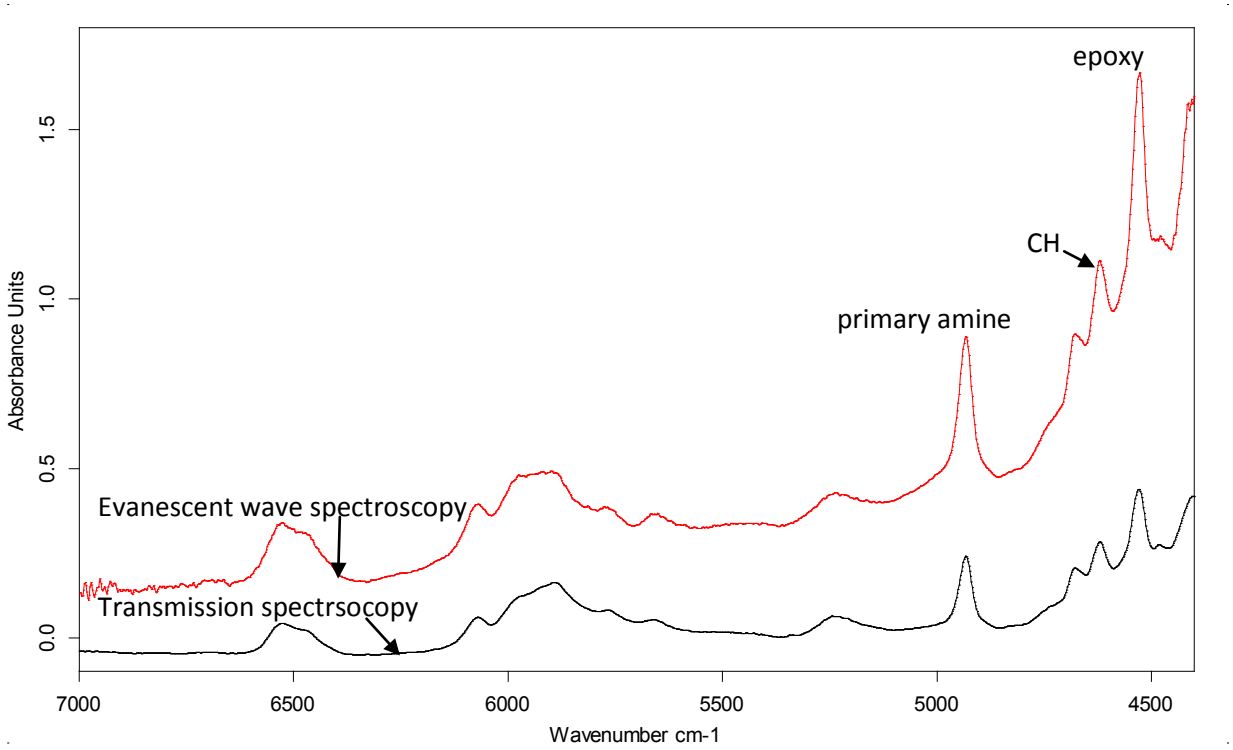

Figures 4.2 and 4.3 illustrate the spectra obtained for the LY3505/XB3403 resin system at different times of cure, at 70 °C via transmission and evanescent wave spectroscopy, respectively. In both cases, the primary amines peak area can be seem to decrease during cure, owing to its involvement

in the primary epoxy-amine addition reaction (Barton, 1985). This is also evident for the epoxy peak and its decreasing area as a function of time (Mijovic and Andjeli, 1995). The CH absorbance peak stays constant, as it does not participate in the cross-linking reactions. During the amine-epoxy reaction, the CH band at 4600 cm^{-1} is not consumed and can therefore be exploited as an internal standard to normalise the epoxy absorbance band (Figure 4.7). The subsequent conversion plots illustrated throughout this chapter were calculated using Equation (16). Percentage consumption for the epoxy peak (or amine peak) as a function of time can be calculated as follows:

$$\alpha_x = 1 - \frac{(A_x / A_{C-H})_t}{(A_x / A_{C-H})_0} \tag{16}$$

where is the conversion of reacting group (amine or epoxy), A_x is the area of the absorption peak, $A_{C\text{-}H}$ represents the area of the reference C-H peak, *t* and *0* are the cure time t in minutes and the start of the cure, respectively.

Figure 4.2: Spectra obtained at 70 °C during cure of the LY3505/XB3403 resin system attained using transmission spectroscopy.

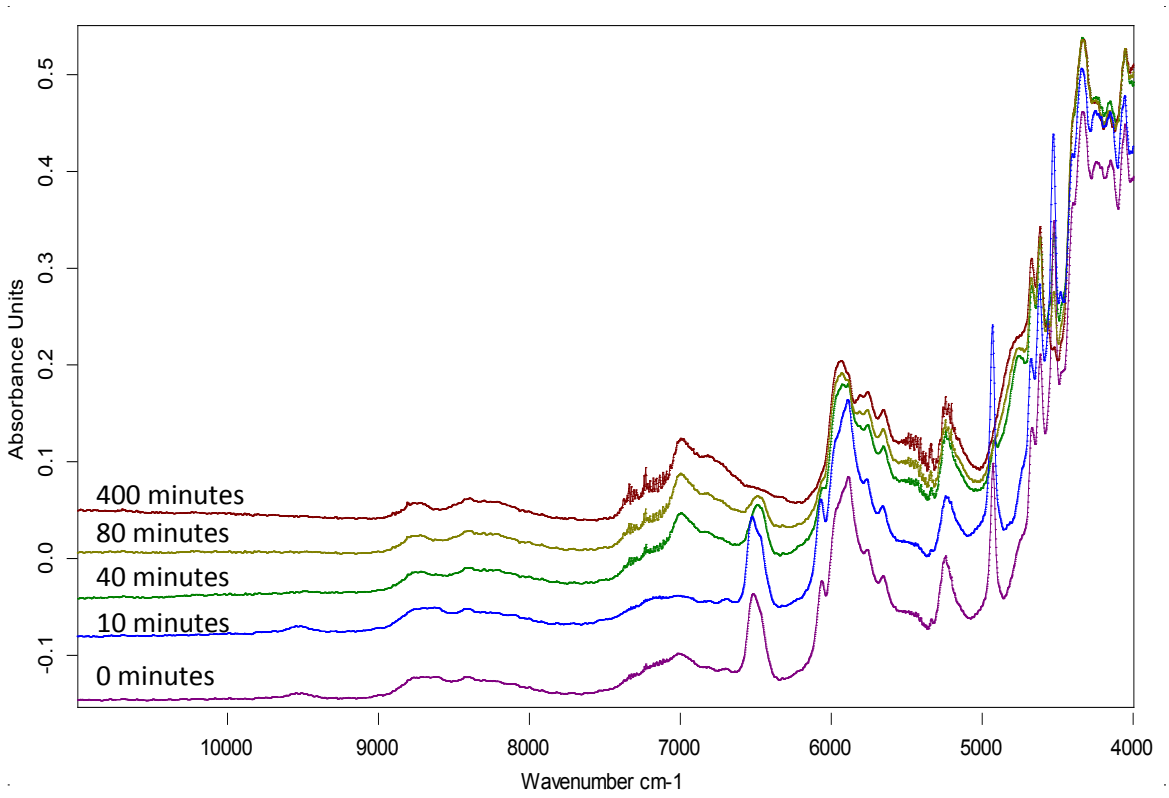

Figure 4.3: Spectra obtained during the cure of the LY3505/XB3403 resin system via evanescent wave spectroscopy showing different times of cure at 70°C.

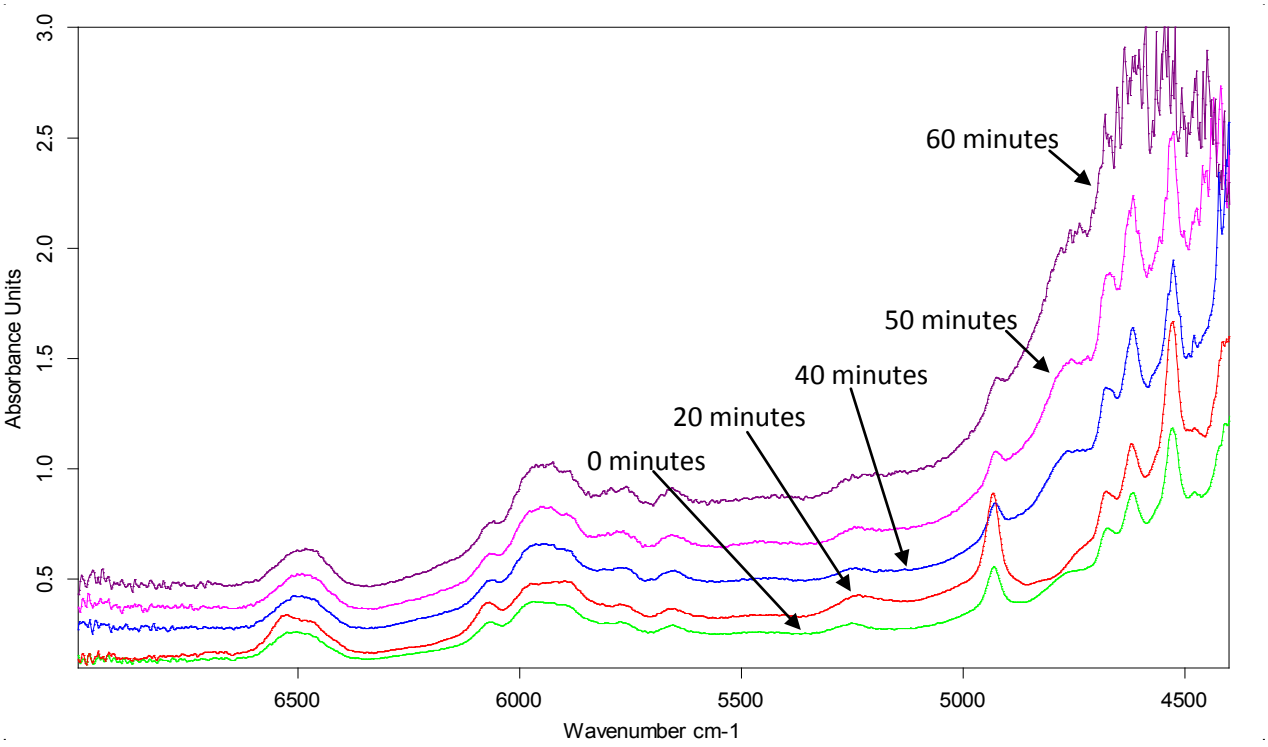

To determine the effectiveness of the of E-glass fibre bundles as light-guides for monitoring the cross-linking reactions via evanescent wave spectroscopy, conversion plots of the absorption of the epoxy functional groups were compared with the conventional transmission spectroscopy technique; isothermal cure experiments at 40, 50, 60 and 70 ^{o}C are illustrated in Figures 4.4a, b, c and d respectively. The evanescent wave spectroscopy experiments were repeated three times.

Figure 4.4: Comparison of the conversion data for the depletion of the epoxy functional groups using transmission spectroscopy and evanescent wave spectroscopy in the LY3505 and XB3403 epoxy resin system at 40, 50, 60 and 70 °C.

a) 40°C

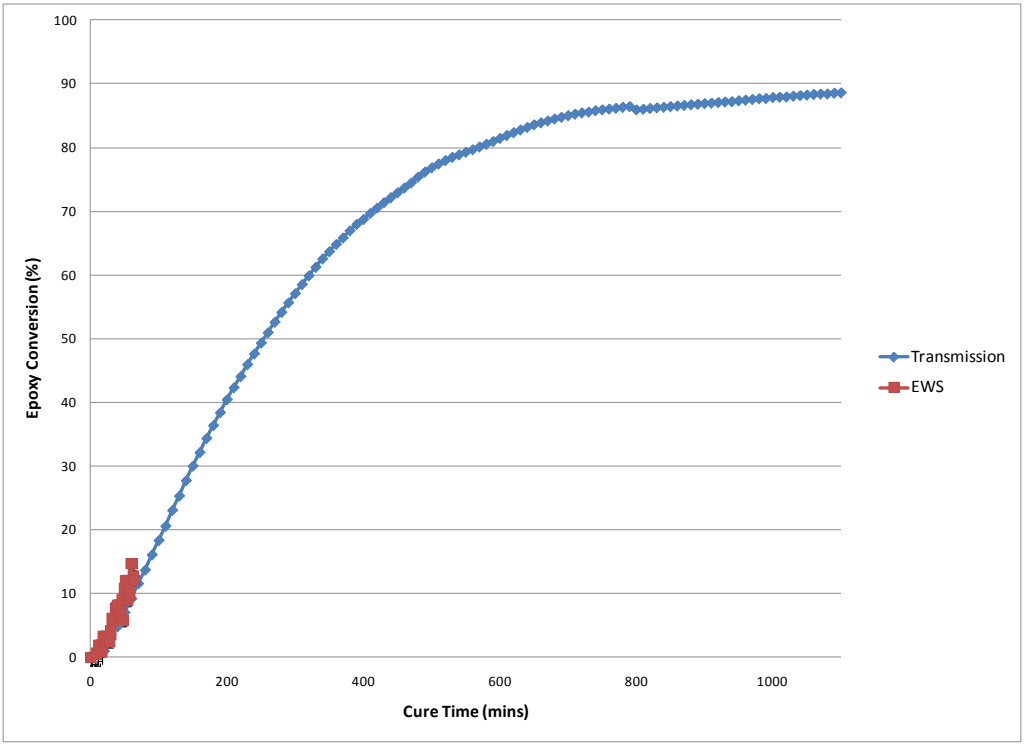

b) 50°C

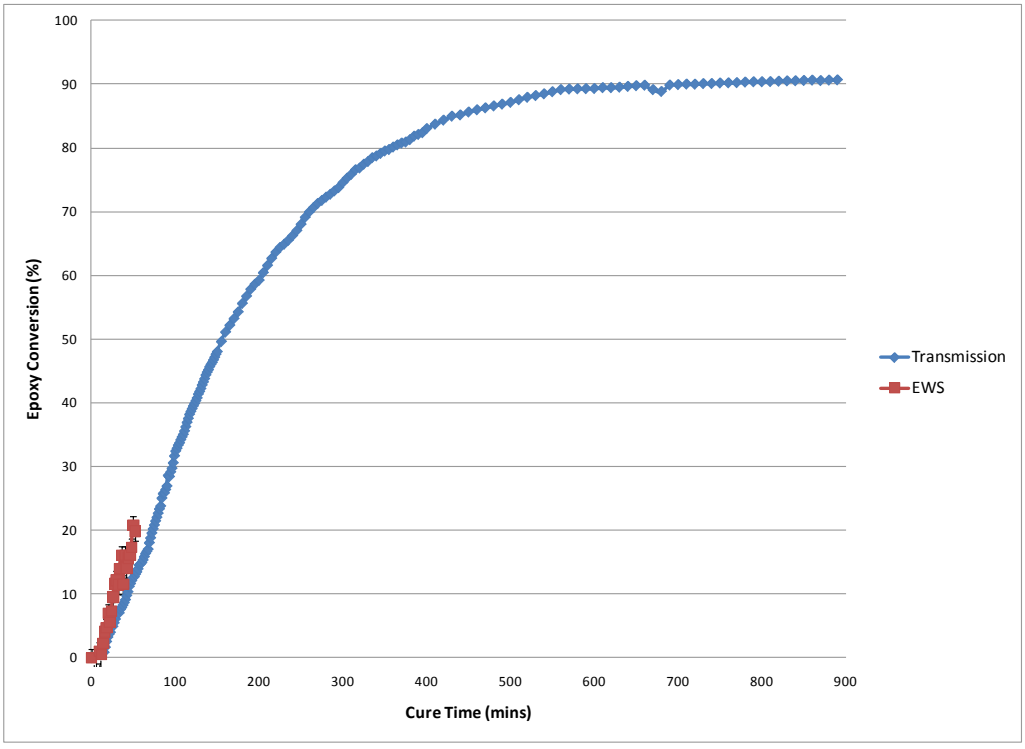

c) 60°C

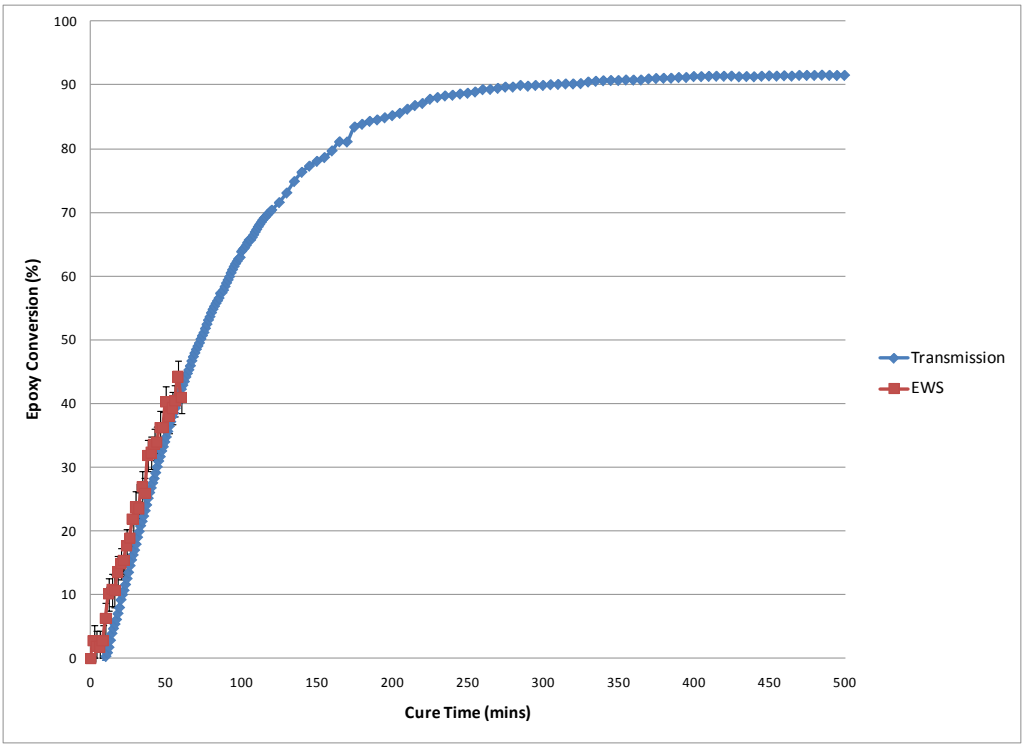
Epoxy Conversion (%)
Cure Time (mins)
Transmission
EWS

d) 70°C

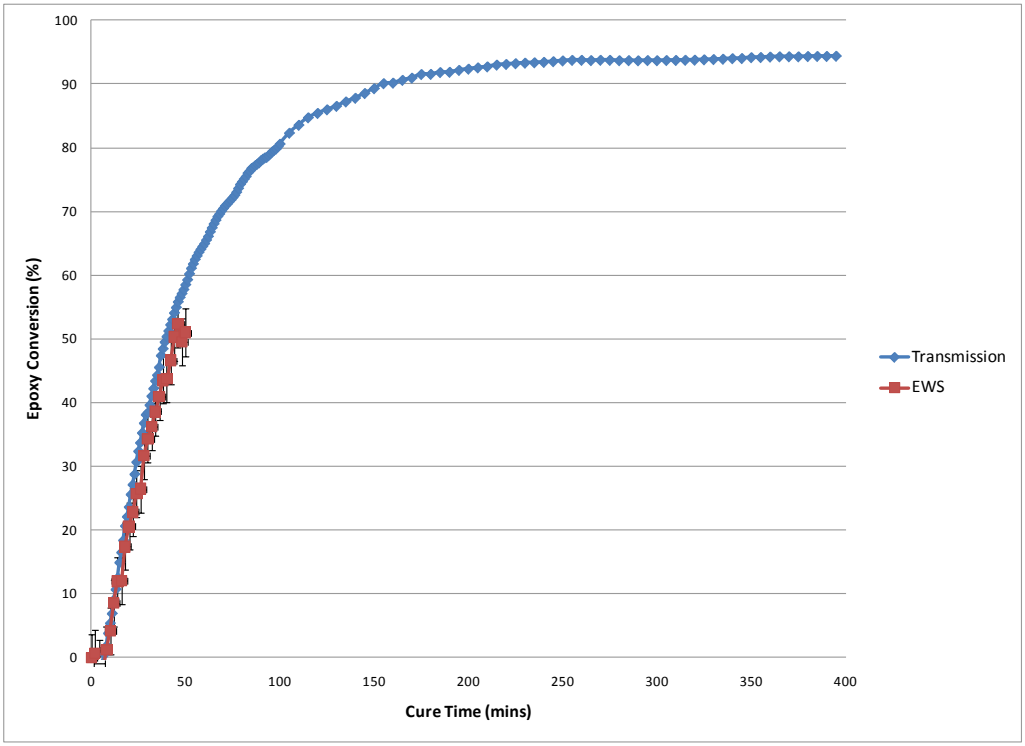
Epoxy Conversion (%)
Cure Time (mins)
Transmission
EWS

Results obtained from the LY3505/XB3403 resin system (Figure 4.4) demonstrate clearly the potential of using reinforcing E-glass fibres as sensors to monitor cross-linking kinetics. Agreeable trends are seen for all conversion plots, albeit they can only be compared at the initial stages of reaction. The higher temperatures of 70 and 60 ^{o}C show better correlation than 50 and 40 ^{o}C, nevertheless an obvious trend is still present for all temperatures. The observed differences may be attributed to the variations in the temperature profile in the two experimental set-ups. It is also worth noting that at the initial stages of cure the epoxy groups are consumed at as a faster rate as the temperature of cure is increased. With respect to the EWS results, error bars were calculated from the standard deviation of the mean conversion of three repeat experiments for all four temperatures.

As mentioned above, the conversion plots only provide data of the initial 60 minutes of the reactions, clearly illustrated when compared to the transmission results. By observing the spectra (Fig. 4.3), a shift in baseline of the spectra illustrates a changing refractive index of the resin; the cross-linking of the uncured resin as the cure proceeds increases the refractive index. This transformation of the liquid resin reduces the signal transmittance of the E-glass fibre sensor as the refractive index of the resin approaches the refractive index of the E-glass fibre. The following equation provides a value that represents a fibre's ability to transmit light, known as the numerical aperture (NA):

(17)

where is the refractive index of the E-glass fibre (fibre core) and is the refractive index of the resin (cladding). is the half-angle of the acceptance cone known as the acceptance angle; light accepted within a certain cone allows the propagation of light through the fibre. The varying refractive index of the cladding will cause a variance to the value of , consequently affecting the critical angle within the fibre and affects the fibre's transmission capabilities. Thus, spectral collection ceases at 60 minutes as the refractive index of the resin reaches that of the E-glass fibre, preventing total internal reflection. EWS can be used up to a certain point for commercially available resins. Further research was undertaken using a resin system with a lower refractive index (EPO-TEK 310M®) to monitor the resin system throughout the whole cure cycle.

4.2 Cure monitoring: EPO-TEK® 310M resin system

4.2.1 Comparison: transmission and evanescent wave spectroscopy

Again, in order to confidently make appropriate conclusions concerning the cure kinetics using this EWS method, the spectra obtained in the near- infrared region of the EPO-TEK® 310M resin system must be compared to the conventional transmission spectroscopic technique to validate its use as a reliable cure monitoring technique (Figure 4.5). On comparing the spectra, both of the spectral acquisition methods yield similar absorbance characteristics. It must be noted that the quality of the EWS spectra is hindered to some extent, due to a lower signal throughput; nevertheless in the future this is negligible and can be rectified by employing a more powerful light source. Characteristic absorbance peaks have been identified for the EPO-TEK 310M resin system; the peak at 6500 cm^{-1} corresponds to the primary and secondary amine overtones. As a result of the primary amines involvement with the epoxy group, a carbon-oxygen bond is broken, consequently producing a secondary amine which further reacts with the epoxy. The advancement in the reactions lead to the depletion of the primary and secondary amine groups, which is illustrated agreeably by the gradual decrease of the absorbance peak at 6500 cm^{-1} during cure with respect to time (Figure 4.6). The initial epoxy-primary amine reactions that take place can be attributable to the rapidly decreased primary amine absorbance peak at 4935 cm^{-1} (Figure 4.6). The conversion percentage calculation of the active functional groups absorbance peaks involvement in the cross-linking reaction relies on normalising these peaks to a functional group that does not participate in the cross-linking reactions. Situated at 4600 cm^{-1} is the C-H stretching vibration of the aromatic ring; its peak area stays the same during the cross-linking reactions as a function of time (Figure 4.6 and 4.7), justifying its use as an internal standard.

Figure 4.5: Absorbance spectra of EPO-TEK® 310M are shown to be identical for both transmission spectroscopy and evanescent wave spectroscopy.

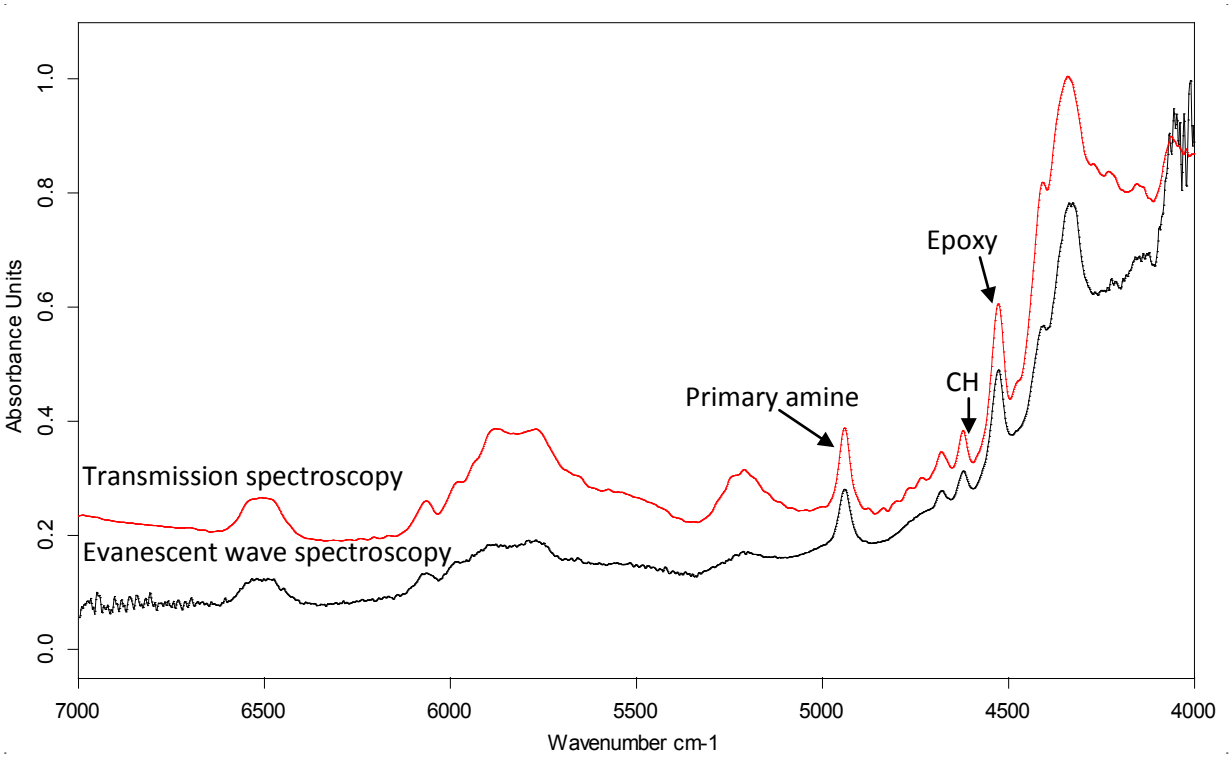

Figure 4.6: Spectra of EPO-TEK® 310M attained using evanescent wave spectroscopy showing different times of cure at 65 °C.

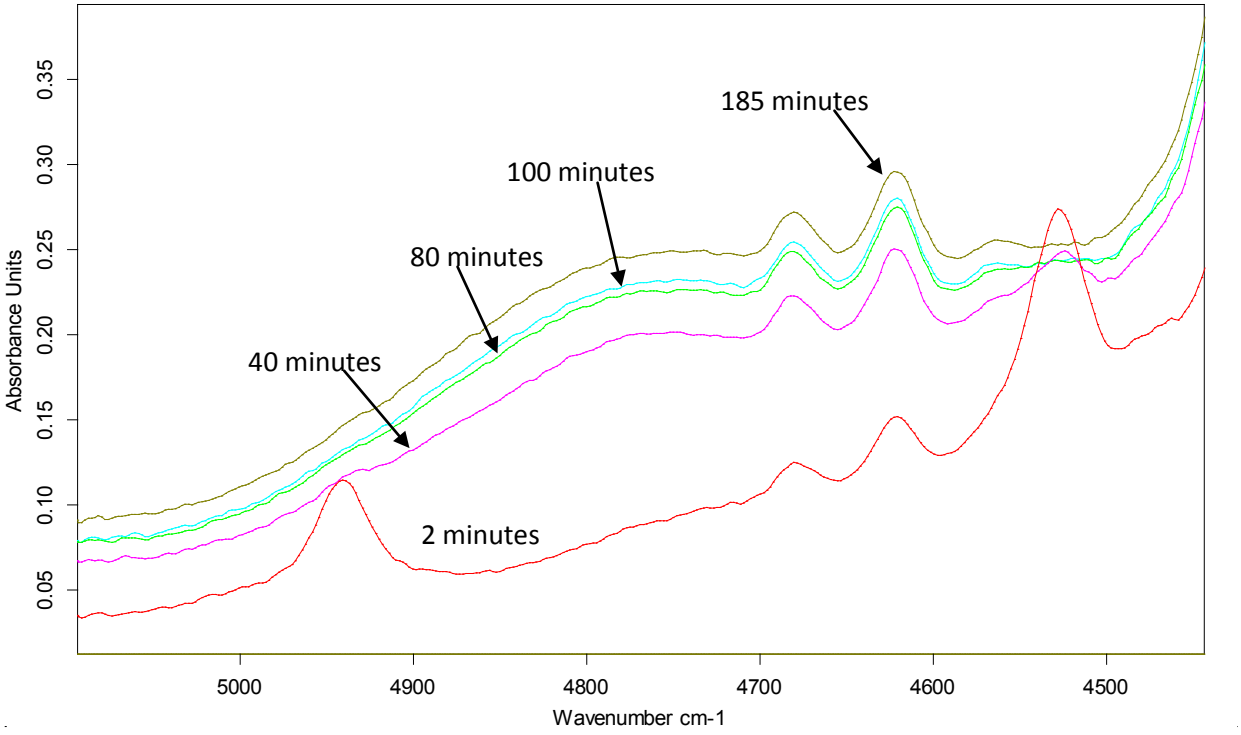

Figure 4.7: A comparison between the integrated areas of the CH and epoxy peak with respects to cure time, demonstrating their different involvement in the cure reactions of the EPO-TEK® 310M resin system.

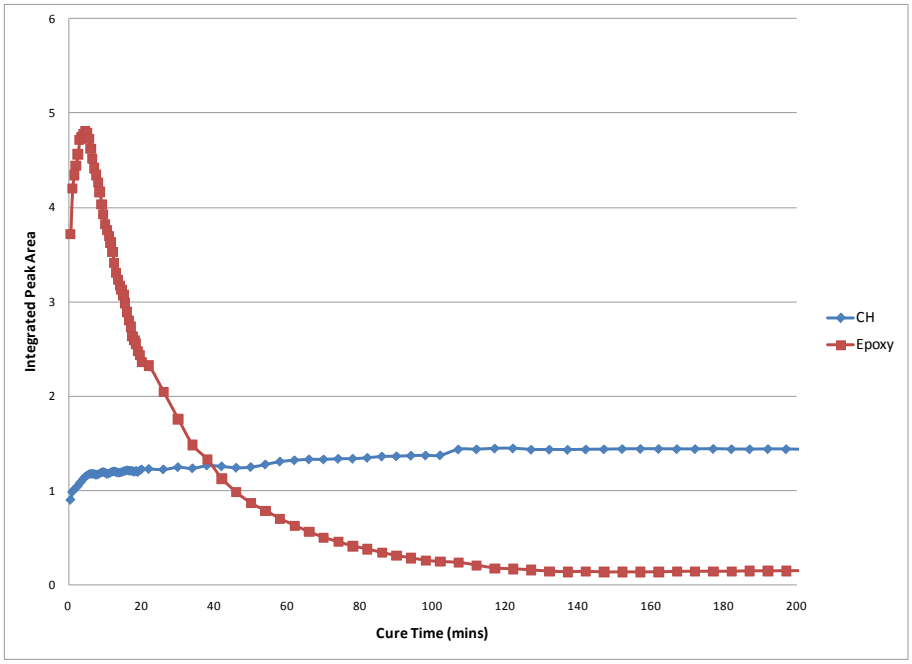

The epoxy and primary amine absorbance bands were chosen to allow comparison between transmission and evanescent wave spectroscopy data. From the conversion plots, Figures 4.8 and 4.9, there are two main regions evident: firstly, the initial stages of cure see a rapid reaction rate credited to the cross linking reactions taking place, the 2nd region concerns the later stages of cure where the curves plateau, this observation is thought to be controlled by the diffusion of reactants (Olmos *et al.* 2005). From the conversion plots, both epoxy and amine functional groups rate of consumption increases with increasing cross-linking temperature. This can be attributed to the collision theory (Hill and Holman, 2000), at higher temperatures higher energy collisions are possible between the functional groups, providing they possess at least the activation energy for the reaction. The increased temperature enhances the mixing of the amine-cured epoxy, thus enhancing the functional groups' interaction with one another, increasing the rate of consumption (Hong and Wang, 1994). A marginal increase in the percentage of epoxy groups consumed is also evident at increased cross-linking temperatures (Figure 4.8). The epoxy functional groups were consumed in the cross-linking reactions at a slower rate than the amines consumption in the reactions (Figure 4.8 and 4.9). Good repeatability of the experiments is illustrated by the error bars (Figure 4.8 and 4.9); the error bars were calculated using the standard deviation of the mean results from three repeated experiments (for both transmission and evanescent wave spectroscopy experiments).

Figure 4.8: Comparison of the conversion data for the depletion of the epoxy functional groups using transmission spectroscopy and evanescent wave spectroscopy in the EPO-TEK 310M epoxy resin system at 35, 45, 55 and 65 °C.

a) 35°C

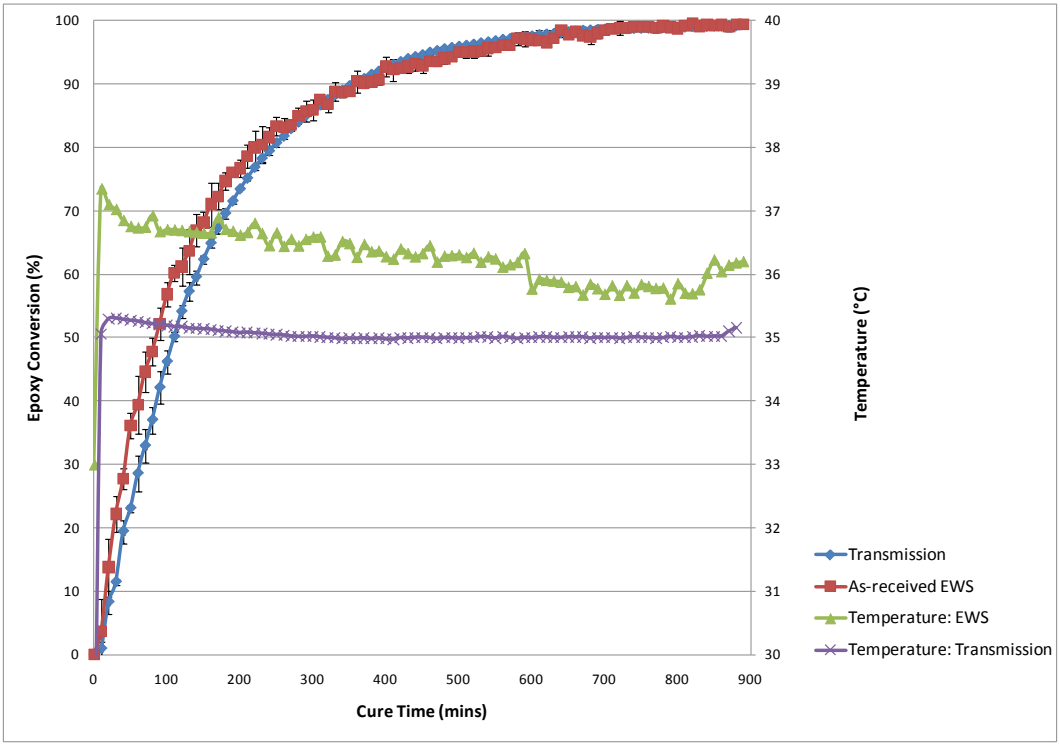

b) 45°C

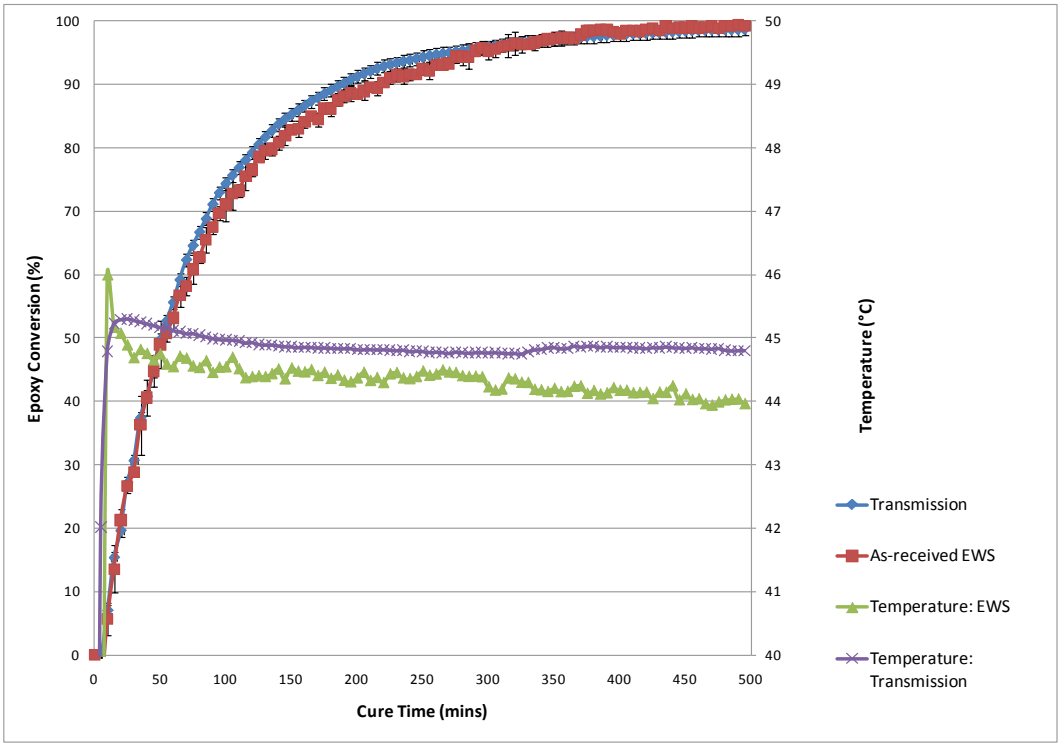

c) 55°C

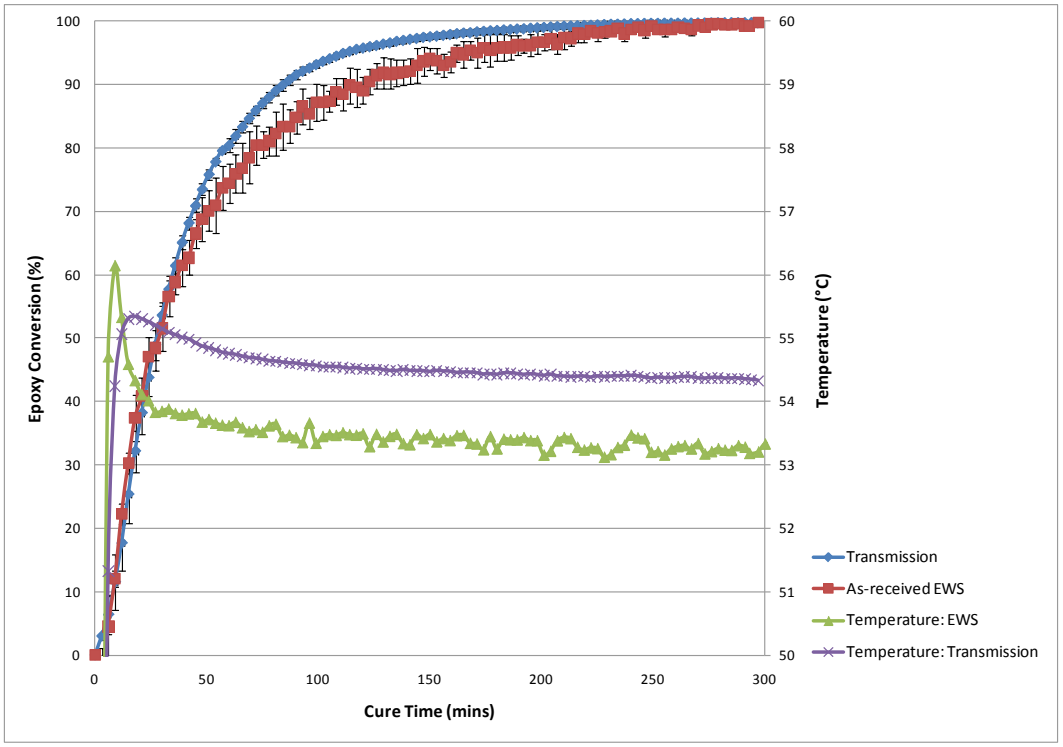
Epoxy Conversion (%)
Temperature (°C)
Cure Time (mins)
Transmission
As-received EWS
Temperature: EWS
Temperature: Transmission

d) 65°C

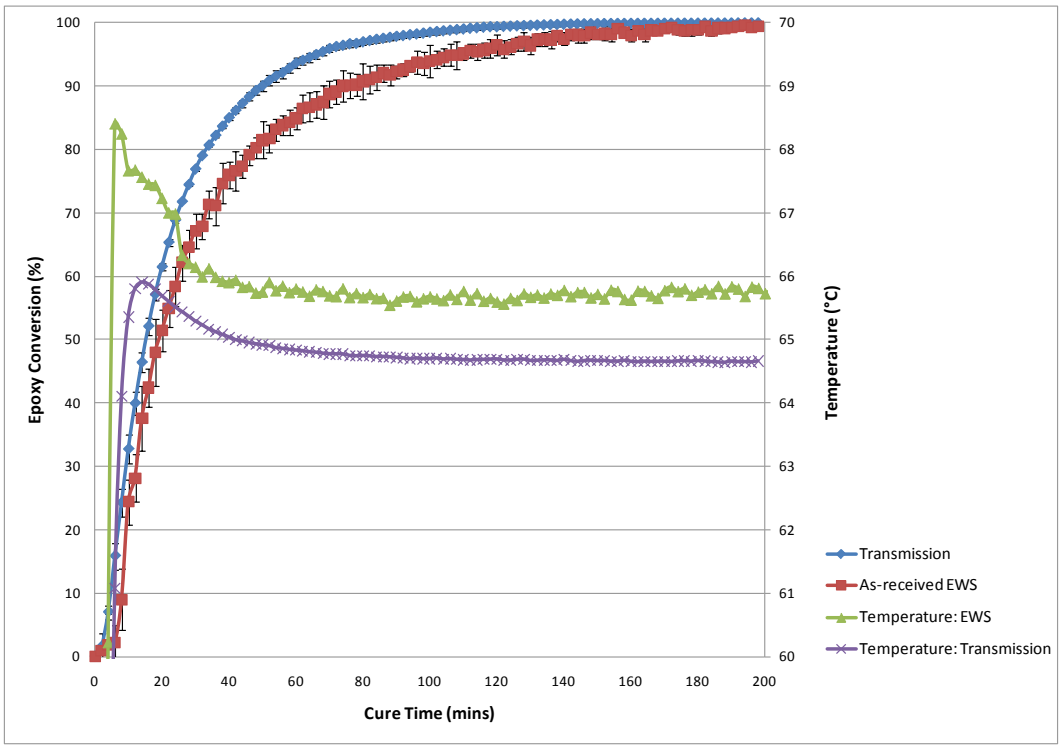
Epoxy Conversion (%)
Temperature (°C)
Cure Time (mins)
Transmission
As-received EWS
Temperature: EWS
Temperature: Transmission

Figure 4.9: Comparison of the conversion data for the depletion of the primary amine functional groups using transmission spectroscopy and evanescent wave spectroscopy in the EPO-TEK 310M epoxy resin system at 35, 45, 55 and 65 °C.

a) 35°C

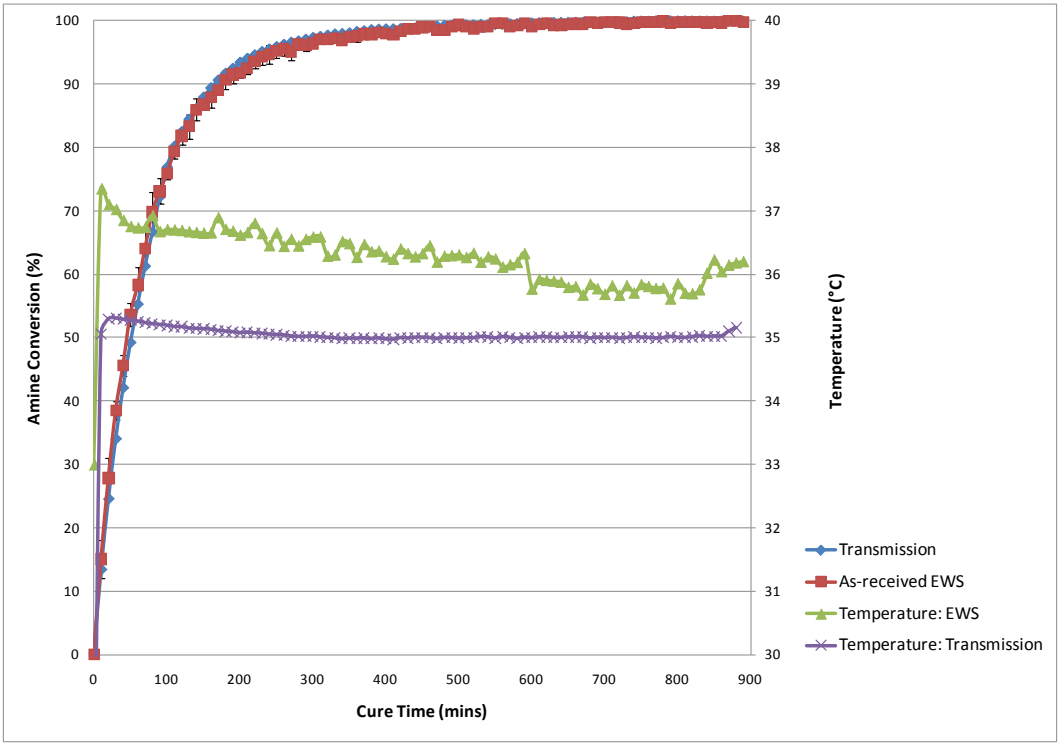

b) 45°C

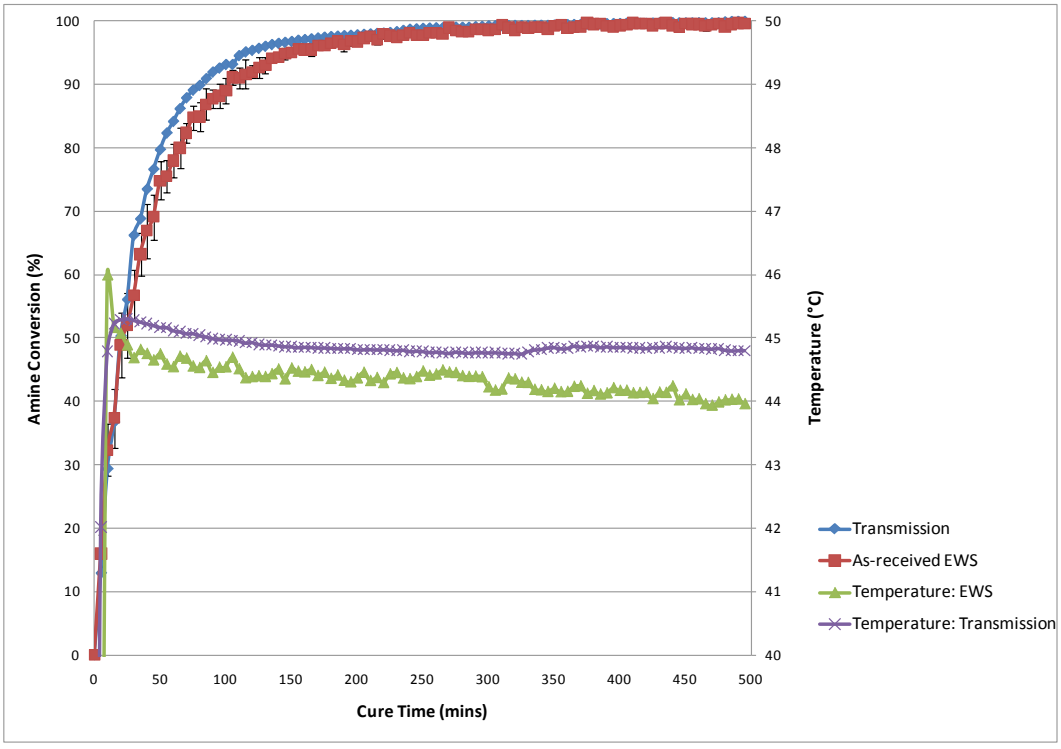

c) 55°C

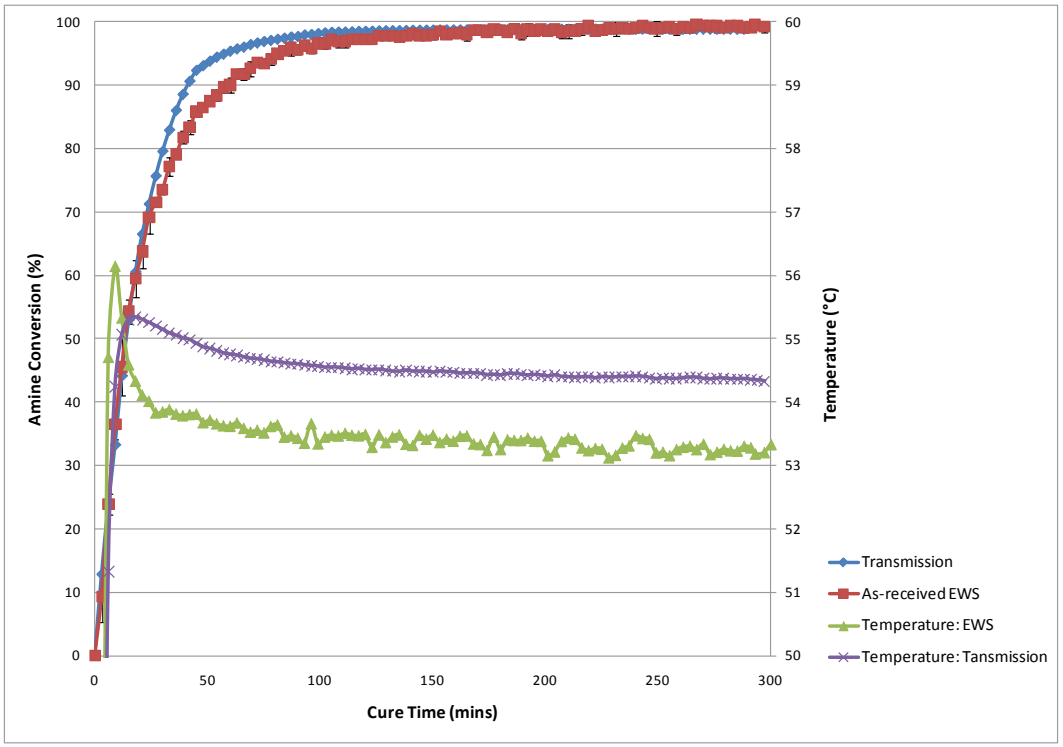
Amine Conversion (%)
Temperature (°C)
Cure Time (mins)
Transmission
As-received EWS
Temperature: EWS
Temperature: Tansmission

d) 65°C

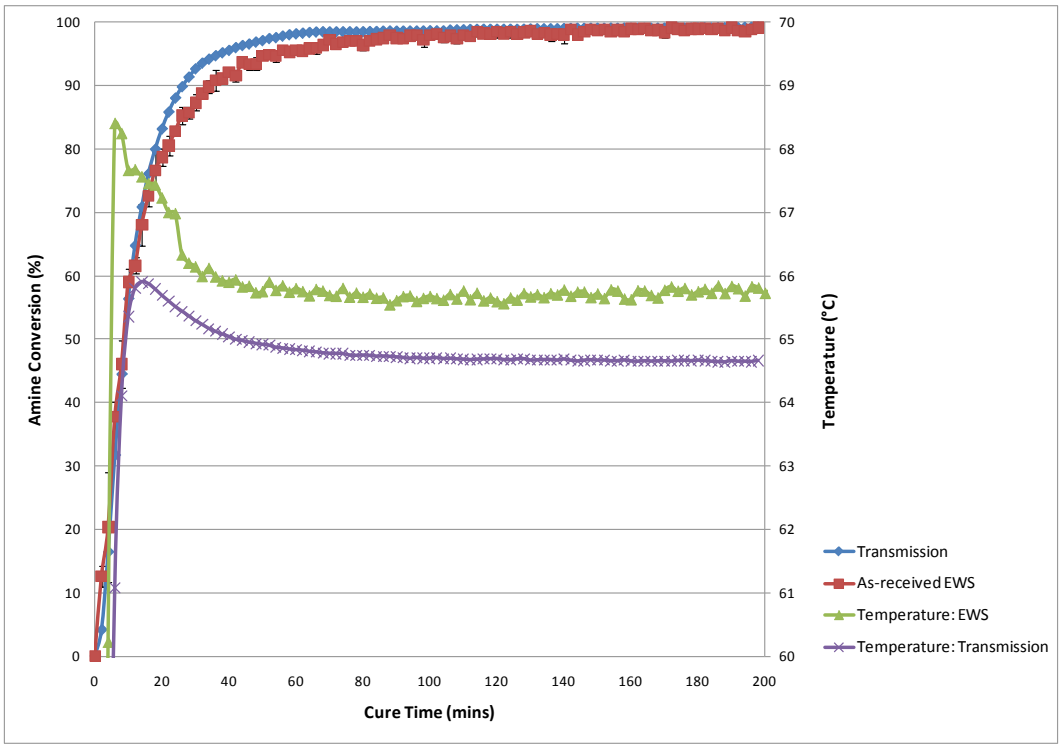
Amine Conversion (%)
Temperature (°C)
Cure Time (mins)
Transmission
As-received EWS
Temperature: EWS
Temperature: Transmission

In all cases of the above conversion plots (Figures 4.8 and 4.9) general agreement is seen between the two methods with respects to the cross-linking rate and the degrees of conversion, nevertheless slight differences are still noticeable. The evanescent wave spectroscopy approach yields slightly lower final degrees of conversion for the epoxy group in comparison to the transmission technique (Figure 4.8); final degree of conversion of the amine group are more similar between the two techniques (Figure 4.9). For example, at 65 °C final degree of conversion of the epoxy group was 99.9% and 99.4% (within experimental error) for evanescent wave and transmission spectroscopy (Figure 4.8d), respectively. At the same temperature the final degree of conversion of the amine group was 99.2% for the evanescent wave method and 99.1% for the transmission technique (Figure 4.9d). Though the trends of the curves are in accord, at higher temperatures inconsistencies are more pronounced concerning the two practices. Figure 4.8d illustrates epoxy conversion for NIR transmission FTIR spectroscopy and evanescent wave spectroscopy at an isothermal of 65 °C; there is an obvious disagreement in the trend of the two datasets.

This result highlights a potential issue concerned with the volatility of the resin system being used. In the case of the transmission experiment, evaporation is not much of a concern, because the resin is contained in a cell with a 1mm aperture at the top. The fibre bundle used in the evanescent wave spectroscopy set-up, is suspended at either end in a cylindrical oven, thus increasing the surface area of the resin and therefore increasing its susceptibility to evaporation.

Also, a temperature control difference of ± 0.02 °C and ± 0.2 °C is present for the conventional transmission technique and EWS technique, respectively. The slight discrepancies could also be attributed to the effect E-glass has on the cross-linking kinetics of the resin, when compared to the bulk resin measured via the transmission technique. The presence of the E-glass fibres can influence and change polymer chain movements and the surrounding residual stresses; this can induce preferential adsorption of the active epoxy and amine functional groups on the E-glass fibres (Petrovic and Stojakovic, 1988). It has been suggested that the reinforcement can “increase” the resins viscosity consequently hindering resin flow and reducing the rate of epoxy-amine cure reactions (Hong and Lin, 1997). Ishida and Koenig (1979) established that the cross-linking of an epoxy resin can be repressed in the presence of a silica surface.

However, it has been established that the EWS technique can mimic the conventional technique of transmission spectroscopy. The technique of using reinforcing E-glass fibres as light-guides to monitor highly localised regions has provided access to cross-linking kinetics at the fibre matrix interface. This can enable process optimisation for the cure kinetics of the resin matrix, especially

regarding the presence of surface treatments on the reinforcing E-glass and their effect towards cross-linking.

4.2.1.1 Effect of heat-treated E-glass fibres on cross-linking

Prior to cure monitoring, SEM was used to characterise the as-received and heat-treated E-glass fibres (Figure 4.10, 4.11 & 4.12). As expected, the fibres were generally clean, but localised debris was present at the fibre ends, which could be attributable to handling. Heat-treated fibres at 600 °C, were cleaner and a reduced number of blisters were present, when compared to the as-received fibres and heat-treated fibres at 450 °C. These surface contaminants of the as-received E-glass fibres could potentially affect the cure kinetics of the resin system used in this study and hence be responsible for the discrepancies observed between the EWS technique and transmission method.

Figure 4.10: SEM micrographs of different locations of Au coated as-received E-glass fibres.

a)

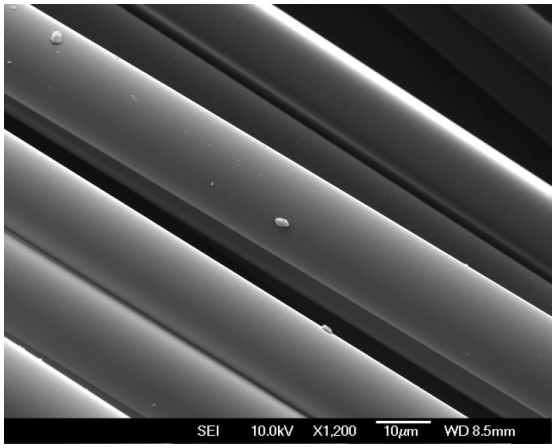

Debris is visible at the ends of the as-received fibres; this contamination is expected due to handling, as the occurance of this debirs is reduced in the other areas of the fibres.

b)

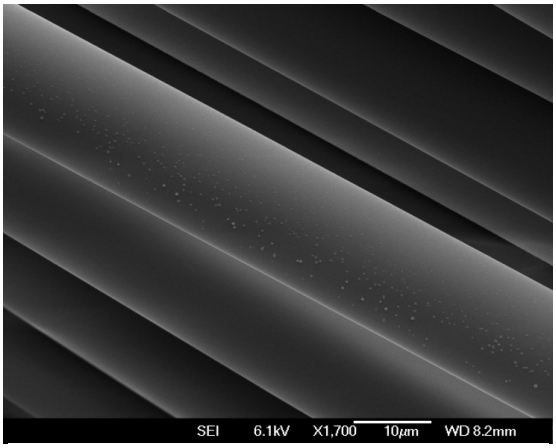

As-received E-glass fibre surface with a raised blistered topography.

c)

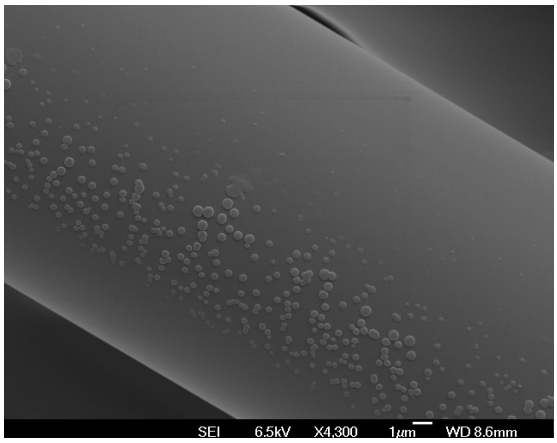

This image illustrates a closer look at the 'blisters' present on the E-glass fibre, it is difficult to determine the nature of the blisters and the potential effects they could have on the cure kinetics.

d)

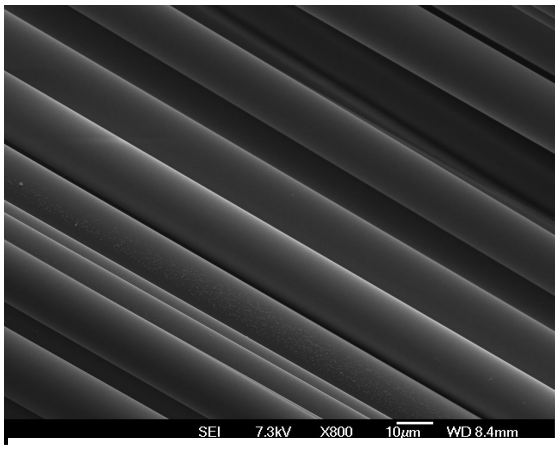

As-received E-glass fibres showing a generally clean surface.

Figure 4.11: SEM micrographs of different locations of Au coated E-glass fibres heat-treated at 450°C for 4 hours.

a)

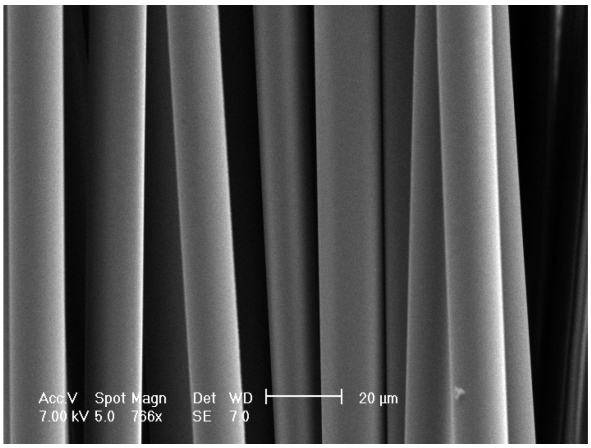

E-glass fibre surfaces heat-treated at 450 °C for 4 hours. A cleaner fibre surface is visible.

b)

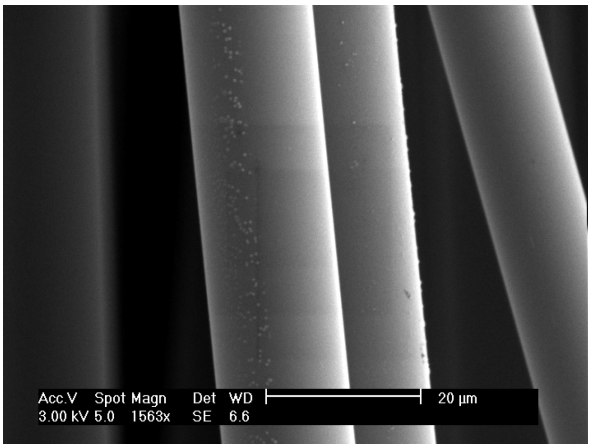

Heat-treated E-glass fibre surface still with the presence of the raised blisters.

c)

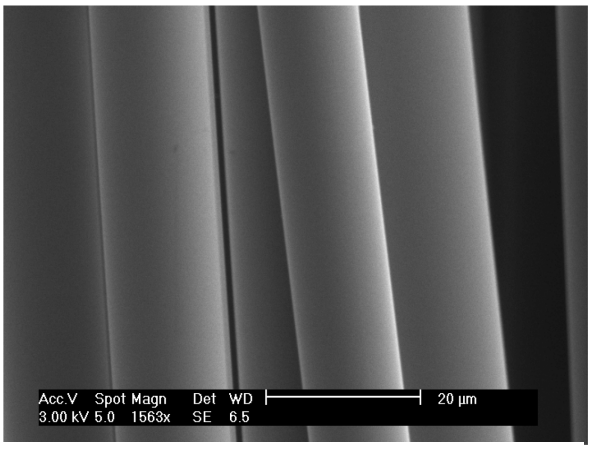

Heat-treated E-glass fibres near the centre show a clean surface.

d)

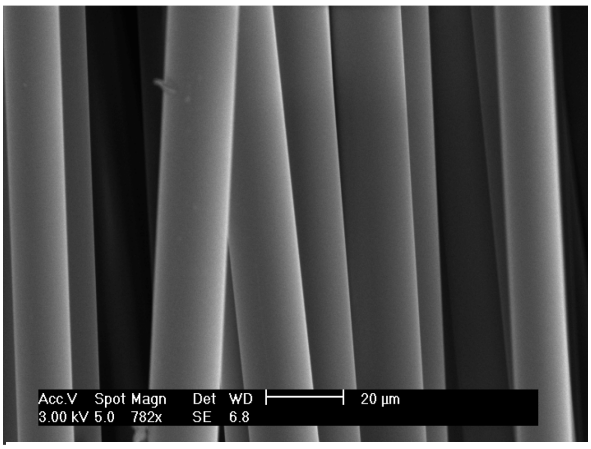

Heat-treated E-glass fibre ends are generally clean, but some debris is visible.

Figure 4.12: SEM micrographs of different locations of Au coated E-glass fibres heat-treated fibres at 600°C for 2 hours.

a)

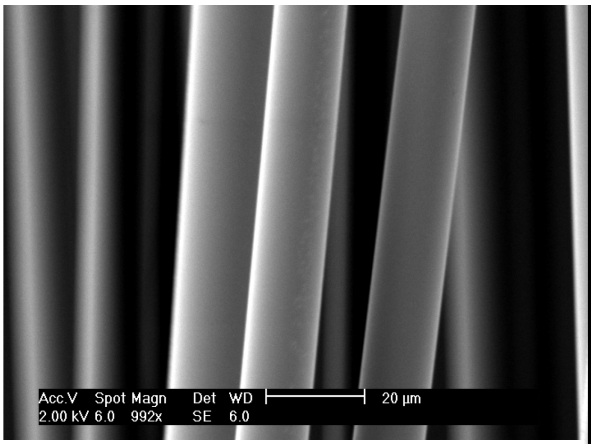

E-glass fibres heat-treated at 600°C provide the “cleanest” fibre.

b)

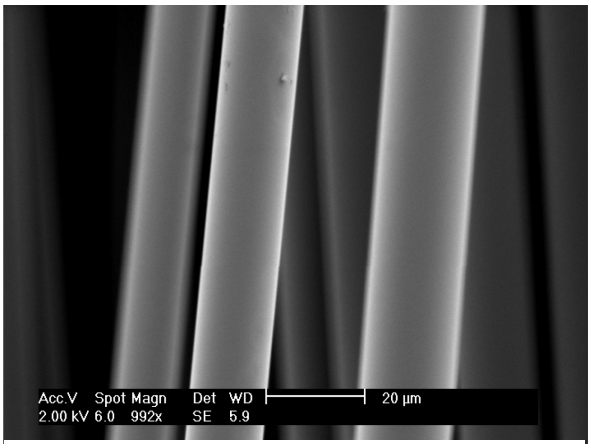

Heat treated E-glass fibre surfaces with no blisters providing a “clean” fibre.

c)

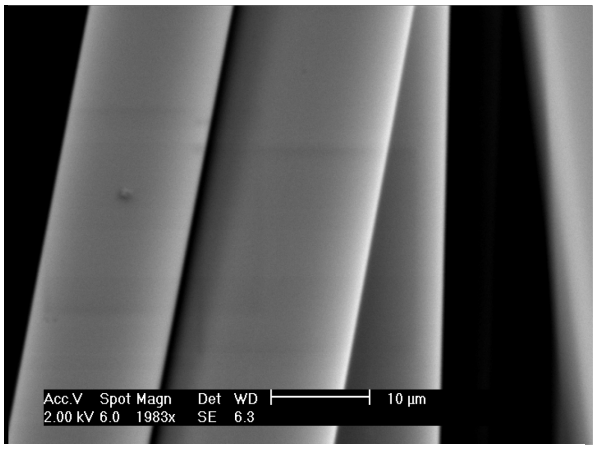

The 600 °C heat treatment has greatly reduced the number of blisters that were present compared to the as-received and 450°C heat-treated E-glass fibres.

d)

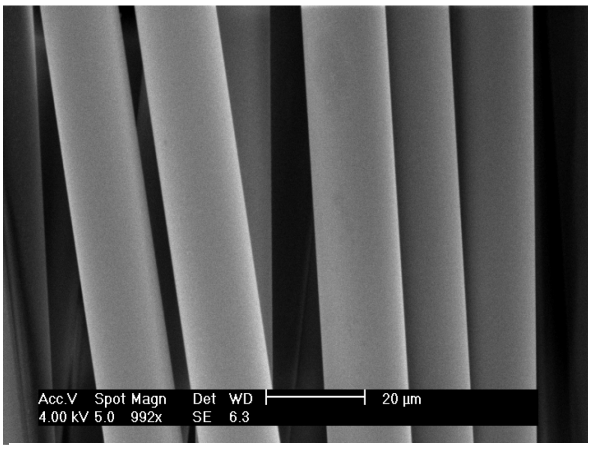

Heat treated E-glass fibres with clean surfaces.

To resolve the concerns with the slight discrepancies seen between the two techniques and the fact that the E-glass fibres being used were as-received; the E-glass fibres were consequently heat-treated for cure monitoring via EWS to eliminate any concerns that contaminants on the surface may be affecting the cure kinetics of the epoxy resin. The E-glass fibres were heated at 600°C for two hours. Two isothermal cure temperatures were chosen (65 °C and 35 °C) to compare as-received E-glass fibres with heat treated E-glass fibres via evanescent wave spectroscopy (Figure 4.13 & 4.14).

Figure 4.13: Comparison of the conversion data for the depletion of the epoxy functional groups of as-received and heat-treated E-glass fibres via evanescent wave spectroscopy in the EPO-TEK 310M epoxy resin system at 35 and 65 °C.

a) 35°C

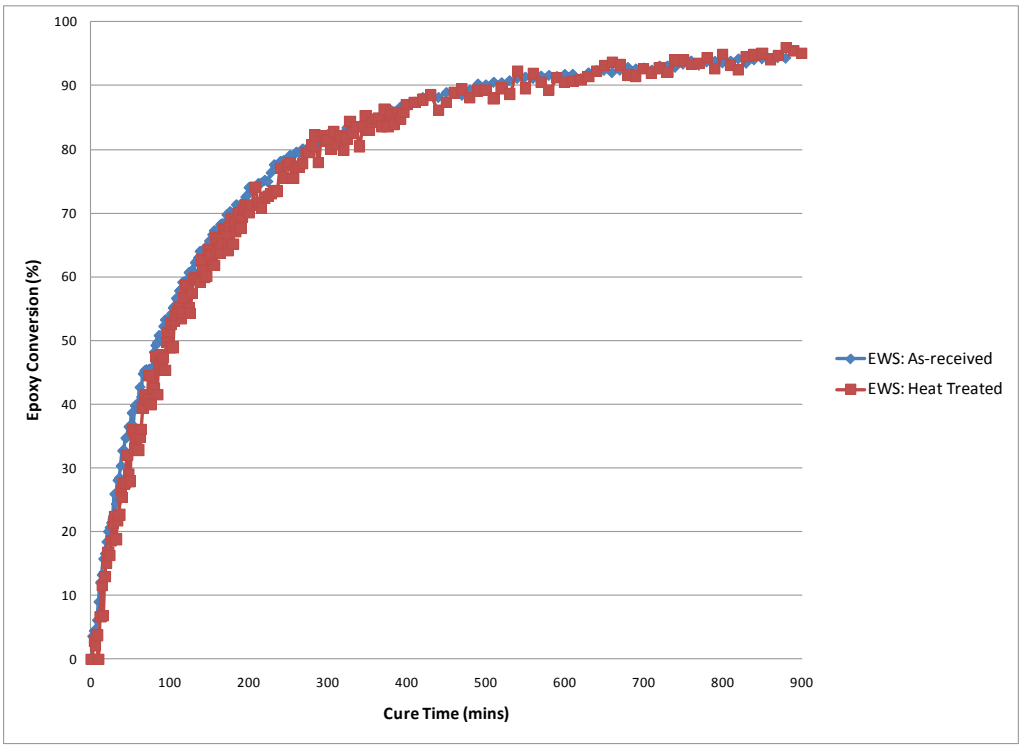

b) 65°C

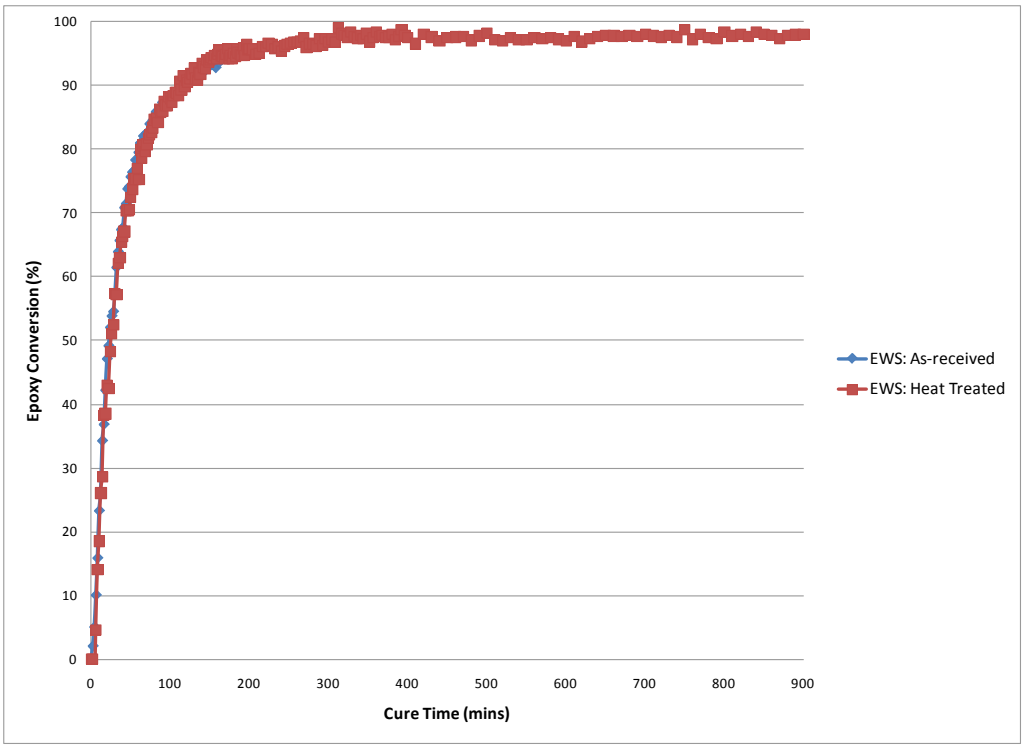

Figure 4.14: Comparison of the conversion data for the depletion of the primary amine functional groups of as-received and heat-treated E-glass fibres via evanescent wave spectroscopy in the EPO-TEK 310M epoxy resin system at 35 and 65 °C.

a) 65°C

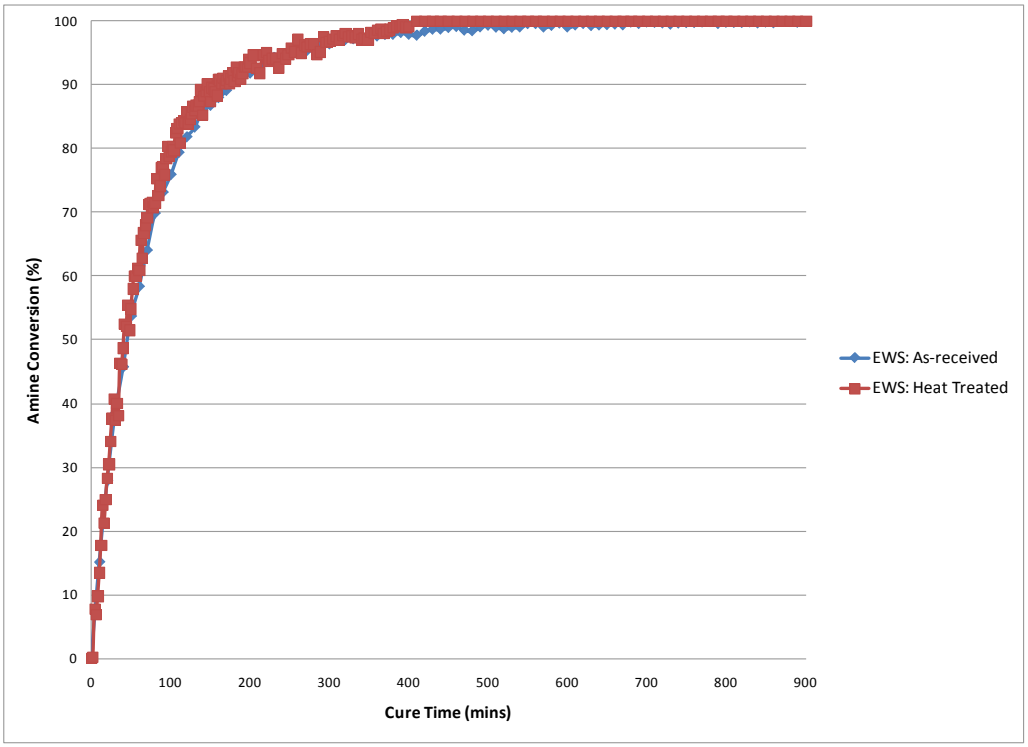

b) 35°C

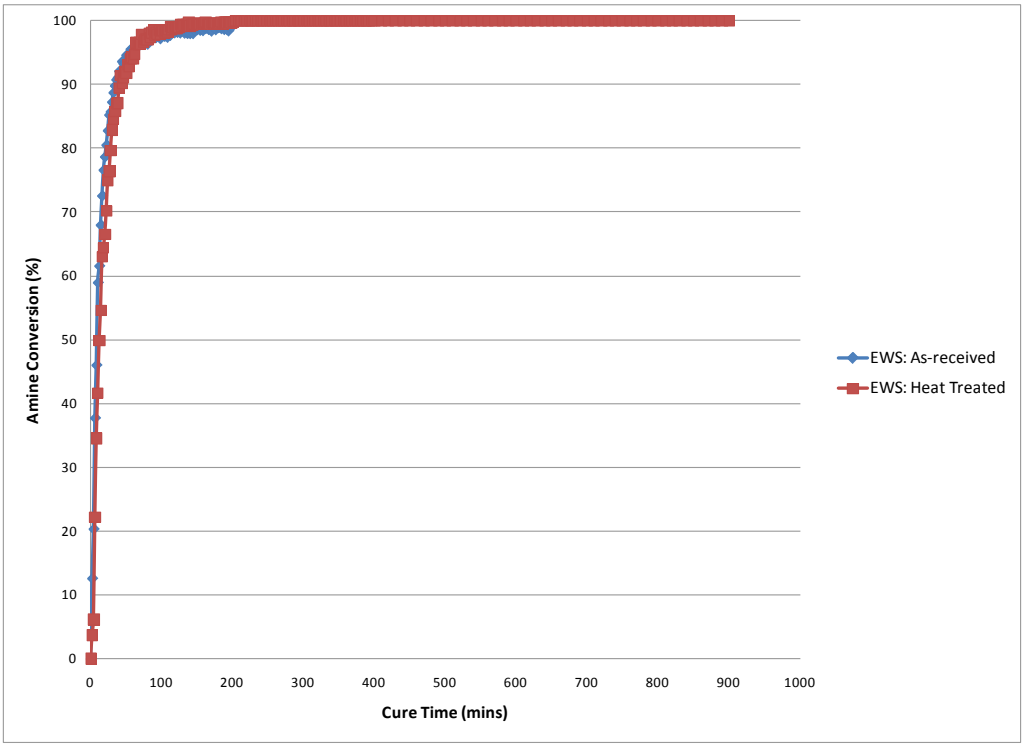

Both of the epoxy and primary amine conversion plots provide identical curves (Fig 4.13 and 4.14), these results help to demonstrate the validity of the subsequent experiments regarding the effects of silane treatments on the E-glass fibres have on the cure kinetics; because the likelihood that any changes to the rate and extent of consumption of the functional groups during cure can be attributed to the presence of the silane treatment.

4.2.2 Effect of GPS treatment of E-glass fibres on the cross-linking kinetics of EPO-TEK® 310M

4.2.2.1 Comparison: As-received versus GPS treatment

Figure 4.15 shows the presence of the relevant absorption peaks illustrated by the NIR spectra of 1% GPS treated E-glass fibres cured at 35°C; this indicates that the E-glass fibre bundle can detect the presence of the coupling agent and therefore be monitored to investigate its effect on the cure reactions.

Figure 4.15: Spectra of EPO-TEK® 310M attained using evanescent wave spectroscopy and GPS (1%) treated E-glass fibres showing different times of cure at 65 °C.

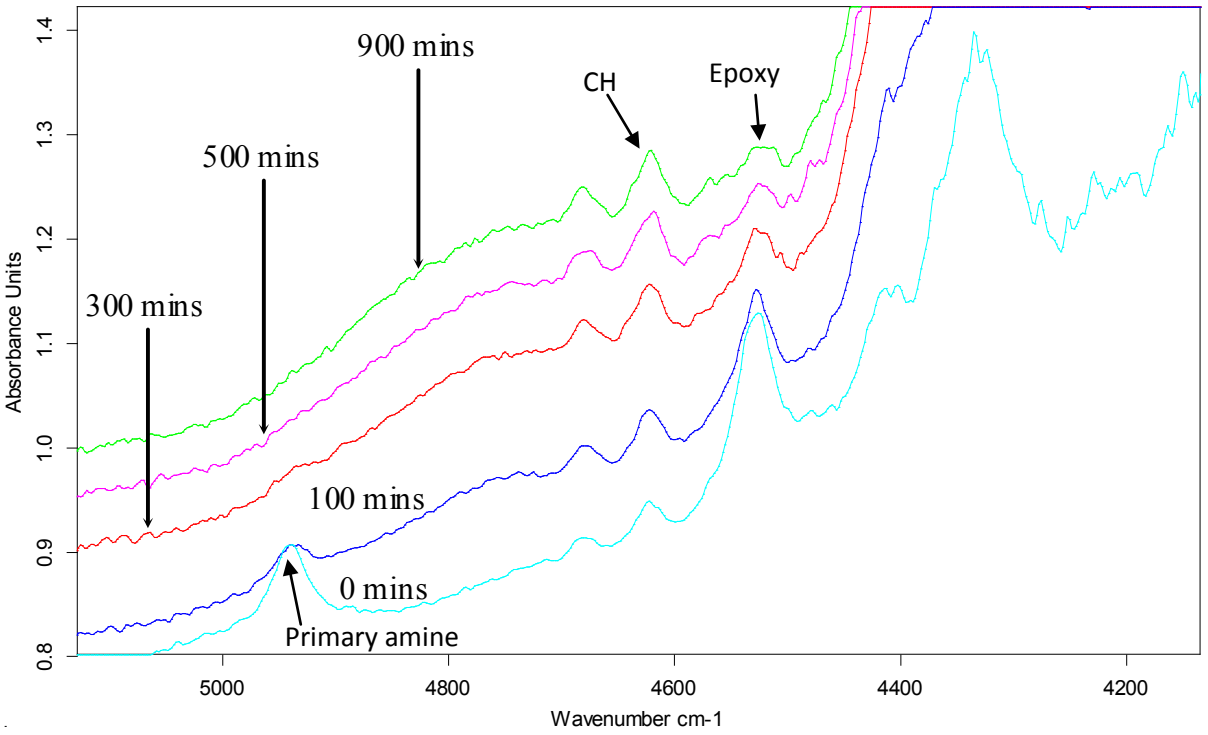

At different time intervals during the cross-linking process it can be clearly seen (Figure 4.15) that the epoxy and primary amine groups are gradually being consumed by the primary and secondary epoxy-amine addition reactions made evident with the decreasing epoxy and amine peak areas. Once again the CH peak absorption is constant.

The treatment of 1% GPS on the E-glass fibres has provided clear evidence that the silane inhibits epoxy consumption in the cross-linking reactions in comparison to the as-received E-glass fibres for all four temperatures (Figure 4.16). The application of a surface treatment will modify the surface chemistry and morphology of the E-glass fibre, therefore affecting its interaction with the epoxy-amine resin system.

Figure 4.16: Comparison of the conversion data for the depletion of the epoxy functional groups of as-received and GPS (1%) treated E-glass fibres via evanescent wave spectroscopy in the EPO-TEK 310M resin system at 35, 45, 55 and 65 °C.

a) 35°C

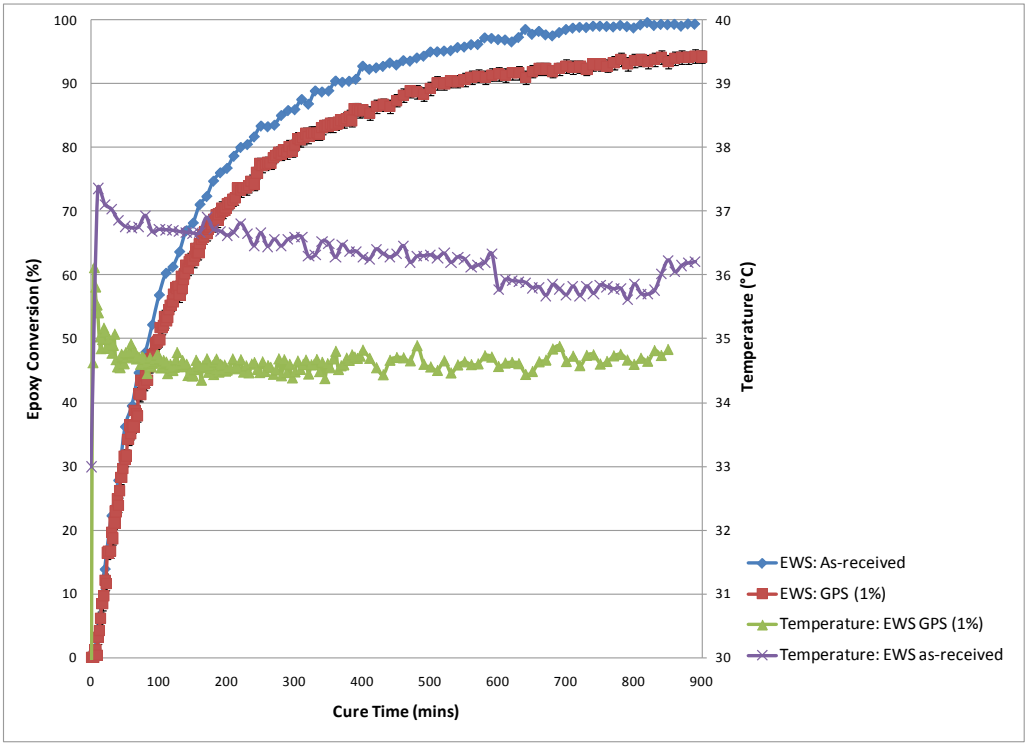

b) 45°C

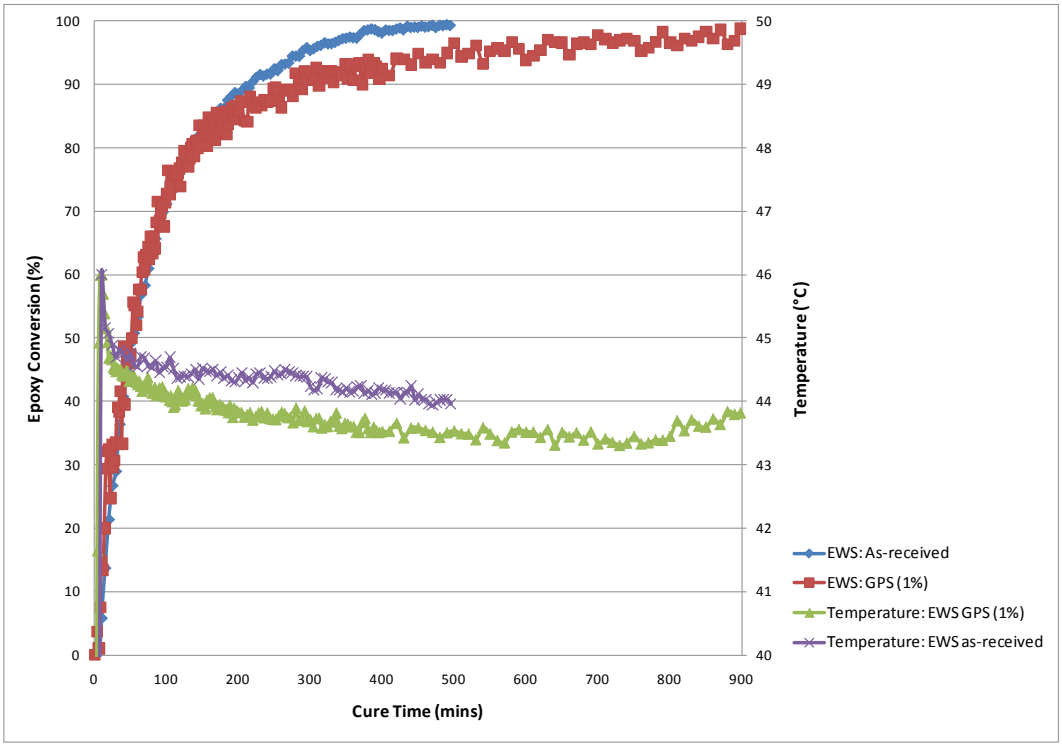

c) 55°C

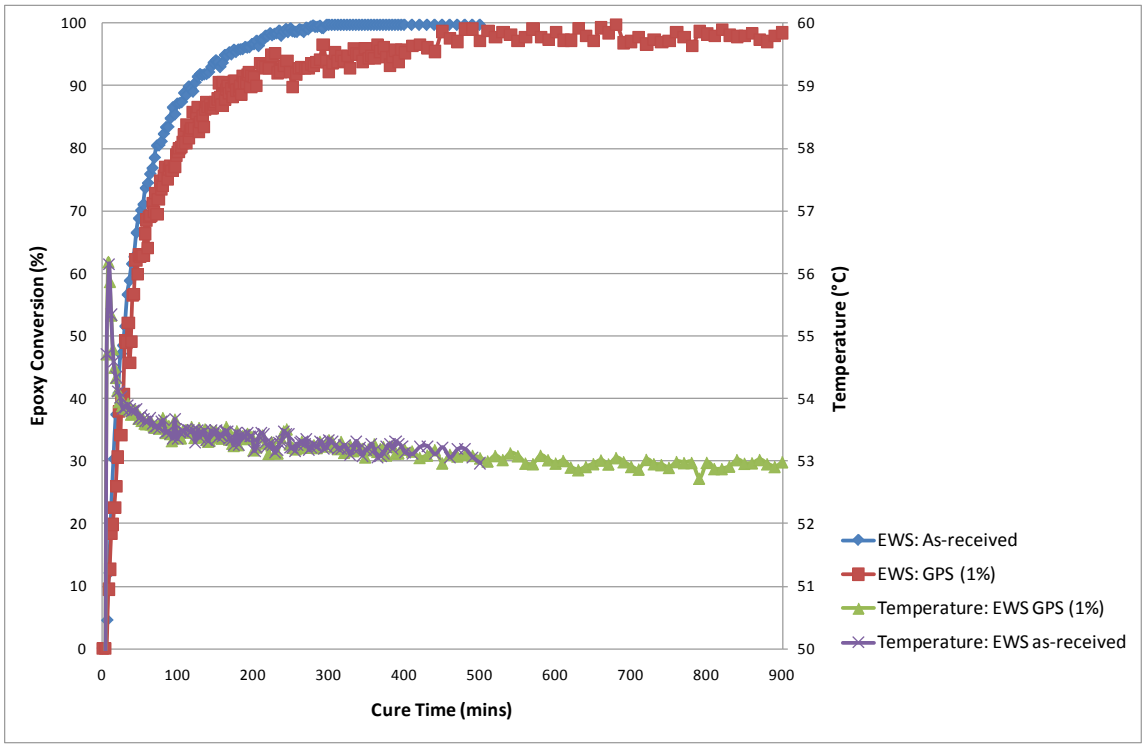
Epoxy Conversion (%)
Temperature (°C)
Cure Time (mins)
EWS: As-received
EWS: GPS (1%)
Temperature: EWS GPS (1%)
Temperature: EWS as-received

d) 65°C

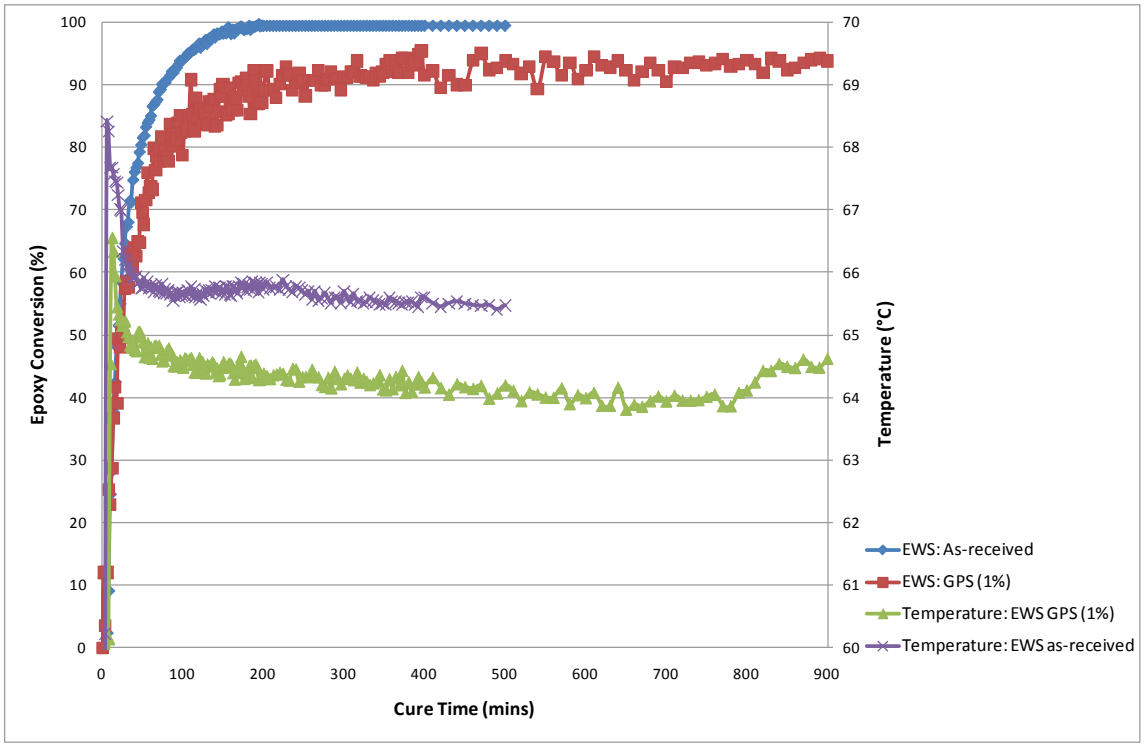
Epoxy Conversion (%)
Temperature (°C)
Cure Time (mins)
EWS: As-received
EWS: GPS (1%)
Temperature: EWS GPS (1%)
Temperature: EWS as-received

During all temperatures the rate of epoxy conversion was similar until it reached approximately 60%, where the epoxy conversion rate starts to slow down for the GPS (1%) treated E-glass fibres. At 35, 45, 55 and 65 °C the final degree of epoxy conversion was reduced by 1, 2, 2 and 5%, respectively (Fig. 4.16a-d).

Figure 4.17: Comparison of the conversion data for the depletion of the primary amine functional groups of as-received and GPS (1%) treated E-glass fibres via evanescent wave spectroscopy in the EPO-TEK 310M resin system at 35, 45, 55 and 65 °C.

a) 35°C

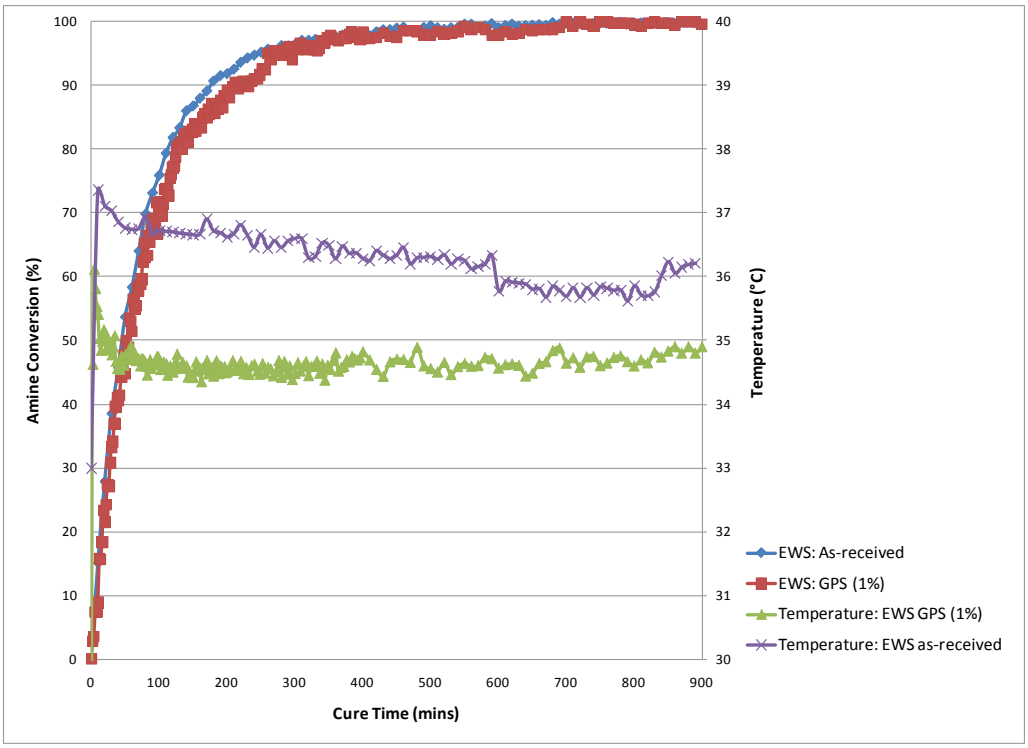

b) 45°C

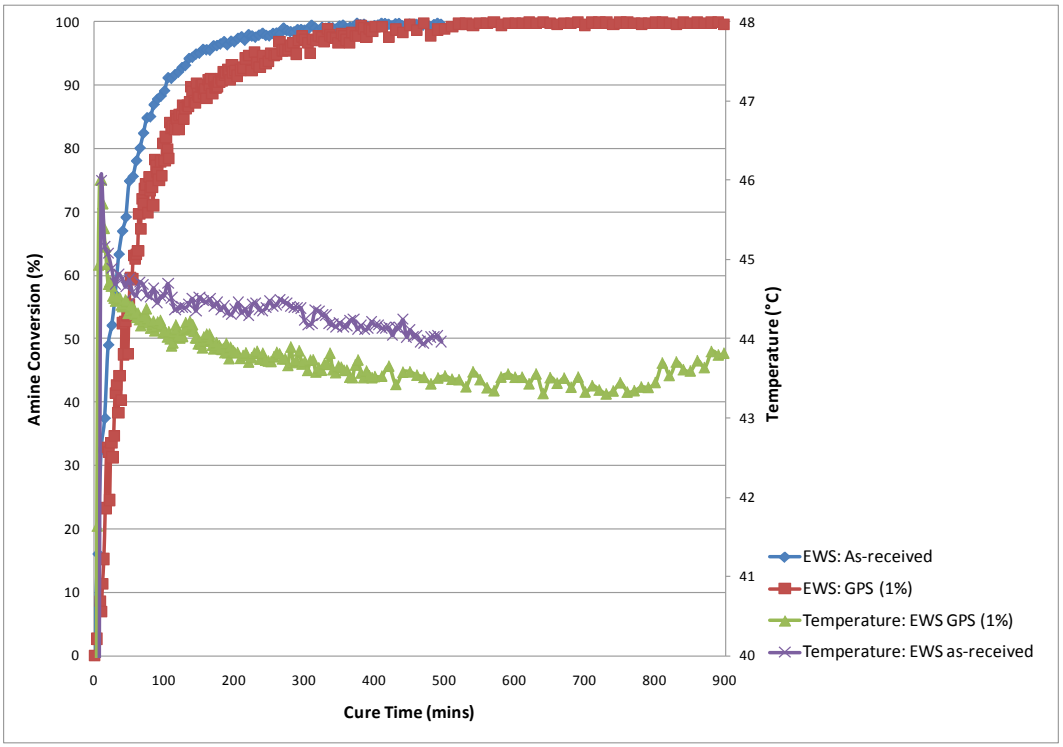
Amine Conversion (%)
Temperature (°C)
Cure Time (mins)
EWS: As-received
EWS: GPS (1%)
Temperature: EWS GPS (1%)
Temperature: EWS as-received

c) 55°C

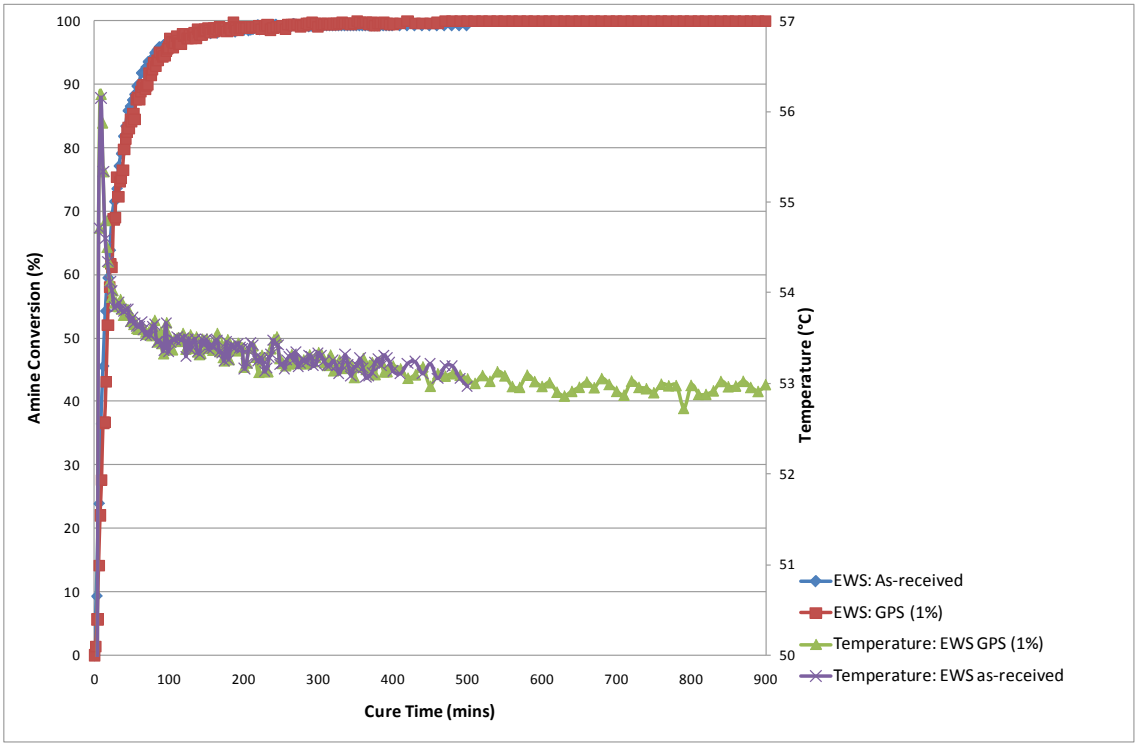
Amine Conversion (%)
Temperature (°C)
Cure Time (mins)
EWS: As-received
EWS: GPS (1%)
Temperature: EWS GPS (1%)
Temperature: EWS as-received

d) 65°C

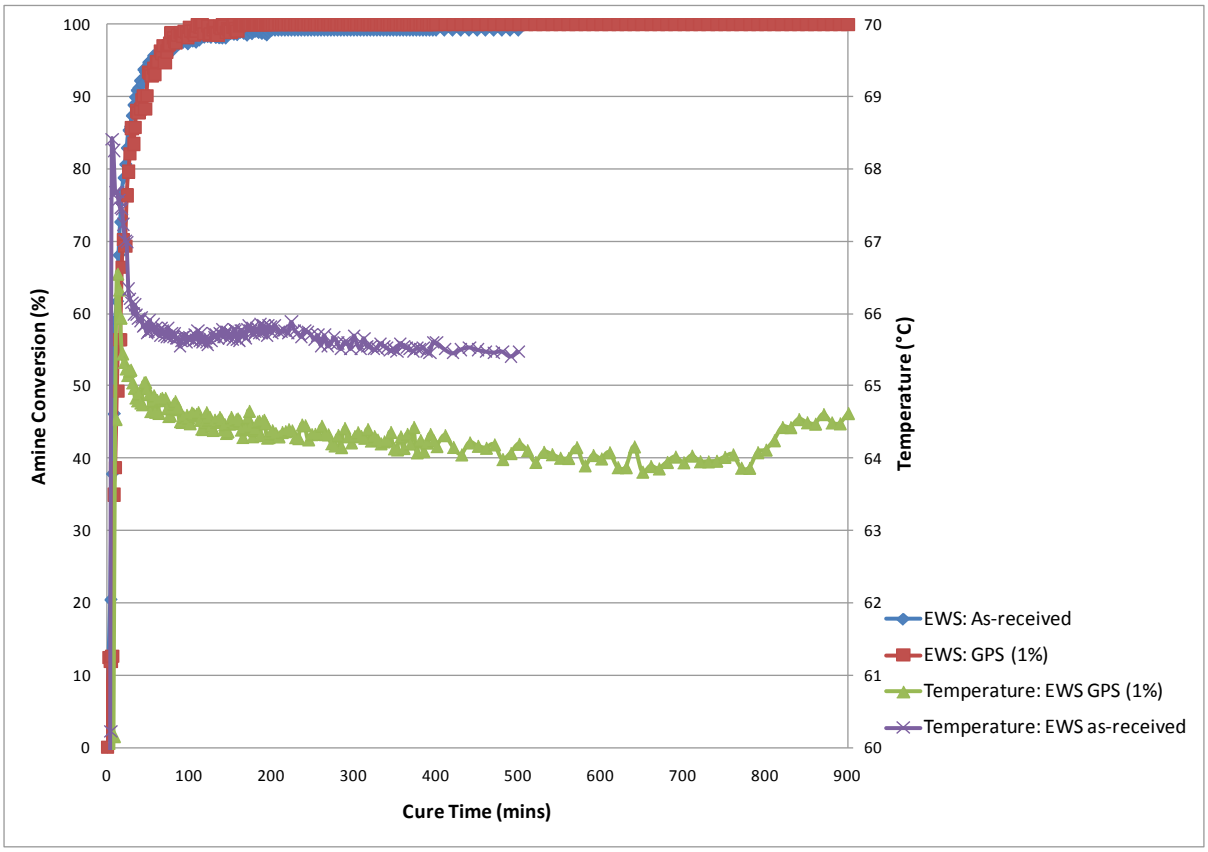

The effect of GPS (1%) treatment on amine consumption during cure was minimal, illustrated by the agreeing trend of curve between the as-received and GPS (1%) treated E-glass fibres (Fig. 4.17a-d). GPS is an epoxy-terminated silane and so at the E-glass fibre surface the amine concentration is expected to not be affected if either GPS treated or as-received E-glass fibres are used. However, there is an issue with respects to the GPS layer acting as a barrier between the E-glass surface and the cross-linking resin system. An explanation exists in that the amine molecules are much smaller than the epoxy molecules and this facilitates their diffusion through the 'silane barrier' (Gonzalez-Benito, 2003) and here they react with the available epoxy groups, producing similar amine consumption as with an as-received fibre.

Epoxy consumption however has been effected by the presence of the GPS treatment. The nature of epoxy cured with the presence of amine being an addition polymerisation, it can be postulated that the presence of GPS on the E-glass fibres surface can lead to preferential adsorption of a particular functional group of the resin onto the E-glass surface (Palmese *et al.* 1999). In addition, the concentration of the reactive groups may have been weakened by dissolving of the GPS with the resin. It could be suggested that the GPS layer may prevent the diffusion of the bulky epoxy functional group (compare to the primary amine) into the silane interphase, thus restricting its

ability to participate in the cross-linking reactions (Culler *et al.* 1986), hence the reduction in epoxy conversion.

4.2.2.2 Effect of GPS treatment at different concentrations of E-glass fibres on the cross-linking kinetics

By increasing the concentration of GPS treatment to the E-glass fibres, the rate and degree of epoxy and amine conversion was consequently affected. 35 °C was chosen as the isothermal cure temperature as it had shown good repeatability from the previous results. During the first 400 minutes of cure the rate of epoxy consumption is seen to increase with increasing concentration of GPS treatment, but after this point the rate of epoxy conversion decreases with increasing GPS treatment, which led to a reduction of the final degree of epoxy conversion. The effect of GPS concentration on amine consumption is not as profound as the differences seen with epoxy consumption. The final degree of amine consumption was similar between all concentrations, but it was during the first 400 minutes where slight differences were observed. As with the rate of epoxy consumption, accelerated amine consumption was also observed with increasing GPS concentration during this time period. The accelerated rate of cure in the case of the silane treated fibres is in agreement with Palmese et al. (1999) and Yu and Sung (1997).

The choice of background spectrum may have contributed to these differences. In these experiments the background spectrum was taken of the as-received E-glass fibre bundle. Thus, the application of the GPS treatment would increases the concentration of epoxy groups at the E-glass interface and the epoxy concentration would seem to further increase by increasing the relative concentration percentage of the GPS. Consequently, evanescent wave spectroscopy supposes an increased rate of consumption of the epoxy and amine functional groups, only apparent during the first 400 minutes. This finding is in agreement with Hong and Lin (1997); the authors measured the (the time to reach maximal curing rate) of a brominated epoxy resin/dicyandiamide (DICY) system via DSC analysis. It was concluded that GPS treated glass beads increased the curing rate of the resin system, particularly at the early stages of cure. This observation was not only attributed to the GPS reacting with the DICY, but also its ability to experience anionic polymerisation induced by the ongoing hydrolysis reactions and the residence of hydroxide ions (Horr and Reynolds, 1997). The reduced extent of functional group consumption with increasing relative GPS concentration treatment, could be credited to a more condense and thicker silane layer. It has been suggested that after the GPS has polymerised, spiral structures are formed of –Si-O-Si-O- and beside the centre of this structure exists pendant hydroxy groups (Allen, 1992). These hydroxy groups are not available for reaction and so the epoxy groups will not be utilised to their fullest extent, potentially explaining the reduced epoxy consumption observed in Figure 4.18a.

Figure 4.18: Comparison of the conversion data for the depletion of the epoxy (a) and amine (b) functional groups of GPS (0.1%, 0.5%, 1% and 3%) treated E-glass fibres via evanescent wave spectroscopy in the EPO-TEK 310M resin system at 35°C.

a) 35°C

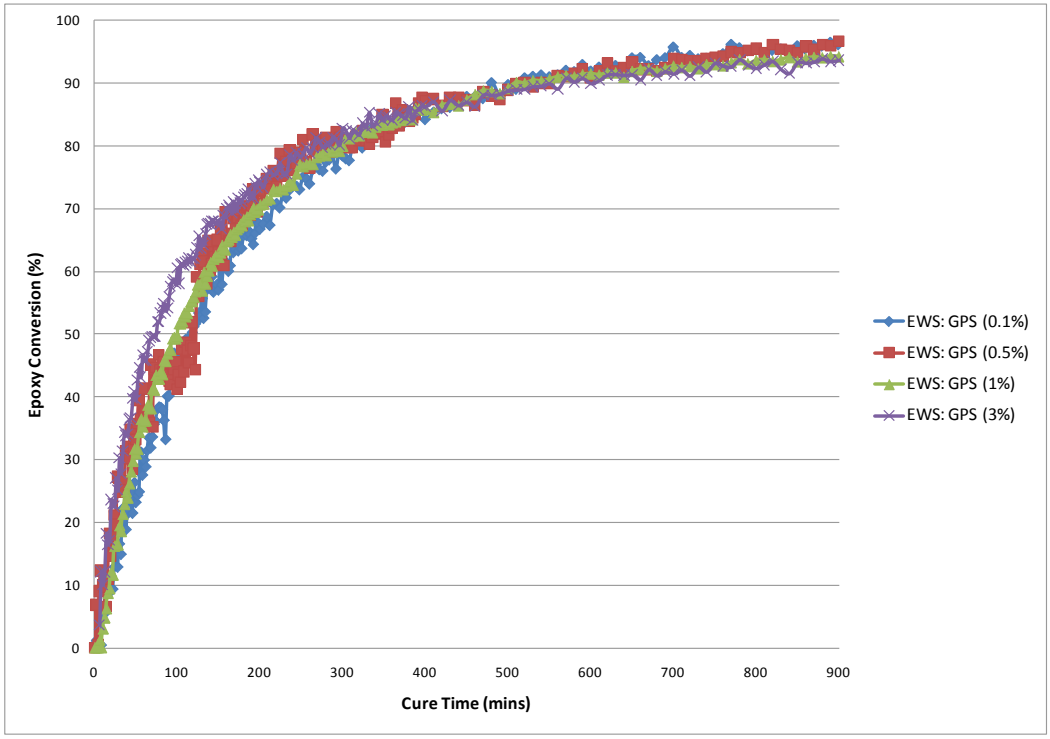

b) 35°C

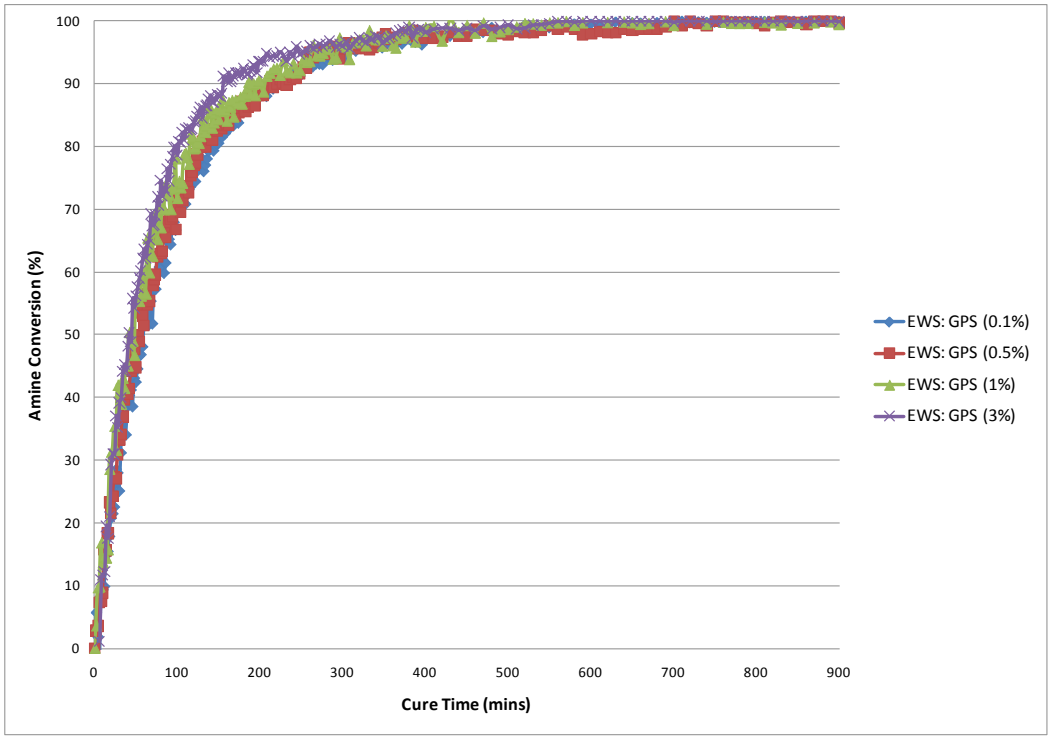

4.2.3 Effect of APS treatment of E-glass fibres on the cross-linking kinetics of EPO-TEK® 310M

4.2.3.1 Comparison: As-received Vs. APS treatment

The chemical nature of the APS treatment induces a pronounced hindrance to the E-glass fibres transmittance in comparison to GPS treated and as-received E-glass fibres and consequently a higher signal-to-noise ratio is present. Nevertheless, conversion plots were still producible to help distinguish any effects APS treatment may have on the cure kinetics of the amine-cured epoxy resin system. Again, the spectra in Figure 4.19 establish that the APS can be detected by identifying the relevant absorption bands and their fluctuating areas, which are in accord with the cure reactions discussed previously.

Figure 4.19: Spectra of EPO-TEK® 310M attained using evanescent wave spectroscopy and APS (1%) treated E-glass fibres showing different times of cure at 65 °C.

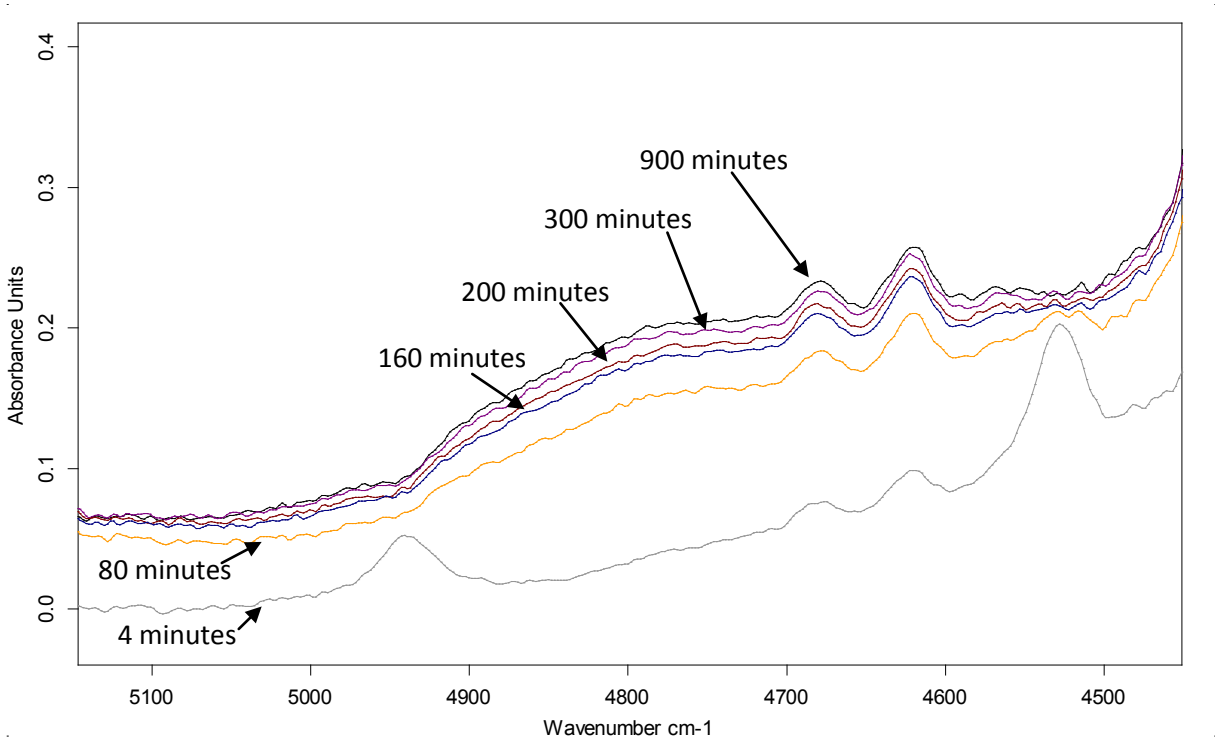

Figure 4.20: Comparison of the conversion data for the depletion of the epoxy functional groups of as-received and APS (1%) treated E-glass fibres via evanescent wave spectroscopy in the EPO-TEK 310M resin system at 35, 45, 55 and 65 °C.

a) 35°C

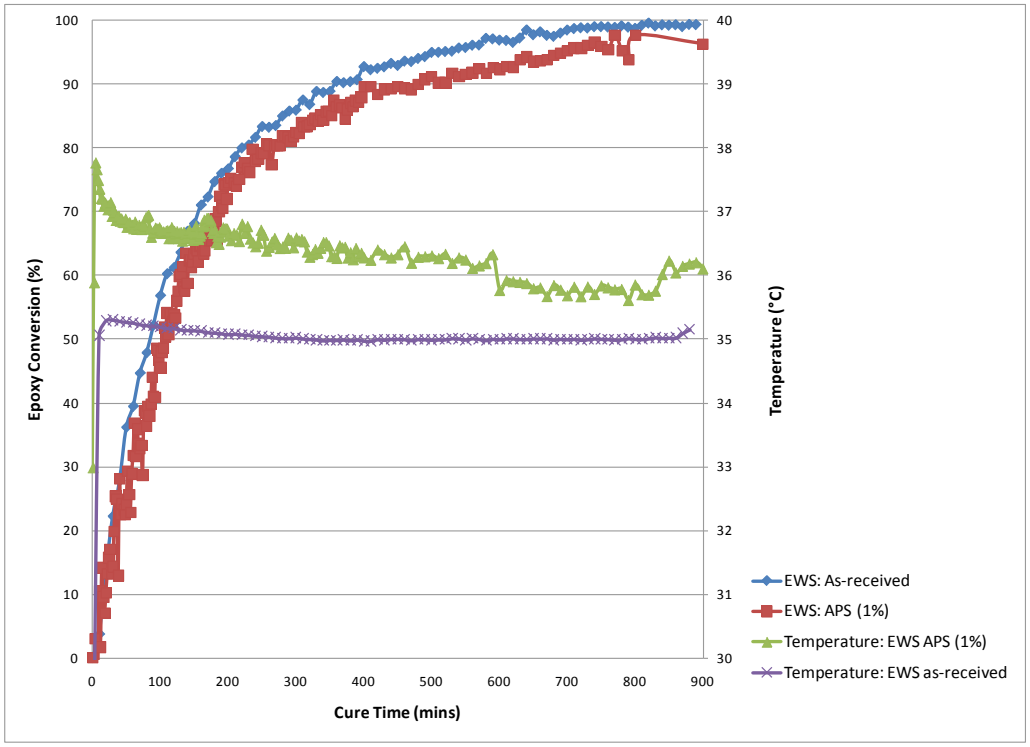

b) 45°C

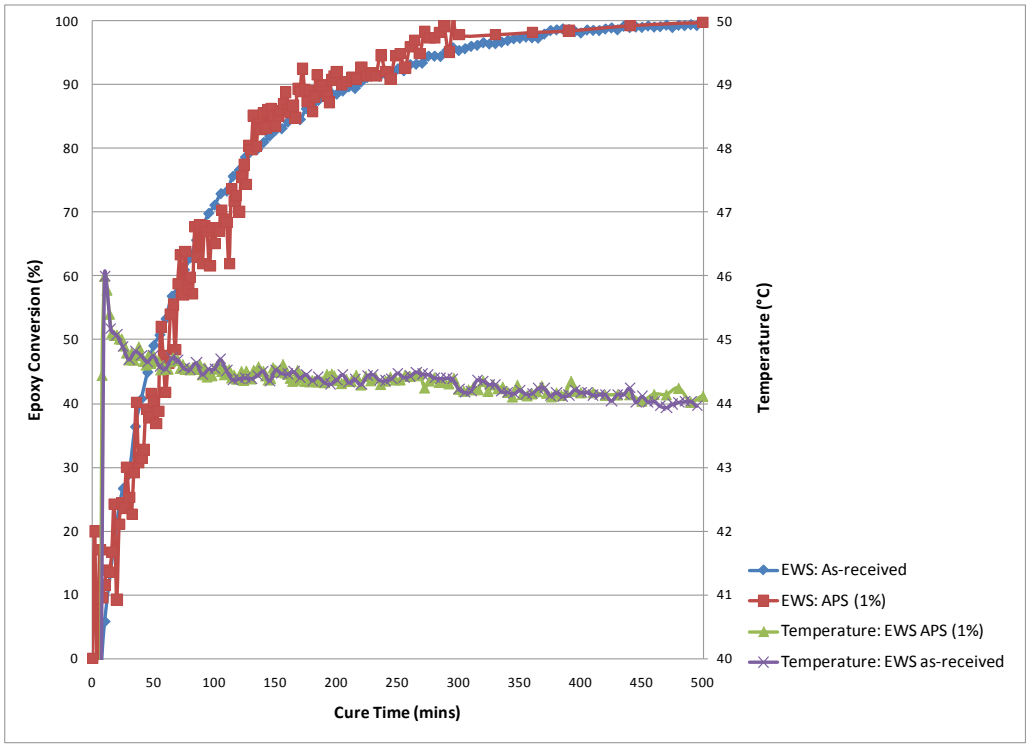

c) 55°C

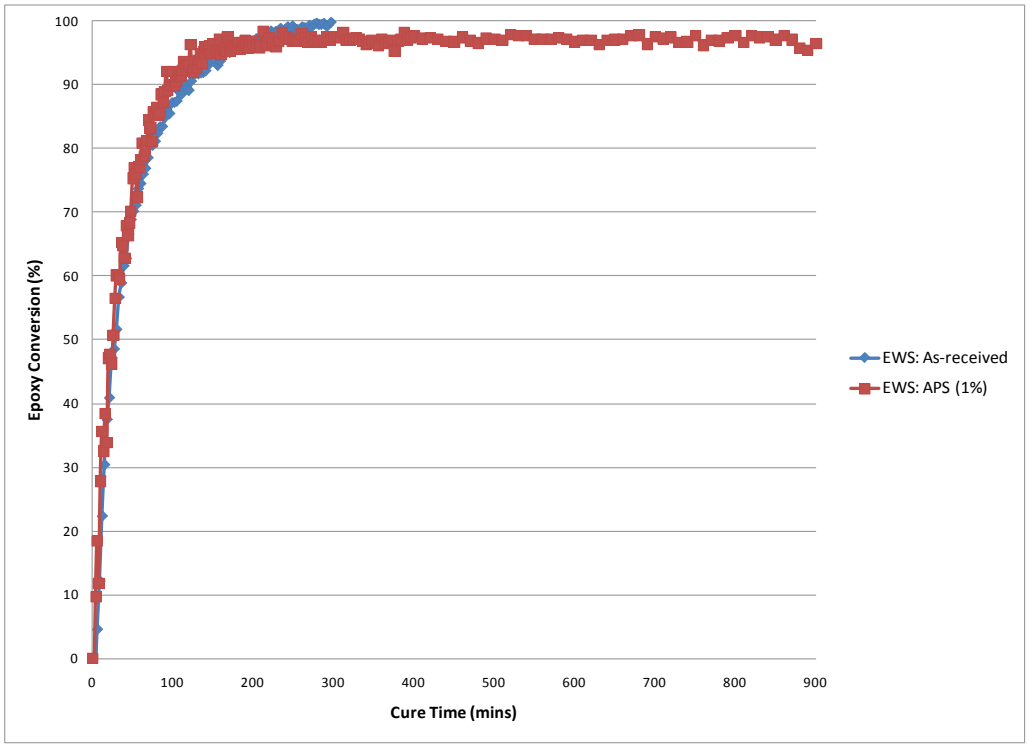
Epoxy Conversion (%)
Cure Time (mins)
EWS: As-received
EWS: APS (1%)

d) 65°C

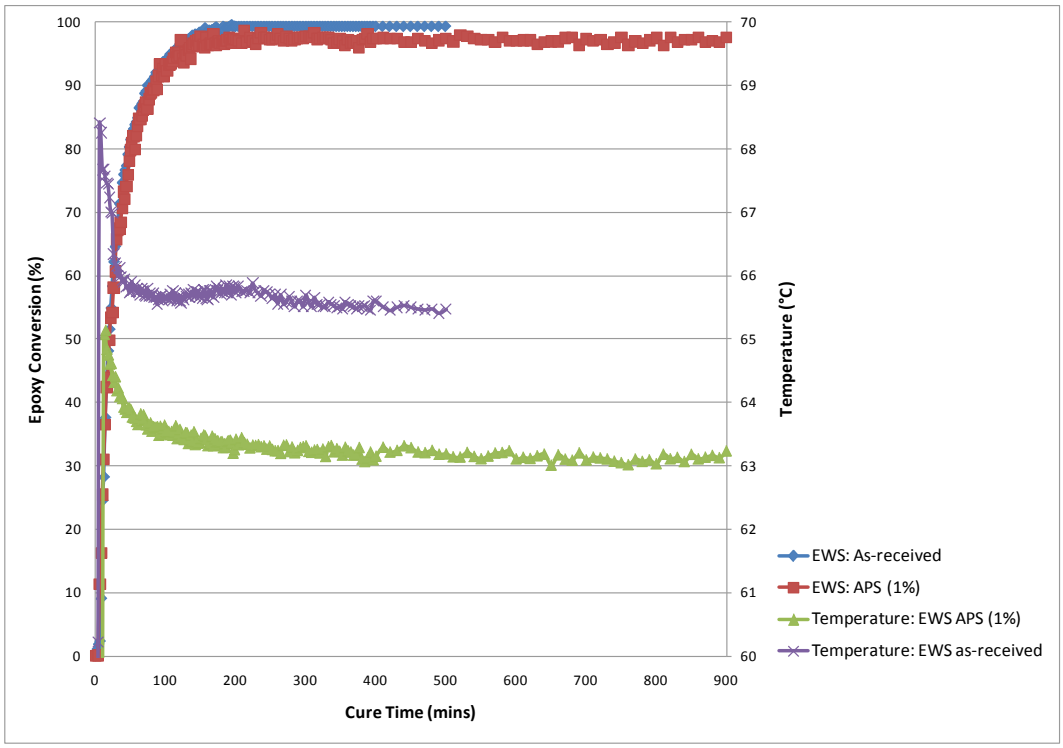
Epoxy Conversion (%)
Temperature (°C)
Cure Time (mins)
EWS: As-received
EWS: APS (1%)
Temperature: EWS APS (1%)
Temperature: EWS as-received

It can be inferred from the epoxy conversion plots (Fig. 4.20a-d) that the presence of APS (1%) on the E-glass fibres did not greatly affect the rate or degree of epoxy consumption, especially when compared to the effect GPS had on epoxy consumption.

Figure 4.21: Comparison of the conversion data for the depletion of the primary amine functional groups of as-received and APS (1%) treated E-glass fibres via evanescent wave spectroscopy in the EPO-TEK 310M resin system at 35, 45, 55 and 65 °C.

a) 35°C

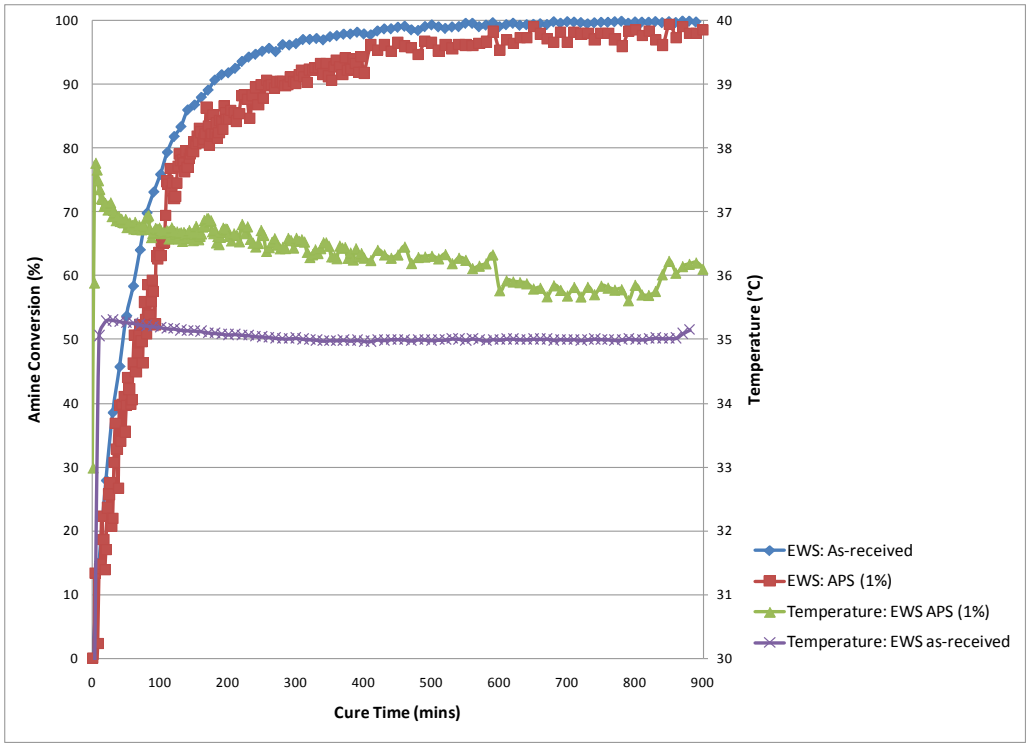

b) 45°C

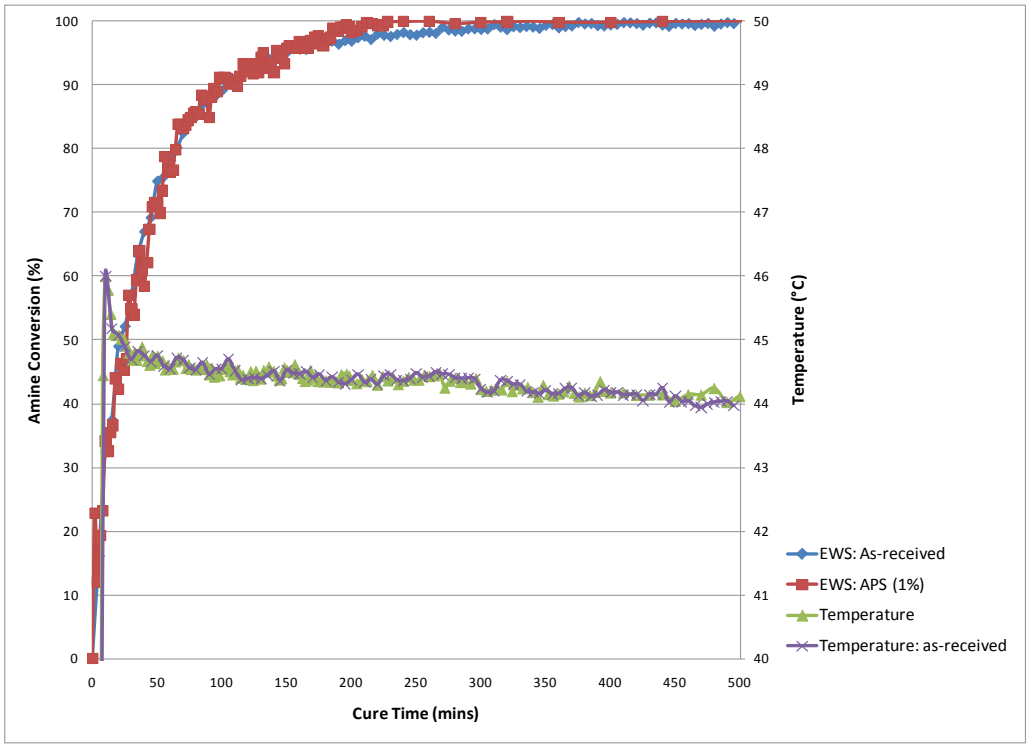
Amine Conversion (%)
Temperature (°C)
Cure Time (mins)
EWS: As-received
EWS: APS (1%)
Temperature
Temperature: as-received

c) 55°C

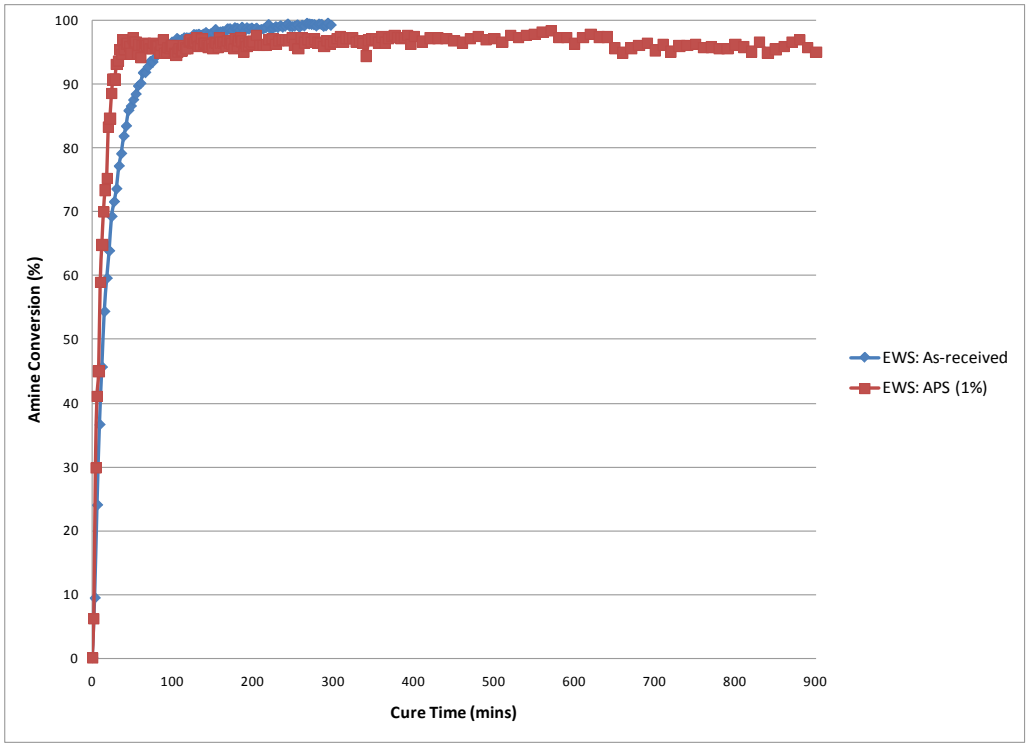
Amine Conversion (%)
Cure Time (mins)
EWS: As-received
EWS: APS (1%)

d) 65°C

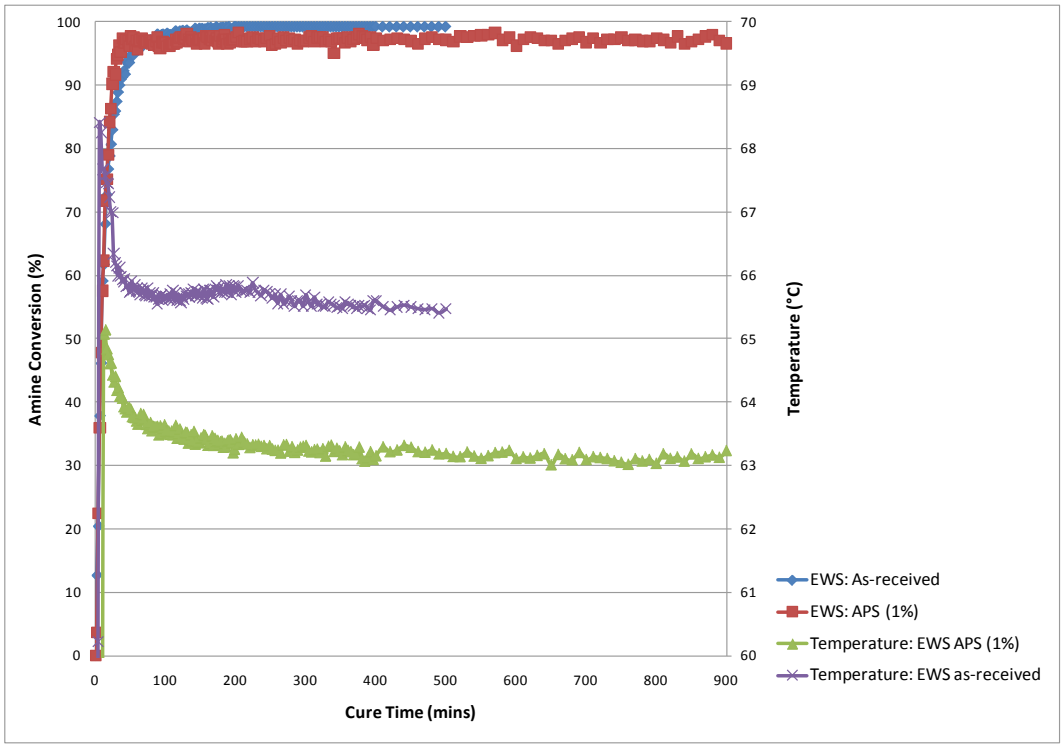

The effect of APS (1%) on amine consumption, is negligible, however it can be observed for all temperatures except at 35°C (Figure 4.21a), that the presence of the silane has induced a quicker amine consumption over the first 60 minutes. In addition a slight reduction in the extent of amine consumption is evident for all temperatures (Figure 4.21a-d). The APS is an amine-terminated coupling agent and so its deposition onto the E-glass surface is expected to increase the number of amino groups, as would be deduced by the EWS technique by using the as-received E-glass fibre as the background spectrum. The increased concentration of amino groups is expected to increase siloxane cross-linking, which reduces interfacial strength (Hamada *et al.* 1994), hence the increased consumption of amino groups observed in Figure 4.21b-d. Because of the increased rate of amine consumption as a result of APS providing an increased relative concentration of amino groups at the E-glass fibre surface, the reduction in amine consumption could be attributed to the cross-linked structure of the APS layer; it can obstruct any further reactions between the epoxy-amine resin system and organofunctional groups of the silane (Iglesias *et al.* 2002).

4.2.3.2 Effect of APS treatment at different concentrations of E-glass fibres on the cross-linking kinetics

Changing the concentration percentage of APS treatment had an effect on the cure kinetics of the epoxy-amine resin system (Figure 4.22). Only three concentrations (0.1, 0.5 and 1%) were chosen to compare isothermal cures at 35°C; APS (3%) treatment proved to downgrade the E-glass' transmittance to the extent where the quality of spectra could not be used. In the case of the epoxy conversion plots (Figure 4.22a) any differences were not of a magnitude to postulate any evaluative response. The amine conversion plots (Figure 4.22b) on the other hand, illustrate an obvious effect on amine consumption by altering the concentration of APS treatment. However, a logical sequence of results is not as evident with the APS treatment as it was with GPS treatment. It can be observed that over the first 60 minutes the rate of amine consumption is faster with APS (0.5%) and APS (1%) treatments compared to APS (0.1%) and as the cure continues the final degree of amine consumption is reduced at higher relative concentrations (0.5 and 1%) (Figure 4.22b). But when solely comparing APS (0.5%) treatment with APS (1%) these trends are reversed and so at these concentrations, further experiments need to be conducted to validate the results (Figure 4.22b). Nonetheless, discussion can be considered concerning the increased rate of amine consumption at the initial stages of cure and the reduced final degree of amine consumption as the relative concentration of APS was increased. It has been postulated that the increased concentration of hydroxyl groups at the E-glass fibre surface (when compared to the bulk resin) will induce favourable reactions with the amine functional groups and in addition; the amine molecules are smaller than their epoxy counterparts and are thought to be able to diffuse more easily through the APS layer (Gonzalez-Benito, 2003). These points coupled with the increasing amount of amine concentration with increasing concentration of APS treatment can explain the increase in amine consumption (Figure 4.22b). This however does not explain why the final degree of amine consumption decreases with increasing APS concentration. Epoxy-amine reactions can be affected by the APS thickness and degree of condensation of the APS interphase (Connell *et al.* 1998). A higher concentration of APS will condense the silane layer, therefore diffusion of the small amine molecules will be impeded and so the extent of reaction is expected to decrease. This was deduced by Connell and co-workers (1998); as the density of the APS was increased it 'entrapped' the primary amines of the silane excluding their participation in the reaction with available epoxy groups.

Figure 4.22: Comparison of the conversion data for the depletion of the epoxy (a) and amine (b) functional groups of APS (0.1%, 0.5%, and 1%) treated E-glass fibres via evanescent wave spectroscopy in the EPO-TEK 310M resin system at 35°C.

a)

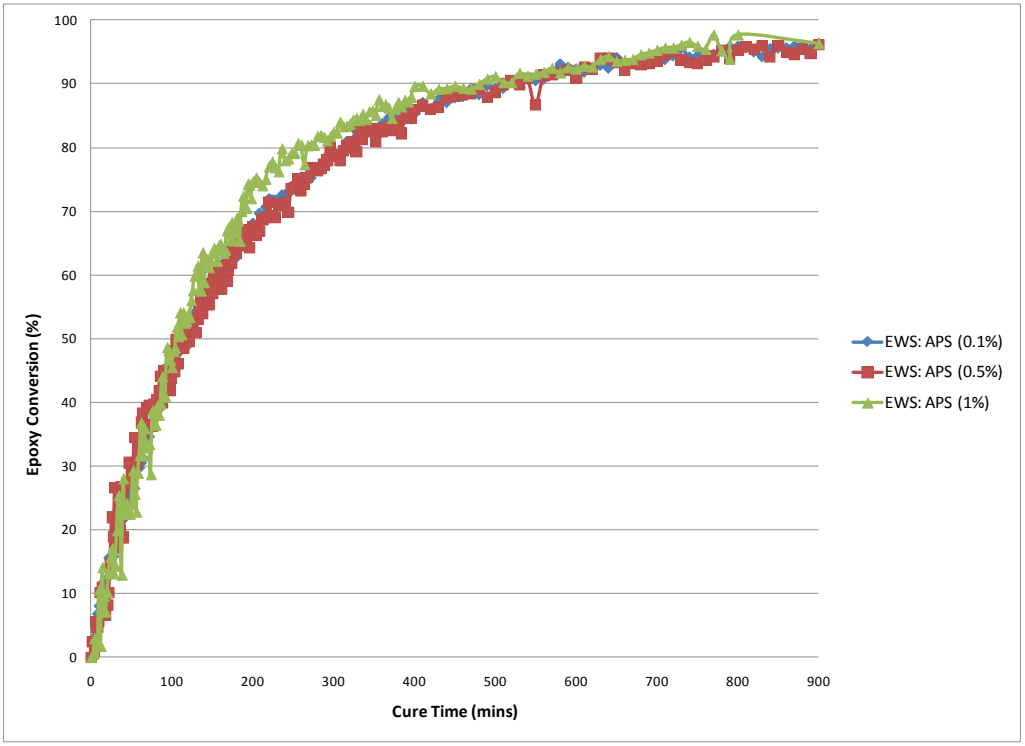

b)

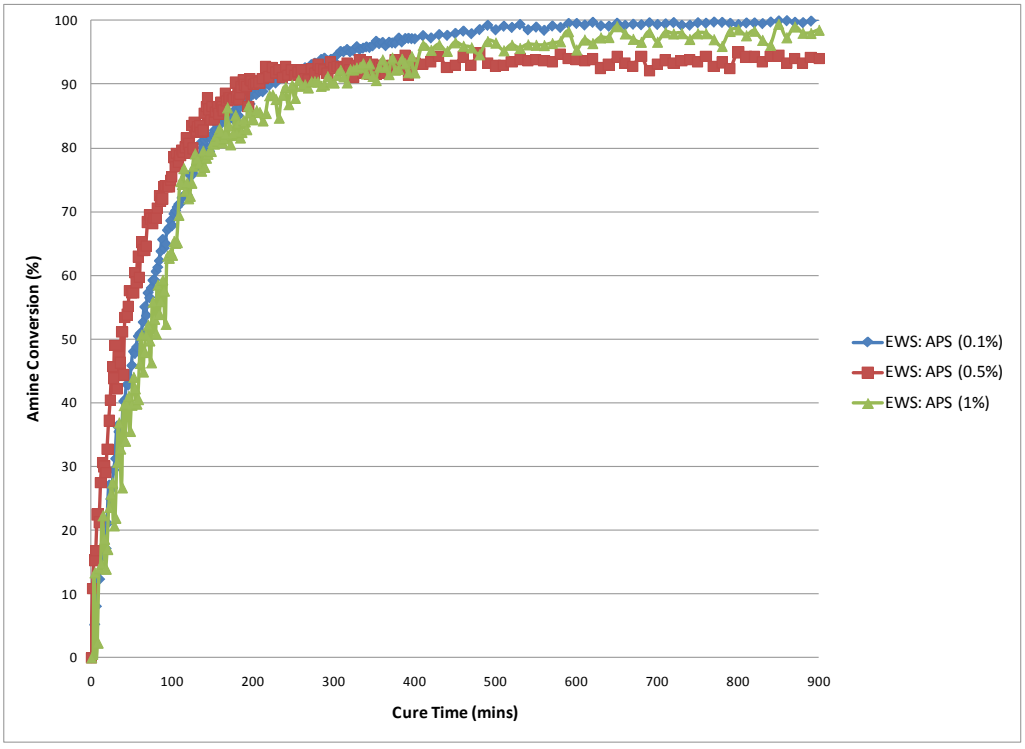

The chemisorbed APS layer is to provide a mechanism for the formation of moleculary sized pores into which the resin molecules can diffuse to form a semi-IPN which promotes adhesion through molecular interlocking. Thus APS can act as an adhesion promoter for a range of matrix polymers independent of chemical coupling (liu *et al.* 2008).

4.2.4 Comparison: Evanescent wave spectroscopy vs. Fourier transform infrared attenuated total reflectance spectroscopy

A preliminary experiment was undertaken to obtain spectra of the EPO-TEK 310M resin in the mid infra-red region. The motivation for this action was to further reinforce the validity of using the E-glass fibres bundles as chemical sensors. The epoxy peak at 915 cm^{-1} (Figure 4.23a) was chosen to track its involvement during cure, its area can be seen to decrease with cure time. The aromatic peak at 1606 cm^{-1} (Figure 4.23b) was chosen as an internal standard, its area is seen to stay constant with cure time. Using Eqn. 16 epoxy consumption was plotted against a cure time of 350 minutes at 35 °C.

Figure 4.23: Mid infra-red FTIR-ATR spectra of EPO-TEK® 310M at different stages of cross-linking at 35 °C: a) Epoxy peak; b) CH peak

a)

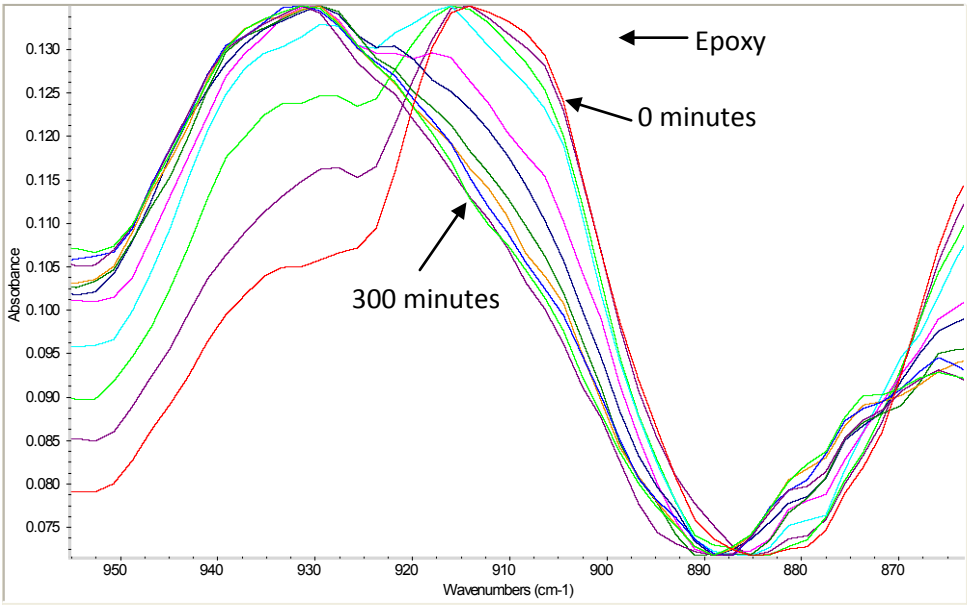

b)

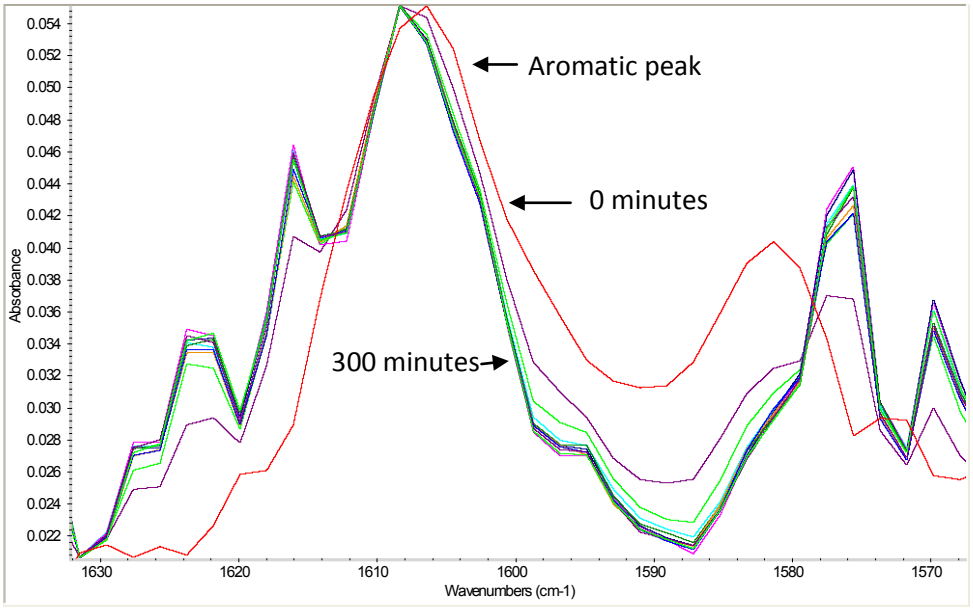

The quality of the epoxy conversion plot (Figure 4.24) obtained via FTIR-ATR spectroscopy is fairly poor, but nevertheless shows some correlation with the conventional transmission technique and EWS method. Caution must be taken when using mid-infrared spectra as it has been reported that individual peaks are more difficult to distinguish than in the near infra-red due to overlapping. Cure could only be monitored up until approximately 300 minutes due to the capabilities of the machine.

Figure 4.24: Comparison of the conversion data for the depletion of the epoxy functional groups using FTIR-ATR spectroscopy and evanescent wave spectroscopy in the EPO-TEK 310M epoxy resin system at an isothermal cure of 35 °C.

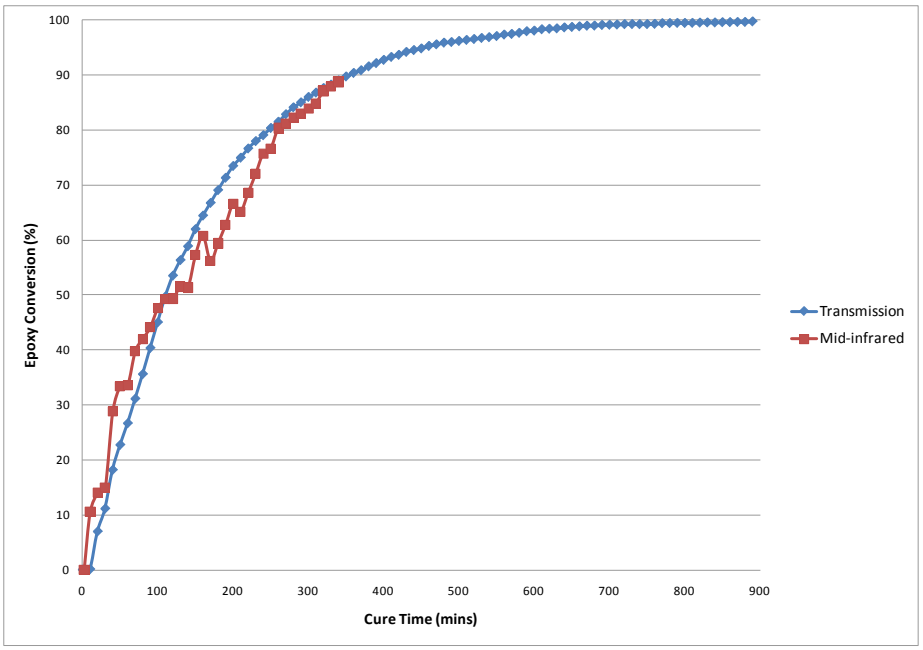

Chapter 5

5. Conclusions

Although the interphase region is minimal in terms of volume compared to the rest of the composite, it has a significant influence on the composites resilience and mechanical performance. Conventional reinforcing E-glass fibres can be used as sensors to monitor the cross-linking kinetics via evanescent wave spectroscopy *in situ*. Absorbance peaks can be readily identified and integrated to track their consumption in the cross-linking reactions during cure. This was established by good correlation between conversion plots of transmission spectroscopy and evanescent wave spectroscopy. Slight discrepancies were observed at higher temperatures; the reasons for this have been discussed. This enabled the study of the effect of silane treatment on the cross-linking kinetics of an amine-cured epoxy resin. GPS and APS treatments affected the cure behaviour of the resin system. Epoxy consumption was affected by GPS treatment more so than amine consumption. As the concentration of GPS increased, faster rates of epoxy conversion were observed at the beginning of cure, but the final degree of epoxy conversion decreased. APS (the amine-terminated silane) affected amine consumption with greater degree than epoxy consumption. Amine was converted at faster rates with increasing amine concentration, but the final degree of amine consumption reduced.

It is not conclusive what has caused these effects, but a number of factors have been postulated: (i) preferential adsorption of one resin component over the other onto the reinforcement surface, e.g. the amine curing agent can migrate into the sizing (Delong et al. 1990); (ii) reactant dilution effects resulting from sizing dissolution; (iii) accelerated cure rate – silane treated fibres may decrease activation energy; (iv) curing rate is higher with GPS treatment because of a higher concentration of epoxy groups (same can be said of APS, higher concentration of amine groups, faster cure rates); (v) amino groups increases rate of viscosity increase due to the higher concentration of epoxy groups and (vi) gradient in reactive amine-epoxy ratio from glass surface to resin, i.e. cross-link density increased nearer the glass surface, as APS is deposited in layers the chemically bonded layer at the glass provides a higher cross-link density.

5.1 Recommendations for future work

The present study established that reinforcing fibres can monitor the cross-linking process of a thermosetting resin. In addition, detection of fibre surface treatments in the form of silane coupling agents has been reported, along with their effect on the cross-linking process. To further enhance

the research continued surface characterisation of as-received, heat-treated and silane treated E-glass should be undertaken. Though extensive time was spent on investigating E-glass fibre surface using AFM, the machine was old and dated and consequently failed to produce images of a quality to be used in this thesis. For instance, nano-indentation used in conjunction with AFM can help characterise the molecular structures and reactions of silane coupling agents at composite interfaces to further develop the choice made concerning compatibility (between the reinforcing fibre, silane coupling agent and matrix). Characterisation of surface area by gas adsorption is another suggestion for further work. Potentially providing a building block, but beyond the scope of this study the feasibility of manufacturing self-sensing bio-composites is an area of research that could provide a wealth of opportunity. Since bone and teeth are naturally occurring polymer composites, questions can be raised if collagen fibres can be used as self-sensors? Already extensive research is progressing; biocompatible electrochemical sensors have been tested, capable of detecting small molecules such as glucose, cholesterol, lactate and urea (Cosnier, 2005). Tactile sensors are being developed to aid the surgeons work; feedback on tissue compliance, texture, contact forces and torques is helping the development of minimally invasive surgery (MIS) (Zbyszewski *et al.* 2008). Though many considerations must be taken, the potential sensors have are paving an exciting future on the development of a wide range of issues.

References

Ahagon, A. and A. N. Gent (1975). "Threshold fracture energies for elastomers." Journal of Polymer Science, Polymer Physics Edition **13**(Copyright 1976, IEE): 1903-1911.

Al-Moussawi, H., E. K. Drown, et al. (1993). "Silane/sizing composite interphase." Polymer Composites **14**(Compendex): 195-200.

Allen, K. W. (1992). "Silanes as the interphase in adhesive bonds." Journal of Adhesion Science and Technology **6**(1): 23-32.

Anderson, D., L. Johnson, et al. (2004). Troubleshooting optical-fiber networks: understanding and using your optical time-domain reflectometer, Elsevier Academic Press.

Anne, M. L., E. L. La Salle, et al. (2009). "Polymerisation of an industrial resin monitored by infrared fiber evanescent wave spectroscopy." Sensors and Actuators B-Chemical **137**(2): 687-691.

Azzarri, M. J., M. S. Cortizo, et al. (2003). "Effect of the curing conditions on the properties of an acrylic denture base resin microwave-polymerised." Journal of Dentistry **31**(7): 463-468.

Bailey, D. and E. Wright (2003). Practical fiber optics, Elsevier.

Bang, K. G., J. W. Kwon, et al. (2001). "Measurement of the degree of cure of glass fiber-epoxy composites using dielectrometry." Journal of Materials Processing Technology **113**(1-3): 209-214.

Barton, J. (1985). “The application of differential scanning calorimetry (DSC) to the study of epoxy resin curing reactions”. Epoxy Resins and Composites I, Springer Berlin / Heidelberg. **72:** 111-154.

Benchekchou, B. and N. S. Ferguson (1998). "The effect of embedded optical fibres on the fatigue behaviour of composite plates." Composite Structures **41**(Copyright 1998, IEE): 113-120.

Bidstrup, S. A., N. F. Sheppard Jr, et al. (1989). "Dielectric analysis of the cure of thermosetting epoxy/amine systems." Polymer Engineering and Science **29**(Compendex): 325-328.

Binnig, G., C. F. Quate, et al. (1986). "Atomic Force Microscope." Physical Review Letters **56**(9): 930.

Bjorksten, J. and L. L. Yaeger (1952). "Vinyl silane size for glass fabric." Modern Plastics **29**(11): 124188.

Bloembergen, N. and P. S. Pershan (1962). "Light waves at the boundary of nonlinear media." Physical Review **128**(Copyright 2004, IEE): 606-622.

Britcher, L., Kempson, S., Matisons, J. (1999). “Silanes on Glass Fibers - Adhesion Promoters for Composite Applications”. In: Mittal, K. L. and Pizzi, A. *Adhesion promotion techniques: technological applications*. New York: CRC Press. 356.

Chailleux, E., Salvia, M., Jaffrezic-Renault, N ., Matejec, V. and Kasik, I. (2001). “In situ study of the epoxy cure process using a fibreoptic sensor”. Smart Materials and Structures, Volume 10, 194–202.

Challis, R. E., M. E. Unwin, et al. (2003). "Following network formation in an epoxy/amine system by ultrasound, dielectric, and nuclear magnetic resonance measurements: a comparative study." Journal of Applied Polymer Science **88**(Copyright 2003, IEE): 1665-1675.

Chang, X., M. Li, et al. (2009). "Recent development and applications of polymer optical fiber sensors for strain measurement." Frontiers of Optoelectronics in China **2**(4): 362-367.

Chen, J. Y., S. V. Hoa, et al. (1999). "Fiber-optic and ultrasonic measurements for in-situ cure monitoring of graphite/epoxy composites." Journal of Composite Materials **33**(Compendex): 1860-1881.

Chen, R., G. F. Fernando, et al. (2004). "A novel ultrasound fibre optic sensor based on a fused-tapered optical fibre coupler." Measurement Science & Technology **15**(8): 1490-1495.

Cole, K. C. (1991). "A new approach to modeling the cure kinetics of epoxy/amine thermosetting resins. 1. Mathematical development." Macromolecules **24**(11): 3093-3097.

Connell, M. E., W. M. Cross, et al. (1998). "Direct monitoring of silane/epoxy interphase chemistry." Composites Part A: Applied Science and Manufacturing **29**(5-6): 495-502.

Conroy, A., S. Halliwell, et al. (2006). "Composite recycling in the construction industry." Composites Part A: Applied Science and Manufacturing **37**(8): 1216-1222.

Cosnier, S. (2005). "Affinity Biosensors Based on Electropolymerized Films." Electroanalysis **17**(19): 1701-1715.

Crosby, P. A., Powell, G. R., Fernando, G. F., Spooncer, R. C., France, C. M. and Waters, D. N. (1996). “In-situ cure monitoring in advanced composites using evanescent wave spectroscopy”. Smart Materials and Structures, Volume 5, 415–28.

Culler, S. R., H. Ishida, et al. (1986). "FT-IR Characterization of the Reaction at the Silane/Matrix resin Interphase of Composite Materials." Journal of Colloid and Interface Science **109**(Compendex): 1-10.

Degamber, B. and G. F. Fernando (2003). "Microwave processing of thermosets: Non-contact cure monitoring and fibre optic temperature sensors." Plastics, Rubber and Composites **32**(Compendex): 327-334.

DeLong, J. D.; Hook, K. J.; Rich, M. J.; Kalantar, J.; Drzal, L. T. *Controlled Interfaces in Composite Materials*, Elesevier Science Publishing Co., **1990**, 87.

Doyle, C., Martin, A., Liu, T., Wu, M., Hayes, S., Crosby, P. A., Powell, G. R., Brooks, D. and Fernando, G. F. (1998). "*In situ* process and condition monitoring of advanced fibre-reinforced composite materials using optical sensors". Smart Materials and Structures, Volume 7, 145–58.

Druy, M. A. and Elandjian, L. (1989). "Composite cure monitoring with infrared transmitting optical fibers". Proceedings of the Society of Photo-optical Instrumentation Engineers (SPIE), Volume 986, 130–134.

Dunkers, J. P., Flynn, K. F. amd Huang, M. T. (1997). "Near Infrared Cure Monitoring and Control of a Resin Transfer Molded Epoxy Composite Using an Evanescent Wave High Index Fiber Optic Sensor". Society of Plastics Engineers Annual Technical Conference, Toronto, Canada, April.

Eaton, P. J. (2010). *Atomic force microscopy*. New York: Oxford University Press. ISBN: 0199570450

Fernando, G. F. (2005). "Fibre optic sensor systems for monitoring composite structures." Reinforced Plastics **49**(11): 41-49.

Fernando, G. F. and Degamber, B. (2006). "Process monitoring of fibre reinforced composites using optical fibre sensors". International Materials Reviews, Volume 51, Issue 2, 65-106.

Feuston, B. P. and S. H. Garofalini (1990). "Water-induced relaxation of the vitreous silica surface." Journal of Applied Physics **68**(Copyright 1991, IEE): 4830-4836.

Gao, X., R. E. Jensen, et al. (2008). "Effect of fiber surface texture created from silane blends on the strength and energy absorption of the glass fiber/epoxy interphase." Journal of Composite Materials **42**(5): 513-534.

Gao, S. L. and E. Mader (2002). "Characterisation of interphase nanoscale property variations in glass fibre reinforced polypropylene and epoxy resin composites." Composites Part a-Applied Science and Manufacturing **33**(4): 559-576.

Garton, A. (1989). "Infrared Spectroscopic Characterization of Epoxy Matrix Composites." **26**(1): 17 - 41.

Gonzalez-Benito, J., J. C. Cabanelas, et al. (1996). "Surface characterization of silanized glass fibers by labeling with environmental sensitive fluorophores." Journal of Applied Polymer Science **62**(Compendex): 375-384.

Gonzalez-Benito, J., J. Baselga, et al. (1999). "Microstructural and wettability study of surface pretreated glass fibres." Journal of Materials Processing Technology **92-93**(Compendex): 129-134.

Gonzalez-Benito, J., F. Mike, et al. (2001). "Fluorescence monitoring of curing process and water accessibility at glass fiber/epoxy interphase on composite materials." Journal of Macromolecular Science - Physics **40 B**(Compendex): 429-441.

González-Benito, J. (2003). "The nature of the structural gradient in epoxy curing at a glass fiber/epoxy matrix interface using FTIR imaging." Journal of Colloid and Interface Science **267**(2): 326-332.

Griswold, C., W. M. Cross, et al. (2005). "Interphase variation in silane-treated glass-fiber-reinforced epoxy composites." Journal of Adhesion Science and Technology **19**(Compendex): 279-290.

Gupta, P. K., D. Inniss, et al. (2000). "Nanoscale roughness of oxide glass surfaces." Journal of Non-Crystalline Solids **262**(1-3): 200-206.

Hahn, H. T. (1984). "Effects of residual stresses in polymer matrix composites." Journal of the Astronautical Sciences **32**(3): 253-267.

Hamada, H., N. Ikuta, et al. (1994). "Effect of interfacial silane network structure on interfacial strength in glass fibre composites." Composites **25**(Compendex): 512-515.

Harrold, R. T. and Z. N. Sanjana (1986). "Acoustic waveguide monitoring of the cure and structural integrity of composite materials." Polymer Engineering & Science **26**(5): 367-372.

Hayes, S., T. Liu, et al. (1997). "In situ self-sensing fibre reinforced composites." Smart Materials and Structures **6**(Compendex): 432-440.

Her, S.-C., B.-R. Yao, et al. (2010). Stress analysis of a resin pocket embedded in laminated composites for an optical fiber sensor, Laubisrutistr.24, Stafa-Zuerich, CH-8712, Switzerland, Trans Tech Publications Ltd.

Hill, G. and Holman, J. (2000). *Chemistry in context*. 5th ed. Walton-on-Thames: Nelson Thornes. 363.

Hong, K. C., T. M. Vess, et al. (1993). Remote cure monitoring of polymeric resins by laser Raman spectroscopy. Proceedings of the 1993 38th International SAMPE Symposium and Exhibition. Part 2 (of 2), May 10, 1993 - May 13, 1993, Anaheim, CA, USA, SAMPE.

Hong, S. G. and J. J. Lin (1997). "Effects of glass beads and silane treatments on the curing behavior of a brominated epoxy resin: DSC analyses." Journal of Polymer Science, Part B: Polymer Physics **35**(Compendex): 2063-2071.

Hong, S. G. and T. C. Wang (1994). "The Effect of Copper Oxides on the Curing of Brominated Epoxy-Resins." Thermochimica Acta **237**(2): 305-316.

Horr, T. J. and G. D. Reynolds (1997). "Reactions of 3-glycidoxypropyltrimethoxysilane in acidic solutions on polymerization and in the presence of silica." Journal of Adhesion Science and Technology **11**(7): 995-1009.

Hull, D. (1981). An Introduction to Composite Materials. Cambridge University Press. Cambridge.

Iglesias, J. G., J. Gonzalez-Benito, et al. (2002). "Effect of glass fiber surface treatments on mechanical strength of epoxy based composite materials." Journal of Colloid and Interface Science **250**(Compendex): 251-260.

Ishida, H. and J. L. Koenig (1979). "An investigation of the coupling agent/matrix interface of fiberglass reinforced plastics by fourier transform infrared spectroscopy." Journal of Polymer Science: Polymer Physics Edition **17**(4): 615-626.

Ishida, H., Naviroj, S., Tripathy, S.K., Fitzgerald, J.J., Koenig, J.L. (1982). “The structure of an aminosaline coupling agent in aqueous-solutions and partially cured solids”. J. Polymer Sci. Polym. Phys. 20,701-718.

Johnson, D. J., D. A. C. Compton, et al. (1992). "Applications of Simultaneous DSC FTIR Analysis." Thermochimica Acta **195**: 5-20.

Johnson, G. A., S. T. Vohra, et al. (1999). Vibration monitoring of a ship waterjet with fiber Bragg gratings. Ofs-13: 13th International Conference on Optical Fiber Sensors & Workshop on Device and

System Technology toward Future Optical Fiber Communication and Sensing. B. Y. Kim and K. Hotate. **3746:** 616-619.

Jones, F. R. (2007). "The Chemical Aspects of Fibre Surfaces and Composite Interfaces and Interphases, and their Influence on the Mechanical Behaviour of Interfaces".

Kalantar, J. and L. T. Drzal (1990). "The bonding mechanism of aramid fibres to epoxy matrices." Journal of Materials Science **25**(10): 4186-4193.

Kang, H. K., D. H. Kang, et al. (2002). "Cure monitoring of composite laminates using fiber optic sensors." Smart Materials & Structures **11**(2): 279-287.

Karkanas, P, I. (1997). Cure Modelling and Monitoring of Epoxy/Amine Resin Systems. Thesis, (Ph.D.). Cranfield University.

Kazilas, M. C. (2002). Acquisition and Interpretation of Dielectric Data For Thermoset Cure Monitoring. Thesis, (Ph.D.). Cranfield University.

Kim, J.-K. and Y.-W. Mai (1998). Engineered Interfaces in Fiber Reinforced Composites, Elsevier.

Kin-Tak, L., Y. Libo, et al. (2001). "Strain monitoring in FRP laminates and concrete beams using FBG sensors." Composite Structures **51**(Copyright 2001, IEE): 9-20.

Kister, G., B. Ralph, et al. (2001). "A chemical sensor based on conventional reinforcing E-Glass fibres." Advanced Engineering Materials **3**(Copyright 2001, IEE): 711-712.

Kister, G., L. Wang, et al. (2003). "Self-sensing E-glass fibres." Optical Materials **21**(Compendex): 713-727.

Koran, P. and R. Kürschner (2001). "effects of sequential versus continuous irradiation of a light-cured resin composite on shrinkage, viscosity, adhesion, and degree of polymerization." Journal of Esthetic and Restorative Dentistry **13**(2): 140-141.

Le Coq, D., K. Michel, et al. (2002). "Infrared glass fibers for in-situ sensing, chemical and biochemical reactions." Comptes Rendus Chimie **5**(12): 907-913.

Lee, B. (2003). "Review of the present status of optical fiber sensors." Optical Fiber Technology **9**(2): 57-79.

Lekakou, C., S. Cook, et al. (2006). "Optical fibre sensor for monitoring flow and resin curing in composites manufacturing." Composites Part a-Applied Science and Manufacturing **37**(6): 934-938.

Leng, J. S. and A. Asundi (2002). "Real-time cure monitoring of smart composite materials using extrinsic Fabry-Perot interferometer and fiber Bragg grating sensors." Smart Materials & Structures **11**(2): 249-255.

Lenhart, J. L., J. H. van Zanten, et al. (2000). "Interfacial response of a fluorescent dye grafted to glass." Langmuir **16**(Copyright 2000, IEE): 8145-8152.

Lew, A., Depeursinge, C., Cochet, F., Berthou, H. and Parriaux, H. *SPIE*, 1984, 514.

Liu, Y. M. (1993). Monitoring the dynamic properties of polymers and composites with a localized micro-vibration methodology. Ph.D. dissertation, Auburn Univ., Dept. of ME., 4-12.

Liu, X., J. L. Thomason, et al. (2008). "XPS and AFM Study of Interaction of Organosilane and Sizing with E-Glass Fibre Surface." The Journal of Adhesion **84**(4): 322 - 338.

Liu, T., G. F. Fernando, et al. (1997). “Simultaneous strain and temperature measurements in composites using a multiplexed fibre Bragg grating sensor and an extrinsic Fabry-Perot sensor”. Smart Structures and Materials 1997: Smart Sensing, Processing, and Instrumentation, 3-5 March 1997, USA, SPIE-Int. Soc. Opt. Eng.

Lodeiro, M.J. and Mulligan, D.R. (2005) “Good practice guide to cure monitoring”. Measurement good practice guide No 75. National Physical Laboratory, Teddington, Middlesex, UK, TW11 0LW, pp 17–32.

Mader, E., H. J. Jacobasch, et al. (1996). "Influence of an optimized interphase on the properties of polypropylene/glass fibre composites." Composites Part a-Applied Science and Manufacturing **27**(9): 907-912.

Martin, Y., C. C. Williams, et al. (1987). "Atomic force microscope-force mapping and profiling on a sub 100-A scale." Journal of Applied Physics **61**(Copyright 1987, IEE): 4723-4729.

Melin, L. G., K. Levin, et al. (1999). "A study of the displacement field around embedded fibre optic sensors." Composites Part A (Applied Science and Manufacturing) **30A**(Copyright 1999, IEE): 1267-1275.

Merad, L., M. Cochez, et al. (2009). "In-situ monitoring of the curing of epoxy resins by Raman spectroscopy." Polymer Testing **28**(Copyright 2009, The Institution of Engineering and Technology): 42-45.

Merschman, S. A. and D. C. Tilotta (1998). "Fiber-optic sensor for aromatic compounds in water based on solid-phase microextraction and ultraviolet evanescent wave absorption spectroscopy." Applied Spectroscopy **52**(1): 106-111.

Mijovic, J. and Andjeli, S. (1995). “A Study of Reaction Kinetics by Near-Infrared Spectroscopy. 1. Comprehensive Analysis of a Model Epoxy/Amine System”. Macromolecules, Volume 28, 2787-2796.

Mike, F., J. Gonzalez-Benito, et al. (2001). "Monitoring of curing process by fluorescence technique. Fluorescence probe and label based on 5-dimethylaminonaphthalene-1-sulfonamide derivatives (DNS)." Journal of Macromolecular Science - Physics **40 B**(Compendex): 405-428.

Miller, J. D. And Ishida, H. "Adhesive-Adherend Interface and Interphase," in "*Adhesion Science*," L.H. Lee, Ed., Plenum, New York (1990) Chapter 10, p.291.

Mitra, B. and D. J. Booth (1998). "Remote cure monitoring of epoxy materials using optical techniques." Ultrasonics **35**(Compendex): 569-572.

Montanini, R. and L. D'Acquisto (2007). "Simultaneous measurement of temperature and strain in glass fiber/epoxy composites by embedded fiber optic sensors: I. Cure monitoring." Smart Materials and Structures **16**(Compendex): 1718-1726.

Muhs, J. D., M. R. Cates, et al. (1990). Fiber-optic sensors for composite cure analysis and lifetime nondestructive evaluation. ICALEO '89. Optical Sensing and Measurement, 15-20 Oct. 1989, USA.

Mulligan, D. (2003). Cure monitoring for composites and adhesives, Rapra Technology.

O'Dwyer, M. J., G. M. Maistros, et al. (1998). "Relating the state of cure to the real-time internal strain development in a curing composite using in-fibre Bragg gratings and dielectric sensors." Measurement Science and Technology **9**(Compendex): 1153-1158.

Okoli, O. I. (2001). "The effects of strain rate and failure modes on the failure energy of fibre reinforced composites." Composite Structures **54**(2-3): 299-303.

Olmos, D., A. J. Aznar, et al. (2005). "Kinetic study of the epoxy curing at the silica particles/epoxy interface using the fluorescence of pyrene label." Polymer Testing **24**(Compendex): 275-283.

Owen, M. J. (2002). Coupling agents: chemical bonding at interfaces. In: Dillard, D. A.; Pocius, A. V.; Chaudhury, M. *Adhesion Science and Engineering Volume 2, The Mechanics of Adhesion/Surfaces, Chemistry Applications*. Elsevier. p403-431.

Palmese, G. R. and R. L. McCullough (1994). "Kinetic and Thermodynamic Considerations Regarding Interphase Formation in Thermosetting Composite Systems." Journal of Adhesion **44**(1-2): 29-49.

Palmese, G. R., O. A. Andersen, et al. (1999). "Effect of glass fiber sizing on the cure kinetics of vinyl-ester resins." Composites Part A (Applied Science and Manufacturing) **30A**(Copyright 1999, IEE): 11-18.

Park, S.-J. and J.-S. Jin (2001). "Effect of silane coupling agent on interphase and performance of glass fibers/unsaturated polyester composites." Journal of Colloid and Interface Science **242**(Compendex): 174-179.

Pedrotti, F. and L. Pedrotti (2006). Introduction to Optics (3rd Edition), Benjamin Cummings.

Petrovic, Z. and N. Stojakovic (1988). "Study of Epoxy Resin-filler Interaction." Polymer Composites **9**(Compendex): 42-50.

Plueddemann, E.P. (1988). Present status and research needs in silane coupling. In *Proc. ICCI-II, Interfaces in Polymer, Ceramic and Metal Matrix Composites* (H. Ishida ed.), Elsevier Sci. Pub. New York.

Plueddemann, E. P. (1991). *Fundamentals of adhesion*. New York: Plenum Press. 279-290.

Plueddemann, E. P. (1991). "Reminiscing on silane coupling agents." Journal of Adhesion Science and Technology **5**: 261-277.

Plueddemann, E.P. and Stark, G.L. (1980). In *Proc. 35th Annual Tech. Conf. Reinf: Plast./Composite.* SPI. Section 20-B.

Powell, G.R., Crosby, P.A. and Waters, D.N. (1998). “In-situ cure monitoring using optical fibre sensors- a comparative study”. Smart Materials and Structures, Volume 7, 557–568.

Provatas, A. and J. G. Matisons (1998). Synthesis of amino acid functional siloxanes. Proceedings of the 1998 Dallas Meeting, March 29, 1998 - April 2, 1998, Dallas, TX, USA, ACS.

Rao, Y. J., S. F. Yuan, et al. (2002). "Simultaneous strain and temperature measurement of advanced 3-D braided composite materials using an improved EFPI/FBG system." Optics and Lasers in Engineering **38**(6): 557-566.

Read, I., P. Foote, et al. (2002). "Optical fibre acoustic emission sensor for damage detection in carbon fibre composite structures." Measurement Science and Technology **13**(Compendex): N5-N9.

Roberts, S. S. J. and R. Davidson (1993). "Cure and fabrication monitoring of composite materials with fibre-optic sensors." Composites Science and Technology **49**(Copyright 1993, IEE): 265-276.

Schweinsberg, D. P. and G. A. George (1986). "A chemiluminescence study of the properties and degradation of epoxy resins as coatings." Corrosion Science **26**(Copyright 1986, IEE): 331-340.

Serway, R., C. Vuille, et al. (2008). College Physics, Thomson Brooks/Cole.

Sever, K., M. Sarikanat, et al. (2008). Effects of fiber surface treatments on mechanical properties of epoxy composites reinforced with glass fabric, Van Godewijckstraat 30, Dordrecht, 3311 GZ, Netherlands, Kluwer Academic Publishers.

Shelby, J. (2005). Introduction to glass science and technology, Royal Society of Chemistry.

Skordos, A. A. (2003). Modelling and monitoring of resin transfer moulding. Thesis, (Ph.D.). Cranfield University.

Smith, I. T. (1961). "The mechanism of the crosslinking of epoxide resins by amines." Polymer **2**: 95-108.

Sourour, S. and M. R. Kamal (1976). "Differential scanning calorimetry of epoxy cure: isothermal cure kinetics." Thermochimica Acta **14**(1-2): 41-59.

Stark, E., K. Luchter, et al. (1986). "Near-Infrared Analysis (NIRA): A Technology for Quantitative and Qualitative Analysis." Applied Spectroscopy Reviews **22**(4): 335 - 399.

Sung, N.H., Kahl, A., Ni, S., Sung, C.S.P., Chin. I.J. (1981). In *Proc.* 36th *Annual Tech. Conf: Reinf. Plast./Composite.* SPI. Section 28.

Thomason, J. L. and D. W. Dwight (1999). "Use of XPS for characterization of glass fibre coatings." Composites Part A: Applied Science and Manufacturing **30**(Compendex): 1401-1413.

Thomason, J. L. and L. J. Adzima (2001). "Sizing up the interphase: an insider's guide to the science of sizing." Composites Part a-Applied Science and Manufacturing **32**(3-4): 313-321.

Troughton, M. J. (2008). *Handbook of Plastics Joining: A Practical Guide*. 2nd ed. New York: William Andrew. 149-150.

Tuncol, G., M. Danisman, et al. (2007). "Constraints on monitoring resin flow in the resin transfer molding (RTM) process by using thermocouple sensors." Composites Part a-Applied Science and Manufacturing **38**(5): 1363-1386.

Udd, E. (1995). "Overview of fiber-optic sensors." Review of Scientific Instruments **66**(Compendex): 4015-4030.

Varma, I. K., G. Gupta, et al. (2001). "Intrinsically conducting polymer blends." Macromolecular Symposia **164**(1): 401-410.

Wang, T. W. H., F. D. Blum, et al. (1999). "Effect of interfacial mobility on flexural strength and fracture toughness of glass/epoxy laminates." Journal of Materials Science **34**(19): 4873-4882.

Wang, L., S. Pandita, et al. (2009). "Characterisation of the cross-linking process in an E-glass fibre/epoxy composite using evanescent wave spectroscopy." Composites Science and Technology **69**(13): 2069-2074.

Weyer, L. G. (1985). "Near-Infrared Spectroscopy of Organic Substances." Applied Spectroscopy Reviews **21**(1): 1 - 43.

Wu, H. F., D. W. Dwight, et al. (1997). Effects of silane coupling agents on the interphase and performance of glass-fiber-reinforced polymer composites. Sixth International Conference on Composite Interfaces (ICCI-6): Microphenomena in Advanced Interfaces, 5-8 May 1996, UK, Elsevier.

Xu, L. and J. R. Schlup (1996). "Application of Near-Infrared Attenuated Total Reflectance Spectroscopy for Monitoring Epoxy Resin/Amine Cure Reactions." Applied Spectroscopy **50**(1): 109-114.

Yongho, S. and J. Wonho (2008). "Atomic force microscopy and spectroscopy." Reports on Progress in Physics **71**(Copyright 2008, The Institution of Engineering and Technology): 016101 (016123 pp.).

Yu, J.-W. and C. S. P. Sung (1997). "Interphase cure characterization in epoxy composites by fluorescence technique." Journal of Applied Polymer Science **63**(13): 1769-1775.

Yu, Y. F., H. H. Su, et al. (2009). "Effects of Storage Aging on the Properties of Epoxy Prepregs." Industrial & Engineering Chemistry Research **48**(9): 4340-4345.

Zbyszewski, D., L. Hongbin, et al. (2008). Wheel/tissue force interaction: A new concept for soft tissue diagnosis during MIS. Engineering in Medicine and Biology Society, 2008. EMBS 2008. 30th Annual International Conference of the IEEE.

Zhang, Z., Y. Liu, et al. (2002). "The effect of carbon-fiber surface properties on the electron-beam curing of epoxy-resin composites." Composites Science and Technology **62**(3): 331-337.

Zhong, Q., D. Inniss, et al. (1993). "Fractured polymer/silica fiber surface studied by tapping mode atomic force microscopy." Surface Science **290**(Copyright 1993, IEE): 688-692.

Zvetkov, V. L., R. K. Krastev, et al. (2008). "Rate equations in the study of the DSC kinetics of epoxy-amine reactions in an excess of epoxy." Thermochimica Acta **478**(Compendex): 17-27.

Appendix

Extensive AFM analysis was also conducted of differently treated E-glass fibre surfaces. Only a couple of the images obtained were included in the study as the following were not of the required standard.

0.1% GPS

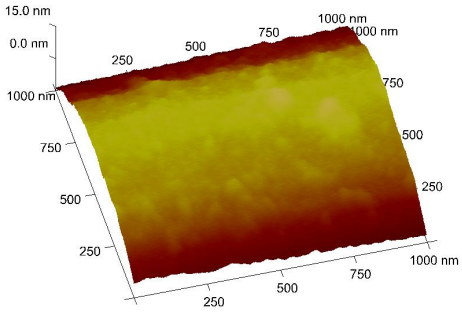

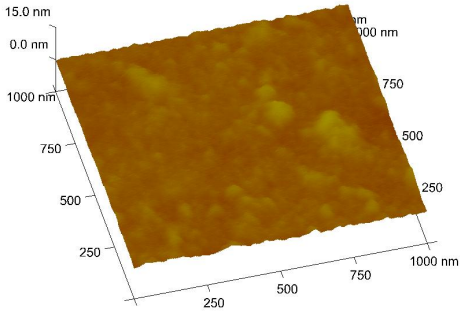

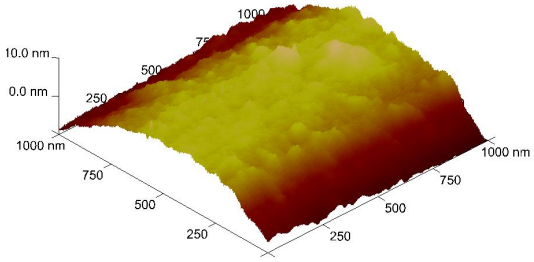

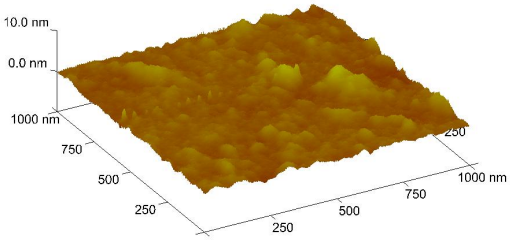

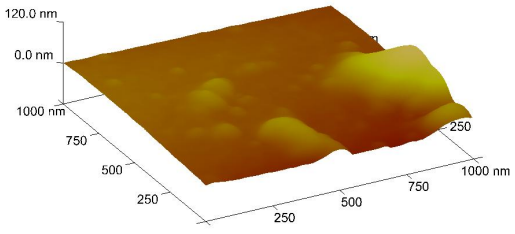

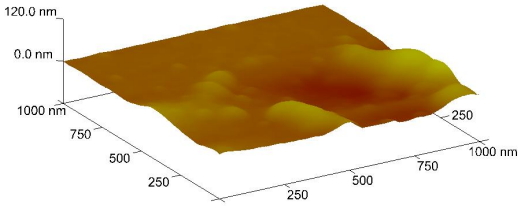

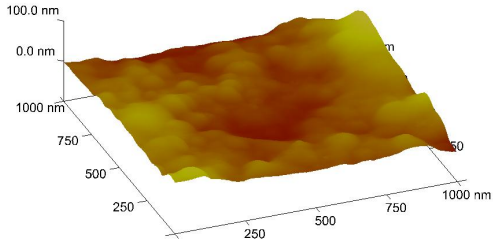
100.0 nm
0.0 nm
1000 nm
750
500
250
250
500
750
1000 nm

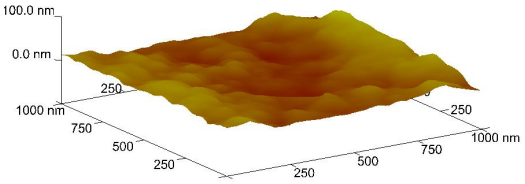
100.0 nm
0.0 nm
1000 nm
750
500
250
250
500
750
1000 nm

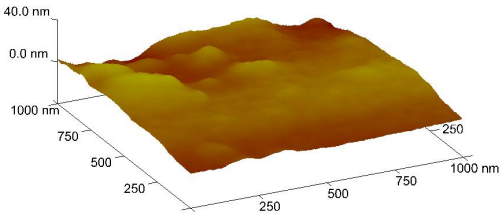
40.0 nm
0.0 nm
1000 nm
750
500
250
250
500
750
1000 nm

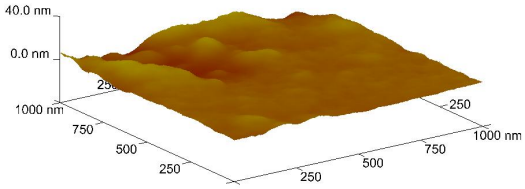
40.0 nm
0.0 nm
1000 nm
750
500
250
250
500
750
1000 nm

0.5% GPS

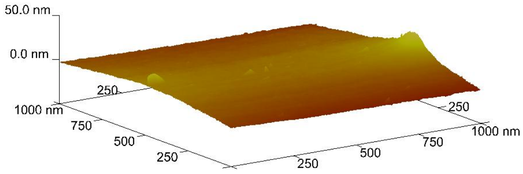
50.0 nm
0.0 nm
250
1000 nm
750
500
250
250
500
750
250
1000 nm

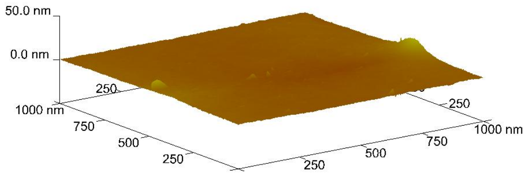
50.0 nm
0.0 nm
250
1000 nm
750
500
250
250
500
750
250
1000 nm

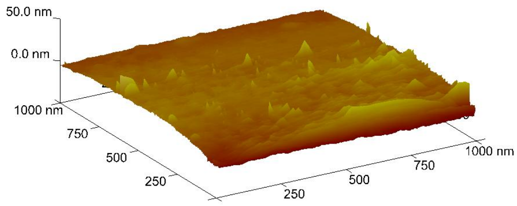
50.0 nm
0.0 nm
1000 nm
750
500
250
250
500
750
1000 nm

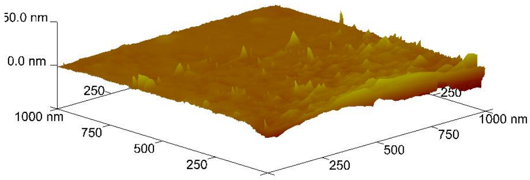
0.0 nm
250
1000 nm
750
500
250
250
500
750
250
1000 nm

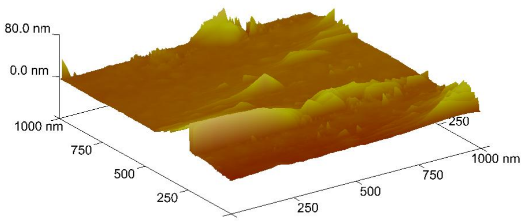
80.0 nm
0.0 nm
1000 nm
750
500
250
250
500
750
250
1000 nm

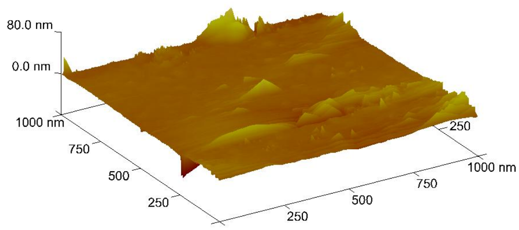
80.0 nm
0.0 nm
1000 nm
750
500
250
250
500
750
250
1000 nm

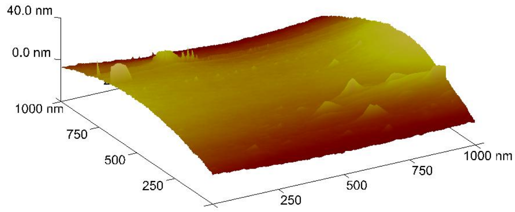
40.0 nm
0.0 nm
1000 nm
750
500
250
250
500
750
1000 nm

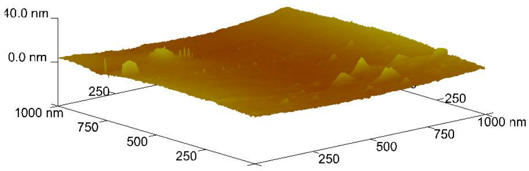
0.0 nm
250
1000 nm
750
500
250
250
500
750
250
1000 nm

1% GPS

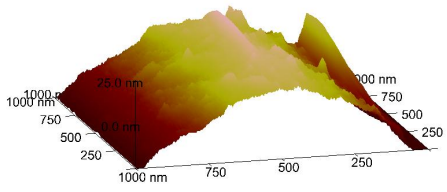
25.0 nm
0.0 nm
1000 nm
750
500
250

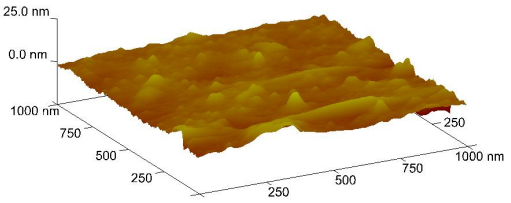
25.0 nm
0.0 nm
1000 nm
750
500
250

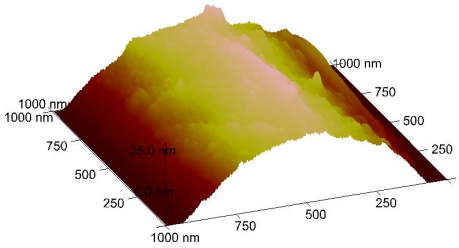
1000 nm
750
500
250
25.0 nm
0.0 nm

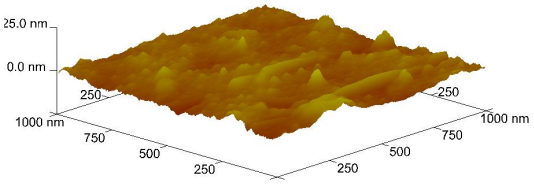
25.0 nm
0.0 nm
1000 nm
750
500
250

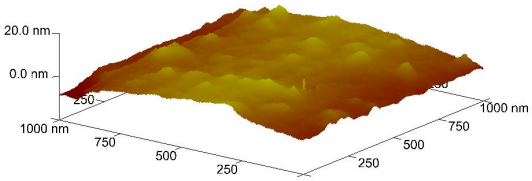
20.0 nm
0.0 nm
1000 nm
750
500
250

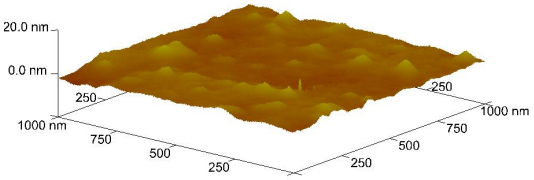
20.0 nm
0.0 nm
1000 nm
750
500
250

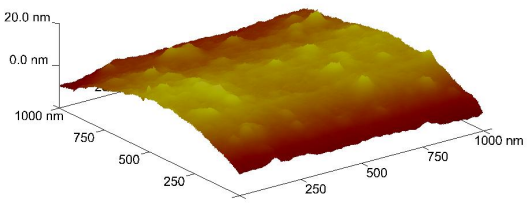
20.0 nm
0.0 nm
1000 nm
750
500
250

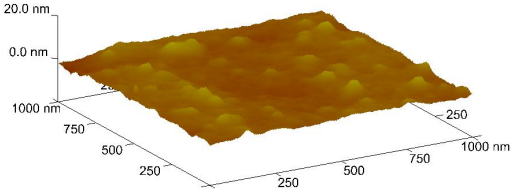
20.0 nm
0.0 nm
1000 nm
750
500
250

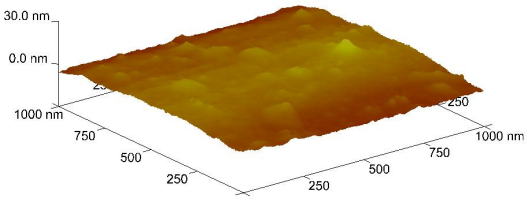
30.0 nm
0.0 nm
1000 nm
750
500
250
250
500
750
1000 nm

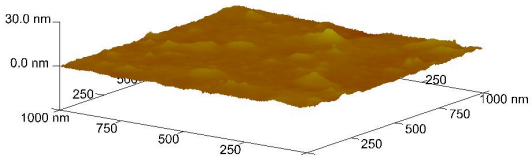
30.0 nm
0.0 nm
250
1000 nm
750
500
250
250
500
750
1000 nm

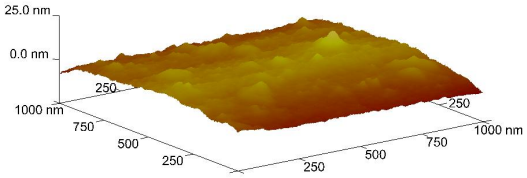
25.0 nm
0.0 nm
250
1000 nm
750
500
250
250
500
750
1000 nm

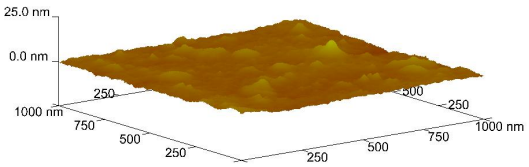
25.0 nm
0.0 nm
250
1000 nm
750
500
250
250
500
750
1000 nm

3% GPS

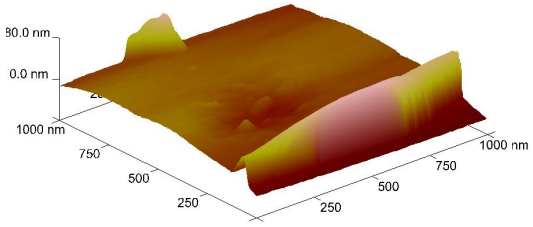
80.0 nm
0.0 nm
1000 nm
750
500
250
250
500
750
1000 nm

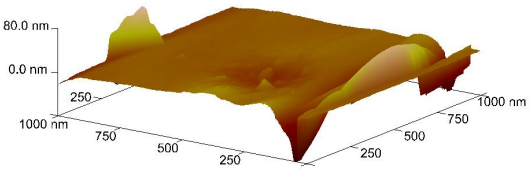
80.0 nm
0.0 nm
250
1000 nm
750
500
250
250
500
750
1000 nm

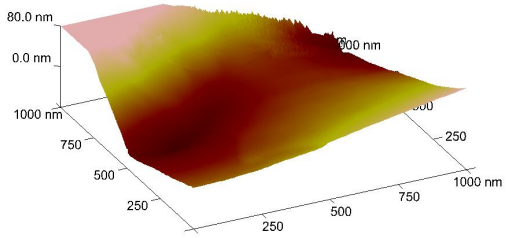
80.0 nm
0.0 nm
1000 nm
750
500
250
250
500
750
1000 nm

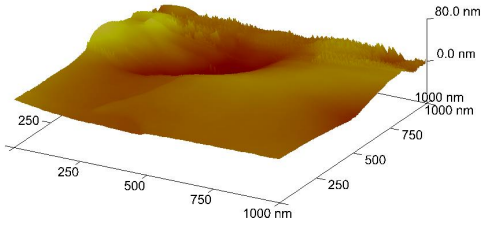
80.0 nm
0.0 nm
1000 nm
1000 nm
750
500
250
250
500
750
1000 nm

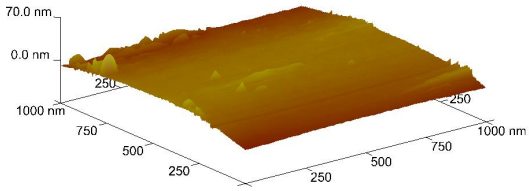
70.0 nm
0.0 nm
250
1000 nm
750
500
250
250
500
750
1000 nm

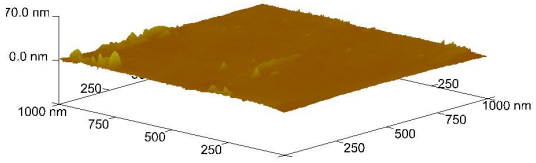
70.0 nm
0.0 nm
250
1000 nm
750
500
250
250
500
750
1000 nm

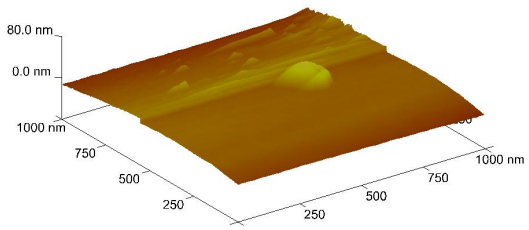
80.0 nm
0.0 nm
1000 nm
750
500
250
250
500
750
1000 nm

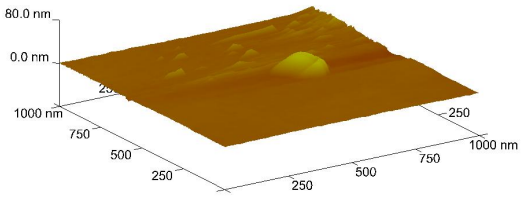
80.0 nm
0.0 nm
1000 nm
750
500
250
250
500
750
1000 nm

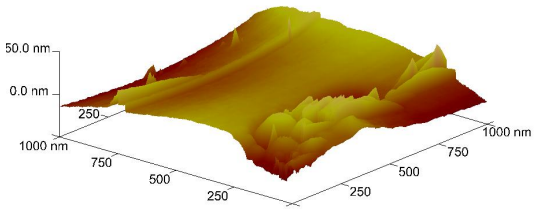
50.0 nm
0.0 nm
250
1000 nm
750
500
250
1000 nm
750
500
250

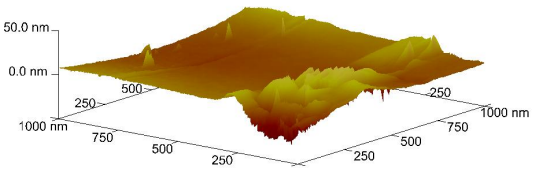
50.0 nm
0.0 nm
500
250
1000 nm
750
500
250
250
1000 nm
750
500
250

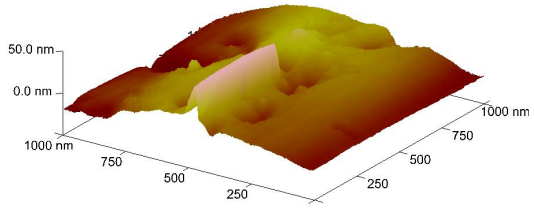
50.0 nm
0.0 nm
1000 nm
750
500
250
1000 nm
750
500
250

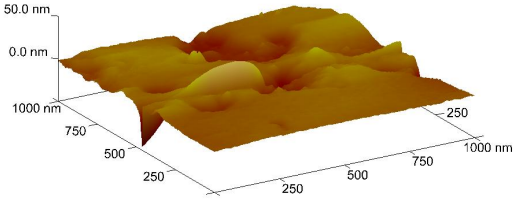
50.0 nm
0.0 nm
1000 nm
750
500
250
250
1000 nm
750
500
250

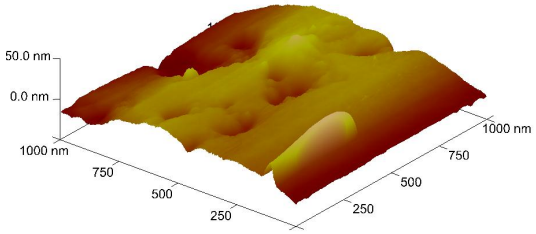
50.0 nm
0.0 nm
1000 nm
750
500
250
1000 nm
750
500
250

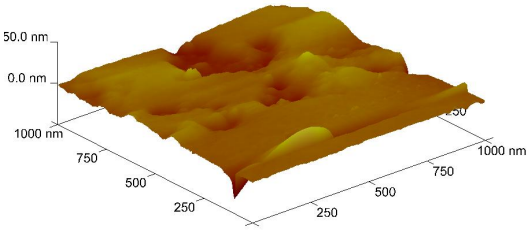
50.0 nm
0.0 nm
1000 nm
750
500
250
1000 nm
750
500
250